http://researchcommons.waikato.ac.nz/

Research Commons at the University of Waikato

Copyright Statement:

The digital copy of this thesis is protected by the Copyright Act 1994 (New Zealand).

The thesis may be consulted by you, provided you comply with the provisions of the Act and the following conditions of use:

- Any use you make of these documents or images must be for research or private study purposes only, and you may not make them available to any other person.
- Authors control the copyright of their thesis. You will recognise the author's right to be identified as the author of the thesis, and due acknowledgement will be made to the author where appropriate.
- You will obtain the author's permission before publishing any material from the thesis.

Late Cenozoic Development of North Taranaki Basin, New Zealand: A Seismic Investigation

A thesis

submitted in partial fulfilment

of the requirements for the degree

of

Master of Science (Research) in Earth and Ocean Sciences

at

The University of Waikato

by

Jessica Eileen Richardson-Land

THE UNIVERSITY OF
WAIKATO
Te Whare Wānanga o Waikato

University of Waikato

2017

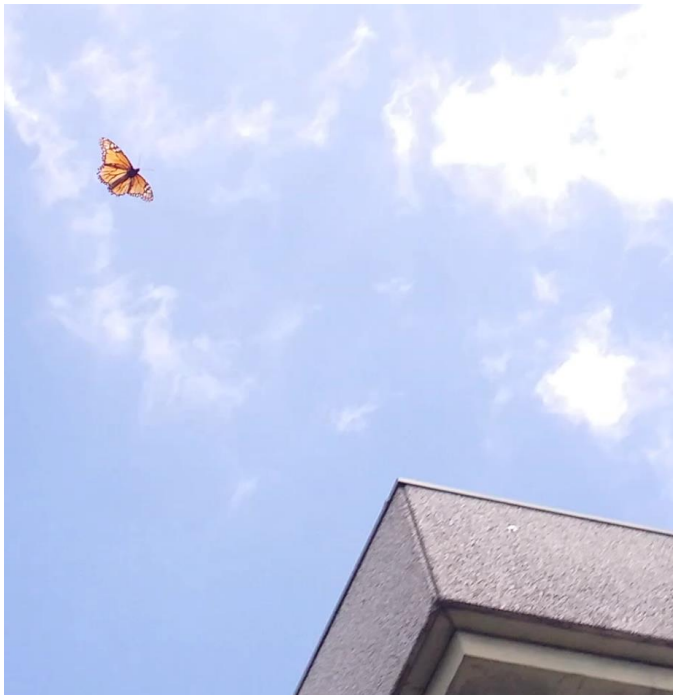

Frontispiece: Monarch butterfly flying above the entrance to my office, E Block, University of Waikato

"Butterflies hover and feathers appear, whenever our guardian angels are near" – Anon

Dedicated to my Dad - Brian Land

This focus of this thesis is on the seismic stratigraphy and structure of the part of North Taranaki Basin immediately north of western Taranaki Peninsula, central-western North Island. In particular, the emphasis is on basin geometry and sedimentation patterns of the Late Cenozoic section. The seismic mapping has been undertaken with open-file industry data archived by New Zealand Petroleum and Minerals (MBIE, Wellington) using industry-standard software (Kingdom TM) under an academic Licence to The University of Waikato.

Seismic reflection mapping made use of 175 2-D seismic profiles and one 3-D seismic survey (Parihaka), all acquired over 6350 km^2 in the study area. Fourteen drill holes in the study area penetrate at least the L. Cenozoic section and from them biostratigraphic data have been previously generated and reported in Petroleum Reports and in papers. An age model has been generated from these data that relies especially upon New Zealand biostratigraphic stage boundaries located in Ariki-1 and Arawa-1, where there is highest confidence about their placement. These are (i) top of Kapitean (5.3 Ma), top of Opoitian (3.6 Ma), top of Waipipian (3.0 Ma), top of Mangapanian (2.4 Ma), and top of Nukumaruan (1.63 Ma). The depths in all 14 drillholes of the newly mapped seismic horizons are illustrated in an enclosure (No. 1) in relation to the biostratigraphic stage boundaries, which documents the age model for the Pliocene-Pleistocene succession in Northern Taranaki Basin. From seismic mapping of horizons selected close to the biostratigraphic stage boundaries (Ariki-1 and Arawa-1), a series of structure contour and isopach maps have been generated for the study area. Parihaka Fault is a major structure revealed by the seismic mapping. It is a segmented fault that bounds a half-graben structure named the Arawa Sub-basin. A second enclosure illustrates this and other structures (e.g. buried volcanoes) on selected seismic reflection profiles and in the structure contour and isopach maps.

The Arawa Sub-basin and Northern Graben developed during the later part of the Kapitean Stage (Late Miocene); that is, prior to 5.3 Ma. Sediment distribution patterns in the Opoitian Stage (Early Pliocene) section were very much influenced by the location of depocentres formed during the Late Kapitean. The Waipipian (Mid-Pliocene) section is comparatively thin and represents a slow down in the sediment supply to North Taranaki Basin, probably because the material being sourced from erosion of the Southern Alps was captured by Wanganui Basin and Toru Trough in southern Taranaki Basin. During the Mangapanian Stage (Late Pliocene) there was a marked increase in sediment flux to North

Taranaki Basin, which resulted in the infilling of Arawa Sub-basin and the formation of a well-defined continental shelf-slope margin, which prograded to the northwest. The Nukumaruan Stage (Early Pleistocene) together with the rest of the Pleistocene was characterised in the study area by further progradation of the shelf-slope basin and a re-orientation of it towards the northwest, forming the modern shelf and slope bathymetry.

Acknowledgements

I wish to thank the many people who provided assistance and support during the preparation of this thesis.

First and foremost, I wish to acknowledge my supervisors for this project, Professor Peter Kamp and Dr Rochelle Hansen. Their knowledge, guidance, and overall support was monumental in providing this project with the direction it needed and its overall success, and for that I am extremely thankful.

I offer my individual thanks to the staff working in 'The Bridge' office, where most of the work was carried out - to Zac Lyon for his expertise, his patience with my endless questions and his teaching of Kingdom SMT; to Yu Shen Liu for his guidance with Adobe Illustrator; to Megan Saunders for her thesis advice and uplifting chats; and to Kirsty Vincent for her occasional baking that made long days easier.

The School of Science and I acknowledge and thank IHS Kingdom for the provision of an Academic Licence to enable seismic mapping of Industry data to have been part of this thesis.

I wish to thank the organisations and people that have provided me financial assistance in the form of scholarships this year: The University of Waikato (Masters Research Scholarship); OMV New Zealand Ltd; and the George Mason Charitable Trust. Studying my Master of Science degree at University would have not been possible without their help and for that I am very grateful.

Lastly, I am both grateful and thankful to all of my friends and my family for their encouragement and welcome distractions. I would like to acknowledge Sylvia Sabbagha and Hannah Josling, who also undertook their thesis research this year too, and I thank them for the numerous 'tearoom motivational talks' and the laughs when I needed them. To my mum, Trish Richardson, I offer my thanks for your unwavering support, your positivity, your help with final proof reading and for always believing in me. To my aunt, Margaret McNeice, who has been on my educational journey since the beginning, I offer my thanks for providing additional help and encouragement. Finally, I wish to give a special thanks to my partner, Shaun McArthur, for always being there for me regardless of sunshine or rain.

Table of Contents

1. Introduction

1.1 An overview

This thesis will examine the development of part of North Taranaki basin from the Late Miocene to the present day. In particular, the study will focus on the basin geometry and sedimentation patterns for late Cenozoic section, primarily through seismic reflection profile mapping and attention to drill hole data archived with New Zealand Petroleum and Minerals (MBIE), as well as biostratigraphic data reported in petroleum reports and in papers.

Taranaki basin is a Cretaceous – Cenozoic sedimentary basin located offshore of the west coast of North Island, New Zealand, occupying an area of approximately 100,000km^2. The basin is the most explored and resource rich sedimentary basin in New Zealand, containing up to 9km of late Cretaceous – Cenozoic sedimentary fill and numerous oil and gas fields.

The basin formed initially due to rifting during the late Cretaceous, and then transitioned into a passive phase, with minimal subsidence and condensed sedimentation (Early Oligocene). From the Late Oligocene, the basin developed as a foreland basin. Shortening along the eastern basin margin continued through into the late Miocene where Southern Taranaki Basin was inverted. Extension developed in Northern Taranaki Basin during the Late Miocene (Kapitean Stage) and during the Mid-Pliocene in the Central Graben to the southwest of Taranaki Peninsula, principally associated with Cape Egmont Fault.

Hansen and Kamp (2002) document the seismic stratigraphy of northern Taranaki Basin using paper trace profiles, and described the Late Neogene evolution of the basin. However, only 39 seismic lines were used in their investigation. Their biostratigraphic work synthesised age control for the late Cenozoic succession, with improvements resulting from the incorporation of new data generated during the past 15 years, provides the age control for this investigation. This study aims to improve the resolution of the seismic stratigraphy of Northern Taranaki Basin, by the use of digital data analysed within the aid of industry standard software (Kingdom TM) and improved biostratigraphic age control.

1.2 Project Objectives

This thesis has 3 main objectives:

- To seismically map a series of horizons within part of Northern Taranaki Basin to better understand the structural and sedimentation history of the basin, using existing biostratigraphy to select and date the mapped horizons.
- From these new data, create a suite of structure contour and isopach maps that will illustrate the basin structure
- Compare the results of seismic mapping with the results of previous basin investigations

1.3 Study Area

The study area (Figure 1.1) covers an area of approximately 6350km^2 in offshore North Taranaki Basin, immediately north of the western part of Taranaki Peninsula, western North Island. This area lies west of an area mapped by Lyon (2015), and north of studies undertaken by Lucas (2013) and Huesser (2014) in south Taranaki Basin. This study area has the following features:

1. This area spans partly across the Northern Graben, as well as across part of the Western Stable Platform, and includes the Arawa sub basin
2. There is good seismic coverage in the area. Numerous 2-D surveys and one major 3-D survey (Parihaka) have acquired data in the southern half of the study area. These data are generally of good quality.
3. There are 14 exploration wells in the vicinity of the study area. This enables satisfactory ties between seismic reflectors across the area as well as to assign ages to mapped stage boundaries based off the biostratigraphy in these holes.
4. The area includes many various structures, including the Mohakatino Volcanic Centre, the Arawa sub-basin and the Parihaka Fault and associated normal faults.
5. The area has a well preserved Late Miocene to present day sedimentary succession, of which the thick Giant Foresets Formation is a prominent feature

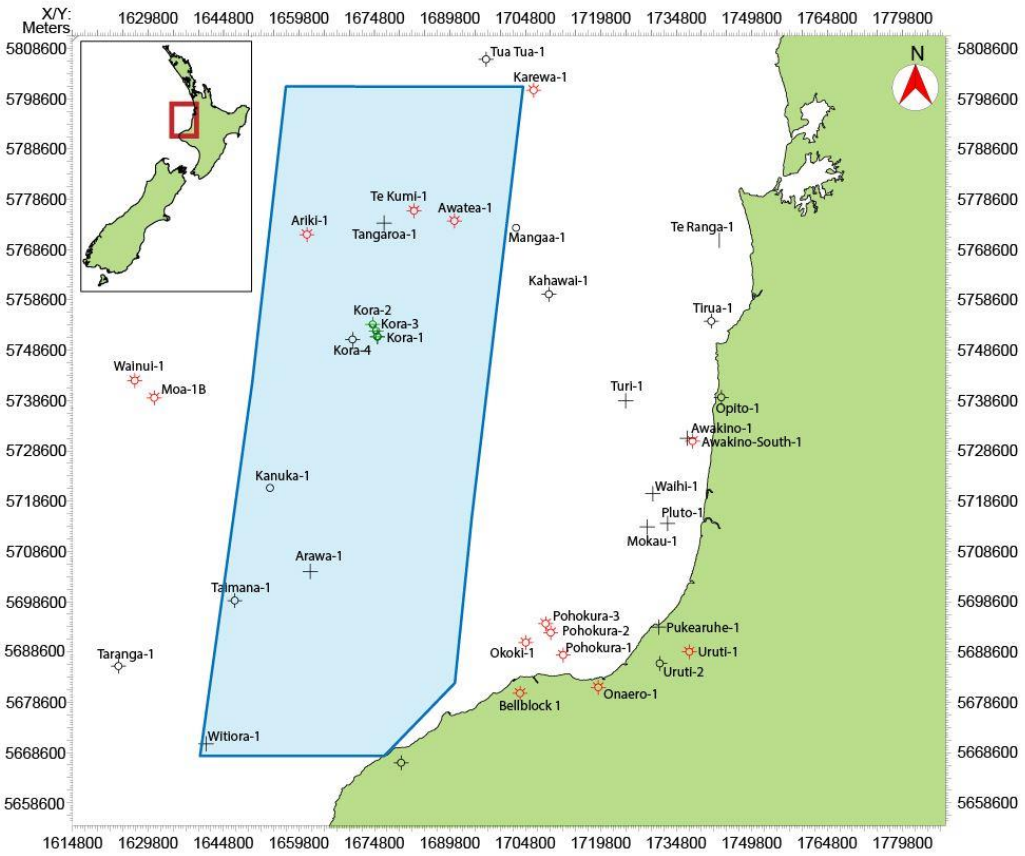

Figure 1.1 Regional Map of offshore Taranaki Basin covering the area directly north of the western Taranaki Peninsula. The study area is outlined by the blue shaded polygon. The locations of the drill holes within the area are also shown.

1.4 Thesis Structure

This thesis has been structured in a way that it covers the objectives listed above. It begins by outlining the geological and tectonic context of Taranaki Basin, followed by the methods used in the study. The stratigraphy of the area is discussed, as is the biostratigraphy (from several sources), focusing on a comparison of the biostratigraphic horizons with the mapped seismic horizons of this study. The geometry of the basin builds on the results of the seismic mapping, while the synthesis merges existing ideas with new ideas proposed in this study, developing the central theme of sediment migration and basin evolution through the Plio-Pleistocene.

Chapter 2: Geological Setting

This chapter outlines the geological setting and tectonic framework of Taranaki Basin, highlighting the important structural regions and the Cretaceous to Cenozoic evolution of the basin, which can generally be separated into three main phases of development.

Hence this chapter will provide a context for the new results presented in this thesis, derived largely from seismic mapping of the Northern Graben and surrounding area.

Chapter 3: Data and Methods

This chapter describes the seismic data and Kingdom SMT software that were used in the investigation. The chapter explains the methods used in seismic mapping from acquisition of seismic surveys, data processing and later seismic line interpretation including seismic facies analysis and production of structure contour and isopach maps. A more detailed methodology for Kingdom SMT is provided in Appendix D.

Chapter 4: Stratigraphy and Biostratigraphy

This chapter describes both the stratigraphy of the study area and biostratigraphy utilized. It briefly covers how biostratigraphy can provide age control for strata in an area, and limitations on the resolution of age from biostratigraphy. This chapter outlines how a practical and fully complete seismic data set was generated for the late Cenozoic section, and then dated using biostratigraphy. This chapter also compares the results of seismic mapping in this investigation with the results of previous investigations.

Chapter 5: Basin Geometry

This chapter outlines the geometry of part of North Taranaki Basin as interpreted from structure contour and isopach maps, and interpreted seismic lines. The chapter is divided into (i) the analysis of key mapped reflectors (structure contour maps of selected horizons) based on Late Cenozoic New Zealand stages, and (ii), an examination of the seismic facies and sediment distribution patterns across the basin from isopach maps.

Chapter 6: Synthesis

This chapter integrates the results reported in preceding chapters and applies them to current thinking. It is mainly concerned with description of the geological history of the basin and how its paleogeography developed.

1.5 References

A reference list of all relevant material used in this study is presented on page ?

1.6 Appendices and Enclosures

Included in the back of this thesis are the following appendices:

Appendix A – New Zealand geological time scale

Appendix B – Seismic lines interpreted in this study

Appendix C – Two way travel time and velocity maps used in the creation of structure contour and isopach maps

Appendix D – Detailed methodology outlining Kingdom SMT and map creation

A CD is included in the pocket at the back of this thesis that contains two large figures presented as Enclosures 1 and 2:

Enclosure 1 depicts a comparison of the mapped stage boundaries from this study and that of Hansen (2003) using biostratigraphic data gathered from several well reports across 14 wells.

Enclosure 2 depicts several seismic lines from the study area showing various structures across the Northern Basin.

2. Geological Setting

2.1 Introduction

Taranaki Basin is a predominantly offshore The Neogene development of Taranaki basin is characterised by subsidence of a foreland basin linked to shortening across the Australia-Pacific plate boundary zone through New Zealand. Later in its history, Taranaki Basin had the Pacific Ocean lithosphere emplaced Cretaceous-Cenozoic sedimentary basin, which initially formed during the Late Cretaceous (Haumurian), following the initial phase of rifting along the New Zealand sector of eastern Gondwanaland and during the early phase (83 Ma) of sea floor spreading in the Tasman sea. The Haumurian rifting essentially initially defined Taranaki Basin. During the Late Palaeocene following the end of sea floor spreading in Tasman Sea (57 Ma), Taranaki Basin developed as a passive margin, characterised by tectonic quiescence, regional subsidence and marine onlap, which continued through to the Early Oligocene. The earliest part of the Oligocene (Lower Whaingaroan) was characterised by paraconformity development over significant parts of Taranaki Peninsula and South Taranaki Basin and minimal sediment accumulation. At the beginning of the Late Oligocene (Upper Whaingaroan) plate motions across New Zealand changed from transtensional to transpressional, causing the initiation of Hikurangi subduction in the eastern Northland and Bay of Plenty areas, and to the south initial formation of the Alpine Fault sector of the Australia-Pacific plate boundary zone beneath it, progressively in a north to south direction (Furlong and Kamp, 2009), and one manifestation of this is the occurrence of mid-Miocene volcanism in Northern Taranaki Basin. This volcanism is still active in the present day in the form of Mt. Taranaki. Another late manifestation of the influence of subduction has been the development of extension, most notably the formation of the Northern Graben during the latest Miocene (Late Kapitean) (King and Thrasher, 1996; Hansen and Kamp, 2004).

This chapter outlines the geological setting and tectonic framework of Taranaki Basin, and the Cretaceous to Cenozoic evolution of the basin. Hence this chapter provides a context for the new results presented in this thesis, derived largely from seismic mapping of the Northern Graben.

2.2. Geological and Structural Setting

Taranaki Basin is located on the western margin of North Island of New Zealand (See Figure 2.1) The basin is primarily a large marine subsurface feature with an area of

approximately 100,000km^2, but also includes onshore areas such as Taranaki Peninsula, coastal regions north of the peninsula extending through to Auckland, as well as the upper reaches of the South Island (King & Thrasher, 1996). Taranaki Basin is bounded to the east by the subsurface Patea-Tongaporutu basement high and the Taranaki Fault, separating the basin from the adjoining King Country and Wanganui Basins (Kamp *et al*., 2004). The western part of the basin has, throughout its entire history, remained open to the sea. Consequently, the western boundary is poorly defined, but is known to extend beyond the present day shelf break in the northwest, before descending into the New Caledonia Basin. To the north, the basin merges into the Reinga-Northland Basin, without an obvious boundary dividing the two (See Figure 2.1). Taranaki Basin lies on the continental Australian plate, and is filled with up to 9 km of Cretaceous to Recent sediment (King & Thrasher, 1996).

King and Thrasher (1996) subdivided the Taranaki Basin into two broad structural regions: The Western Stable Platform and the Eastern Mobile Belt.

2.2.1 The Western Stable Platform

The Western Stable Platform has remained, for the most part, structurally unchanged since the Paleocene aside from subsidence, having not been affected by the shortening along eastern parts of the basin during the Neogene. It is characterised at depth by several preserved half graben structures, formed during the Late Cretaceous rifting, which were concurrently infilled by sediment aggradation, and later (Pliocene-Pleistocene) progradation (King & Thrasher, 1996)

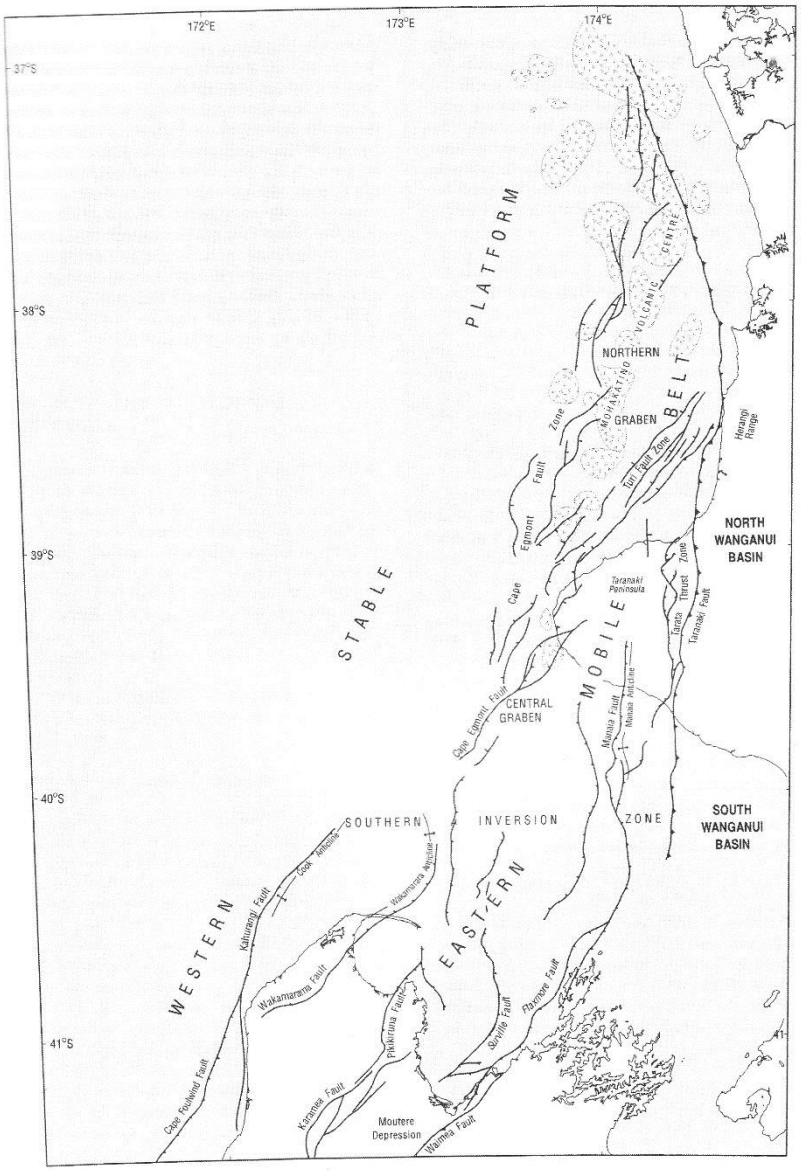

Figure 2.1 Subdivision of Taranaki Basin - Taranaki Basin is separated into four main zones; The Western Stable Platform, Southern Inversion Zone, Central Graben, and Northern Graben. Major fault traces are included. (From: King and Thrasher, 1996).

2.2.2 Eastern Mobile Belt

The Eastern Mobile Belt is a structurally complex zone east of the Western Stable Platform. It can be further divided into two structural sectors comprising various depocentres and sub-provinces which developed under two different tectonic regimes during the Neogene: the Southern Sector (the Tarata Thrust Zone and the Southern Inversion Zone, both formed under a compressional regime), and the Northern Sector (Central and Northern Grabens which formed under an extensional regime) (See Figure 2.1) (King & Thrasher, 1996).

2.2.3 The Tarata Thrust Zone

The Tarata Thrust Zone is a region of north trending en-echelon thrust faults, sub parallel to and located just west of Taranaki Fault, as well as several associated anticlinal structures (See Figure 2.1) These structures formed as a result of crustal shortening across Taranaki Fault zone (initiating during the late Oligocene) and reverse movement along the basin margin on the Taranaki Fault in the Early Miocene (c. 14Ma) (King & Thrasher, 1996).

2.2.4 The Southern Inversion Zone

From the late-Early Oligocene (c. 29 Ma) and throughout the majority of the Miocene, crustal shortening occurred across Taranaki Fault Zone. However, it wasn't until the Late Miocene (c. 10 Ma) that this shortening became regionally more widespread, particularly in the southern half of Taranaki Basin. This caused previously existing normal faults to be reactivated as reverse faults, initiating the uplift of former grabens of Cretaceous-Palaeocene age and the eventual formation of several anticline (inversion) structures (i.e. the Cook, Wakamarama and Maui anticlines) (Vonk & Kamp, 2008).

2.2.5 Central Graben

The Central Graben is a small depocentre, oriented NNE-SSW, which lies south of the Northern Graben (see Figure 2.1). It includes the offshore area directly to the west and south-west of Taranaki Peninsula, as well as sections of the western onshore peninsula itself (NZPAM, 2016). It is bounded by the Cape Egmont Fault to the west. The sedimentary fill within this graben is mainly of post-Mangapanian age (Late Pliocene), making the graben slightly younger than its northern counterpart, in which the oldest sedimentary fill is of Late Kapitean age (King and Thrasher, 1996).

2.2.6 Northern Graben

The Northern Graben is an elongated extensional feature, similar to the Central Graben, also oriented NNE-SSW. Its southern extent is offshore northern Taranaki Peninsula. It is flanked by the Western Platform to the west and the Turi Fault zone to the east, these features providing the ultimate controls on the grabens overall subsidence during the Late Neogene. The northern-most limit is less well defined in literature (See Figure 2.1). Biostratigraphic data from this region supports subsidence during the Late Neogene, as this data suggests that the water depths varied between 1000-1500 m in the Northern Graben during the period of initial graben development (Late Miocene), compared with

the majority of Taranaki Basin, whose water depths varied between 50 m-600 m during this time (King & Thrasher, 1996).

The graben first began to develop during the Late Miocene to the Early Pliocene due to the initial activation of the Kahawai Fault (Hansen and Kamp, 2004) as well as a developing extensional regime in the northern half of the basin. This caused the graben to gradually open up in a triangular wedge like shape (open to the north, eventually generating over 1-3 km of extension in the area over time (Hansen & Kamp, 2004). This shape is thought to be influenced by the clockwise rotation of the Australia plate within the Australia-Pacific plate boundary zone (Giba *et al*., 2010)

The Northern Graben is significant to this study because it has been a major structure attracting sediment through the late Pliocene and into the Pleistocene. It has several distinguishing structural features, including the Mohakatino Volcanic Arc, and the Parihaka Fault/Arawa Sub Basin that impact this study.

2.2.6.1 The Mohakatino Volcanics

The Mohakatino Volcanics are made up of several submarine stratovolcanoes that erupted offshore during the Middle and Late Miocene, forming an arc within and parallel to the Northern Graben (King and Thrasher, 1996) (See Figure 2.1). These volcanoes are either basaltic and/or andesitic in nature, with the magma originating from melting of Pacific Oceanic lithosphere subducted beneath the Australian plate lithosphere (Bergman *et al*., 1992). Active volcanism is thought to have started about 14-11 Ma (Lillburnian through to latest Waiauan) (King & Thrasher, 1996), although evidence suggests there were earlier eruptions that occurred at the Kora volcanic massif around 18-19 Ma (Bergman *et al*., 1992). Eruptions continued through to at least 7-8 Ma (Late Tongaporutuan to early Kapitean) (King and Thrasher, 1996)

2.2.6.2 The Parihaka Fault and Arawa Sub Basin

The Parihaka Fault marks the western margin of the Northern Graben, and is one of the most prominent structures present in the graben at approximately 50 km long. This fault has a complex 3D geometry and is composed up to 5 individual segments of varying lengths, as opposed to one long continuous trace (Giba *et al*., 2012).

Initial displacement on the Parihaka Fault was in response to the west-east extension occurring during the Cretaceous to Paleocene. On seismic reflection profiles, the fault trace strikes north-south to NNW-SSE, is near continuous, and exhibits throws of up to 1800 m in the Late Cretaceous section. The fault was obliquely reactivated during the Early Pliocene around 3.7 Ma, in response to the NW-SE extension occurring in the northern part of the basin at this time. When observing post-Miocene seismic horizons on seismic reflection profiles, the fault trace is seen to be comprised of four parallel segments, with varying strikes from North-South to NNW-SSE. The fault segments in the north show greater vertical displacements than those in the south, with vertical displacements of up to 1450m (Giba *et al*., 2012).

As a result of these displacements on Parihaka Fault, a sedimentary depocentre formed on the eastern side of this fault. This depocentres has recently been informally named the Arawa sub-basin, and is a crucial part of this study in relation to the development of the Northern Graben and overall sediment deposition patterns through time.

2.3. Paleogeographic Maps

Paleogeographical maps of Taranaki Basin presented in this section have been reproduced from Strogen *et al.*, 2011. These maps illustrate sediment pathways, ancient shorelines, and water depths in the basin at various times during the Miocene through to the Pleistocene. The eight maps depicted are as follows: 15.5 Ma, 12 Ma, 7.2 Ma, 5 Ma, 3.3 Ma, 2.7 Ma, 1.6 Ma, and Present Day. These maps represent the best matches to the ages of the horizons mapped in this study - 7.2 Ma (Early Kapitean Stage), 5.3 Ma (Early Opoitian Stage), 3.6 Ma (Early Waipipian Stage), 2.4 Ma (end of the Mangapanian Stage and start of Nukumaruan Stage) and 1.63 Ma (Start of Castlecliffian Stage). The 15.5 Ma and 12 Ma maps have also been included as these ages coincide with the onset of Mohakatino Volcanics (~14-11 Ma), a prominent structural feature in the area of study.

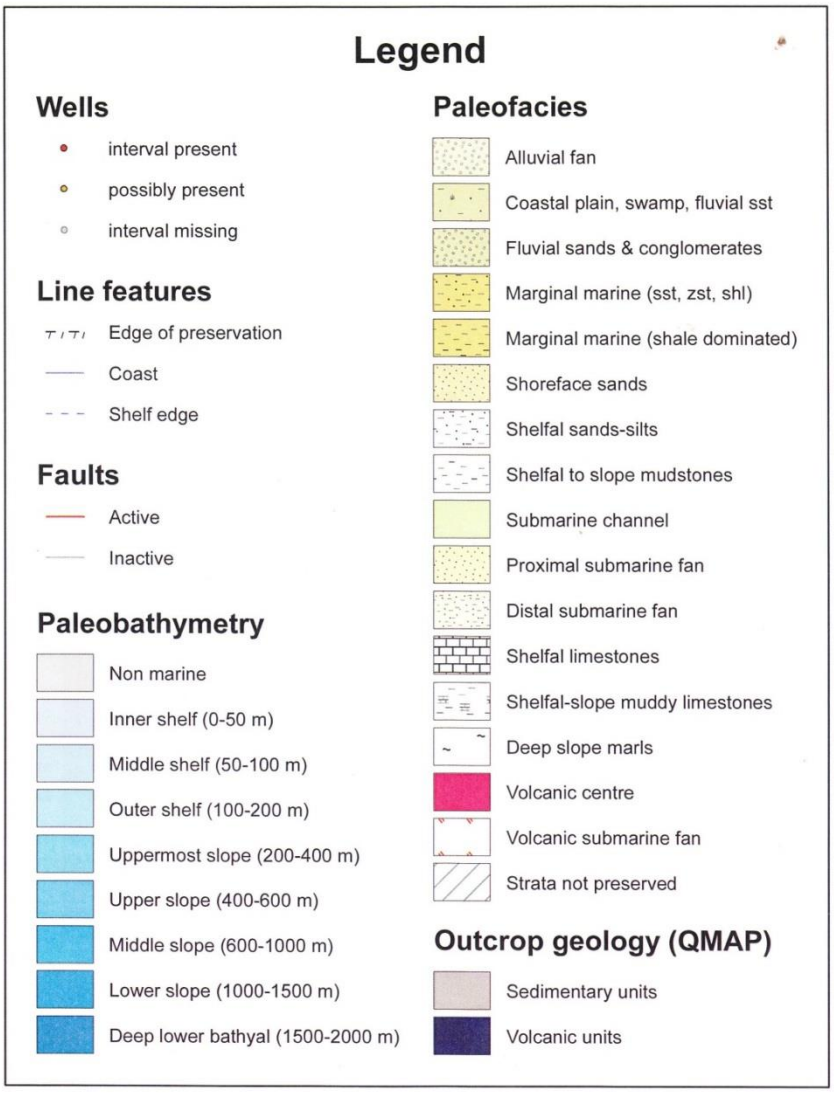

Figure 2.2 Legend for the paleogeography maps presented in the following figures (2.3-2.6) (From: Strogen et al., 2011).

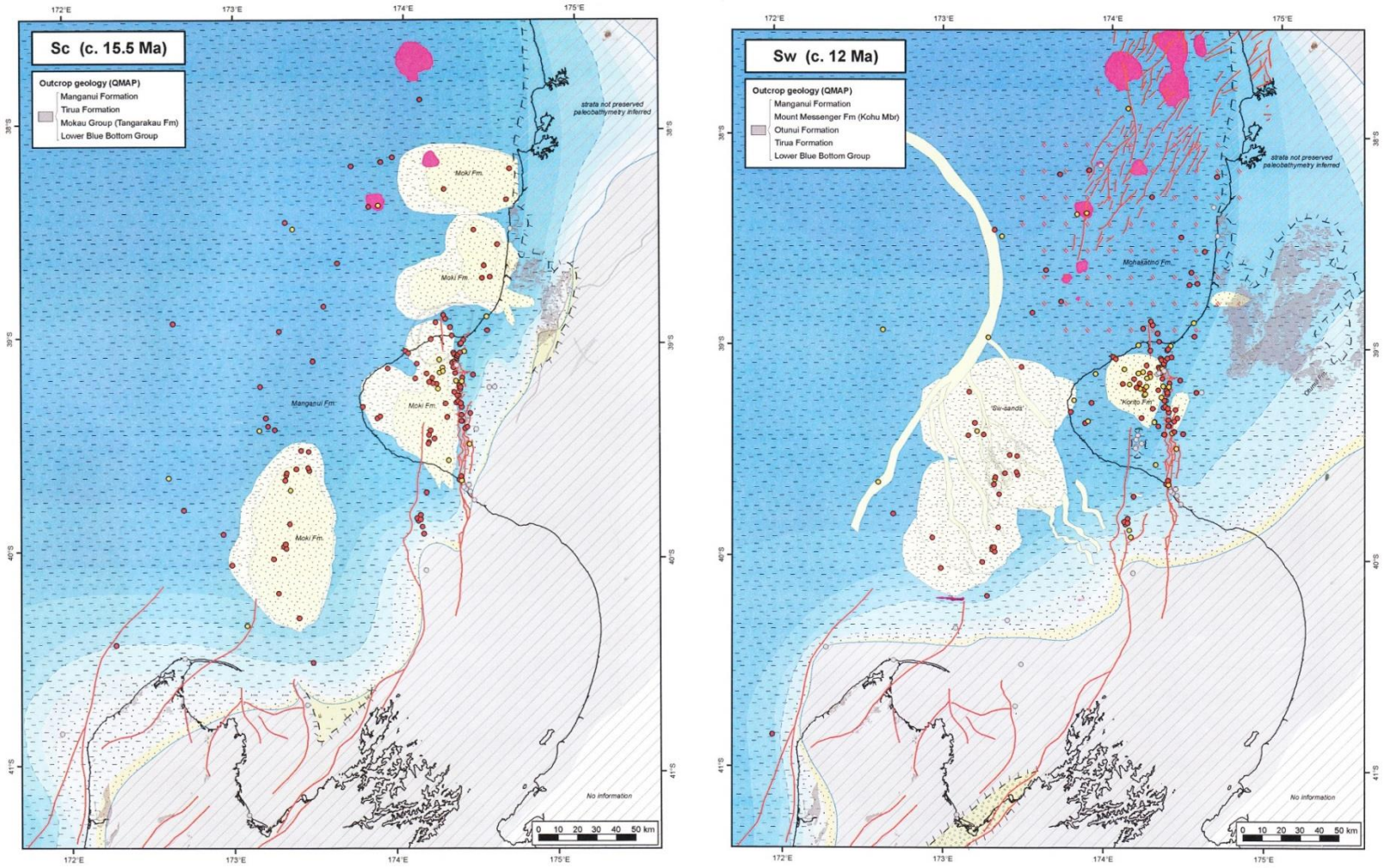

Figure 2.3 – (Left) Paleogeography map of 15.5 Ma. (Right) Paleogeography map of 12 Ma. (From: Strogen et al., 2011).

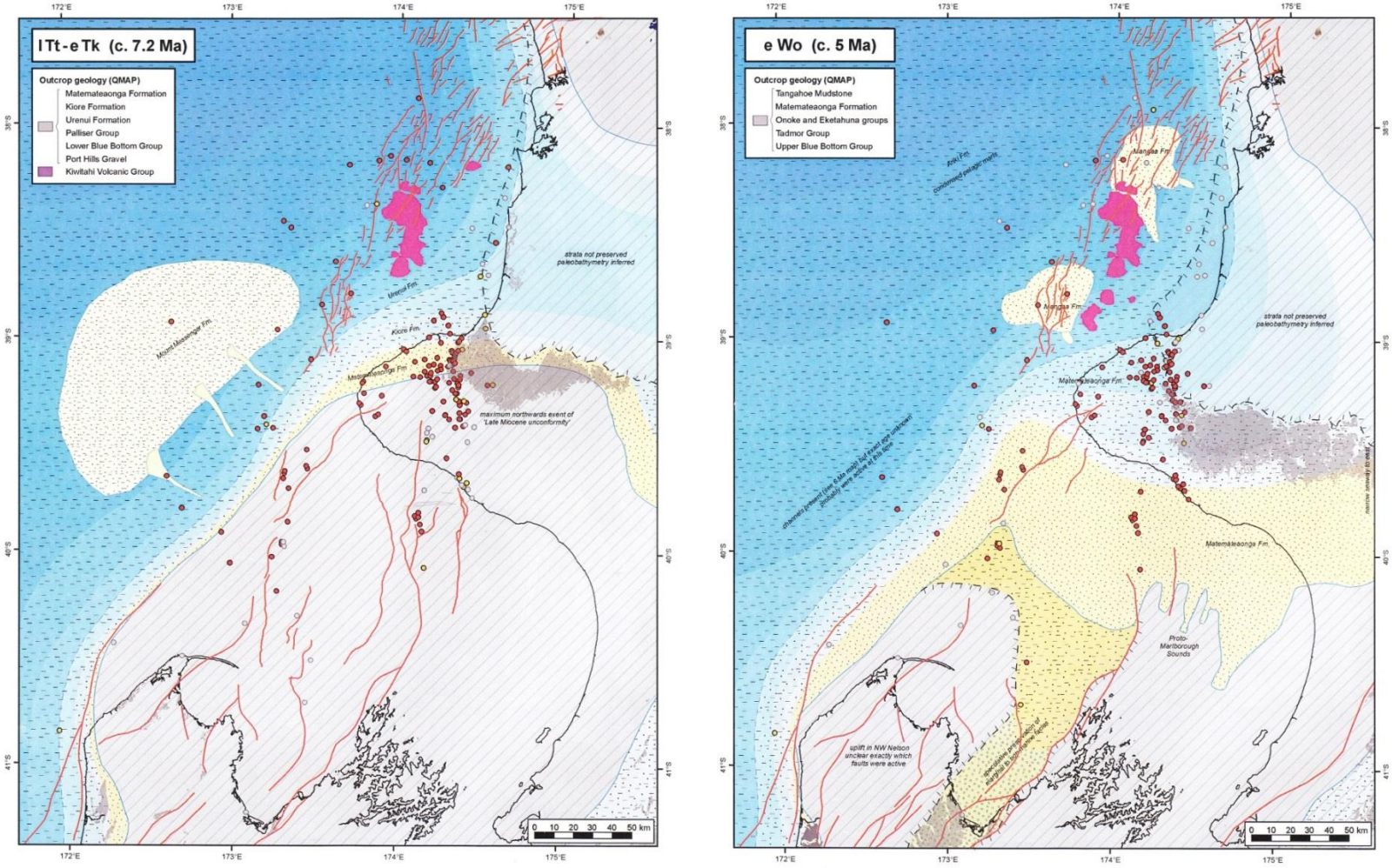

Figure 2.4 – (Left) Paleogeography map of 7.2 Ma. (Right) Paleogeography map of 5 Ma. (From: Strogen et al., 2011).

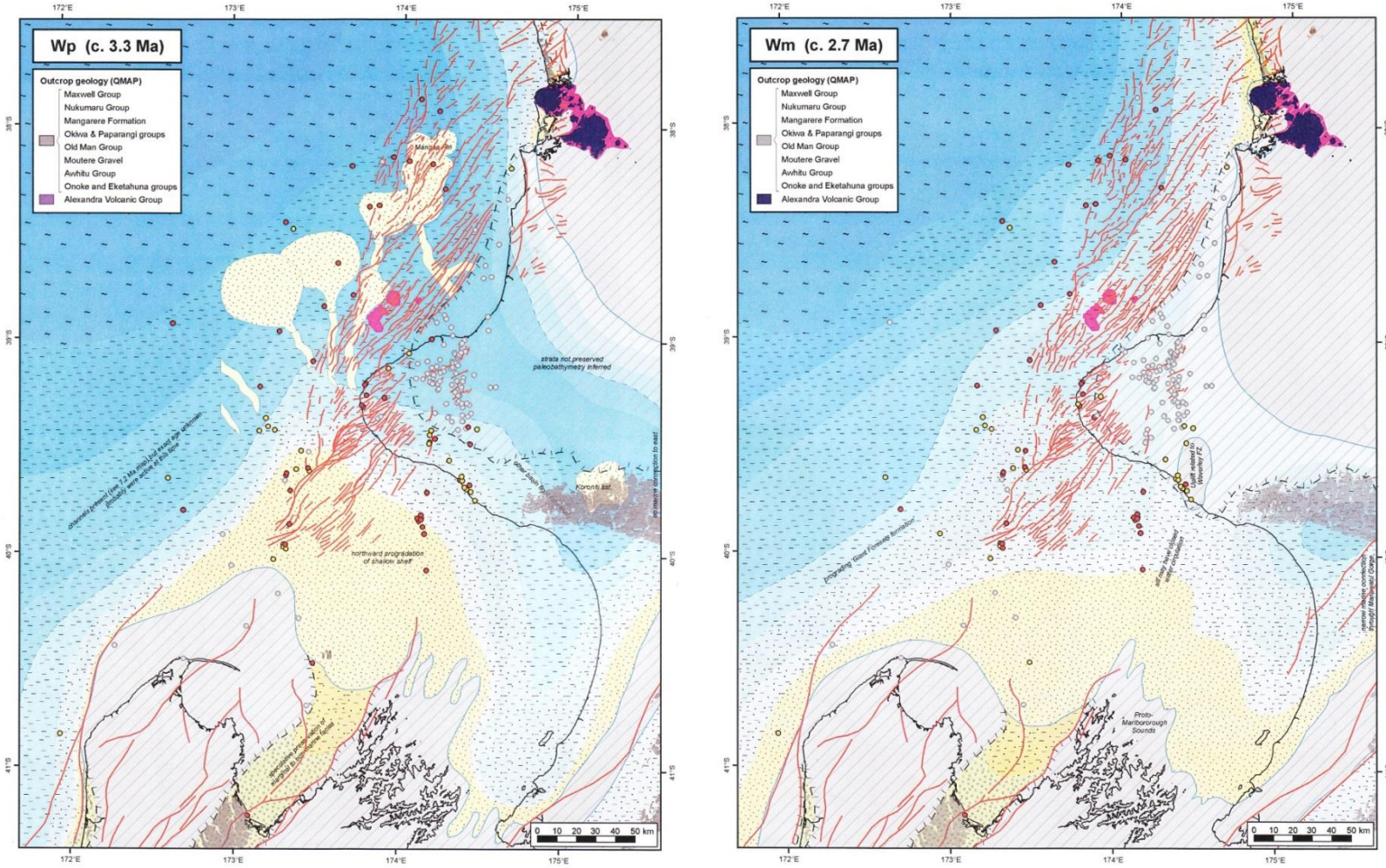

Figure 2.5 – (Left) Paleogeography map of 3.3 Ma. (Right) Paleogeography map of 2.7 Ma. (From: Strogen et al., 2011).

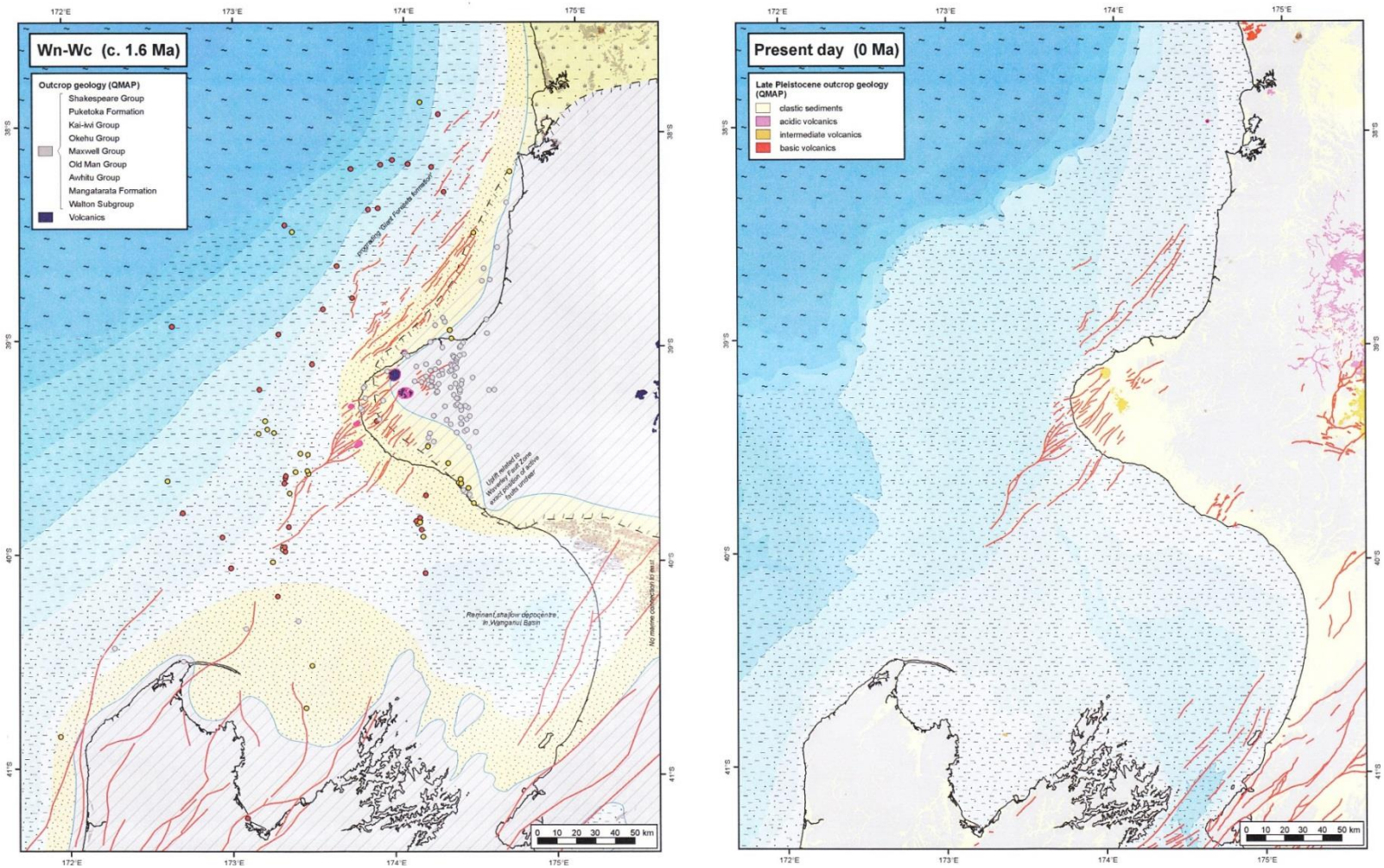

Figure 2.6 – (Left) Paleogeography map of 1.6 Ma. (Right) Paleogeography map of 0 Ma. (From: Strogen et al., 2011).

2.4 Late Cretaceous to Cenozoic Development of Taranaki Basin

The overall development of Taranaki Basin since its initial formation in the Late Cretaceous has been complex, but can generally be separated into three main phases of development (Giba et al., 2010).

Following the end of rifting (Late Paleocene), Taranaki Basin evolved into a passive margin basin and tectonic activity was relatively quiet, apart from regional subsidence and basin wide transgression (Thrasher, 1992). Ongoing subsidence throughout the Late Paleocene and Eocene resulted in an overall deepening across the basin with accumulation of shelfal Turi Formation across much of the southern extent of the basin (See Figure 2.7) (King and Thrasher, 1996).

The beginning of the Late Oligocene (Early to Late Whaingaroan stage boundary, 30-29 Ma) plate motion across New Zealand changed from transtensional to transpressional, and this was reflected in the start of substantial overthrusting of basement into eastern Taranaki Basin (Furlong and Kamp, 2009). This is reflected in the thickness of the Otaraoa Formation (Late Whaingaroan) east of Taranaki Fault in the Taranaki Peninsula area. This sedimentation is mainly calcareous mudstone, later becoming more calcareous (Tikorangi Formation) (Ngatoro Group), and then transitioning back to marl (Taimana Formation) (See Figure 2.7).

Although reverse/thrust faulting on Taranaki Fault was underway at the start of the Late Whaingaroan, it became more marked during the Waitakian Stage, resulting in uplift of the Patea-Tongaporutu Herangi High during this time (Kamp et al., 2004). This movement continuing into the Otaian has resulted in approximately 12-15 km westward displacement of basement over Paleogene strata along the eastern margin of the Taranaki Basin (King, 1989; King and Thrasher, 1996; Kamp et al., 2004; Tripathi and Kamp, 2008). The main effect of continued basement overthrusting in the Late Oligocene and into the Early Miocene was lithospheric loading of the Australian Plate resulting in the development of a foreland basin due to the resultant plate flexural subsidence. During the Altonian (Late Early Miocene about 19 Ma), sediment accumulation started progradation of the basin fill, which continues today (King and Thrasher, 1996).

The main influx of terriginous sediment started during the Late Waitakian and Early Otaian and drove a change from carbonate-dominated sedimentation to terriginous-dominated sedimentation within Taranaki Basin which is representative of the initiation of Wai-iti Group deposition (King & Thrasher, 1996). This includes the deposition of the Manganui

Formation, a bathyal mudstone which is up to 1000 m thick and major interbedded sandstone/mudstone complexes (Moki and Mt Messenger Formations) which were mass emplaced as prograding slope deposits (See Figure 2.7). Increasing sediment supply and lower rates of subsidence during this time is representative of a change from marine transgression to regression and an extended period of north westward progradation of the continental margin sedimentary wedge (King and Thrasher, 1996).

During the Middle to Late Miocene (c. 10 Ma), shortening across southern North Island reactivated Late Cretaceous – Palaeocene normal faults in a reverse sense in southern Taranaki Basin leading to the development of inversion structures. These also developed in the Taranaki Peninsula to North Taranaki transition (Mokau and Pohokura anticlines) (King and Thrasher, 1996).

Shortening within the northern part of the basin (i.e. the reverse faulting on Taranaki Fault) ceased by the Middle Miocene (Hansen and Kamp, 2004), although crustal shortening continued in the southern part of the basin. As the northern part of basin changed from a convergence to extension, normal faults developed (~ 12 Ma; Giba et al., 2010 but probably at a younger time), and the Northern and Central grabens were formed. Most of the normal faults had minimal offset, with exception of the faults within the Cape Egmont Fault Zone, and Parihaka and Kahawai faults.

The timing of extension followed the main phase of eruption of submarine stratovolcanoes of the Mohakatino Volcanic Centre (Middle to Late Miocene at approximately 14 Ma (Giba et al., 2010), but continued concurrently through to later parts of volcanism (7-8 Ma). The volcaniclastic sediments associated with Mohakatino Volcanics (Mohakatino Formation) interfinger with siliciclastic sediment of Manganui Formation and Mt Messenger Formation (See Figure 2.7) (King and Thrasher, 1996).

By the Late Miocene and during the Pliocene, a marl known as Ariki Marl accumulated over parts of the Western Stable Platform (See Figure 2.7) (Hansen and Kamp, 2004). The accumulation of this marl is significant in that it indicates that the large volumes of sediment eroded off the emerging Southern Alps during this time did not reach the northern part of Taranaki Basin (Vonk and Kamp, 2008). As a result, Northern Taranaki Basin was starved of sediment during this time. This lack of sediment can be directly attributed to the majority of the sediment being tied up instead with the accumulation of the thick Kiore and Matemateaonga formations in both King Country and Wanganui Basins during the Late Miocene and Early Pliocene, with only limited progradation into

the Northern Graben area (Mt Messenger fans) (Hansen and Kamp, 2002). It could also be linked with the termination of active volcanism from the Mohakatino volcanic arc sometime in the Late Miocene, which would have reduced the amount of local volcaniclastic sediment to the area (Hansen and Kamp, 2004).

During the Early Pliocene (Opoitian Stage), sandy sediments sourced from uplift and erosion of Southern Alps accumulated in the Northern Graben. These submarine fan deposits are known as Mangaa Formation (See Figure 2.7). These deposits are limited to lie within the fault-bounded graben. They lie east of the mostly extinct Mohakatino Volcanic centre, which provided an upstanding physical barrier to their dispersion in the west. These factors acted to control the sediment pathway and areas of accumulation (Hansen and Kamp, 2004). Accumulation of these submarine fans within the graben continued into the Mangapanian Stage, when sedimentation rates started to surpass the accommodation space in the graben. As a result, the graben was rapidly infilled and eventually overtopped during the latest Pliocene (Nukumaruan). This was followed by progradation of the Giant Foresets Formation (the uppermost stratigraphic unit which underpins the modern shelf and slope) across the northern part of the Western Stable Platform (See Figure 2.7) (Hansen and Kamp, 2002).

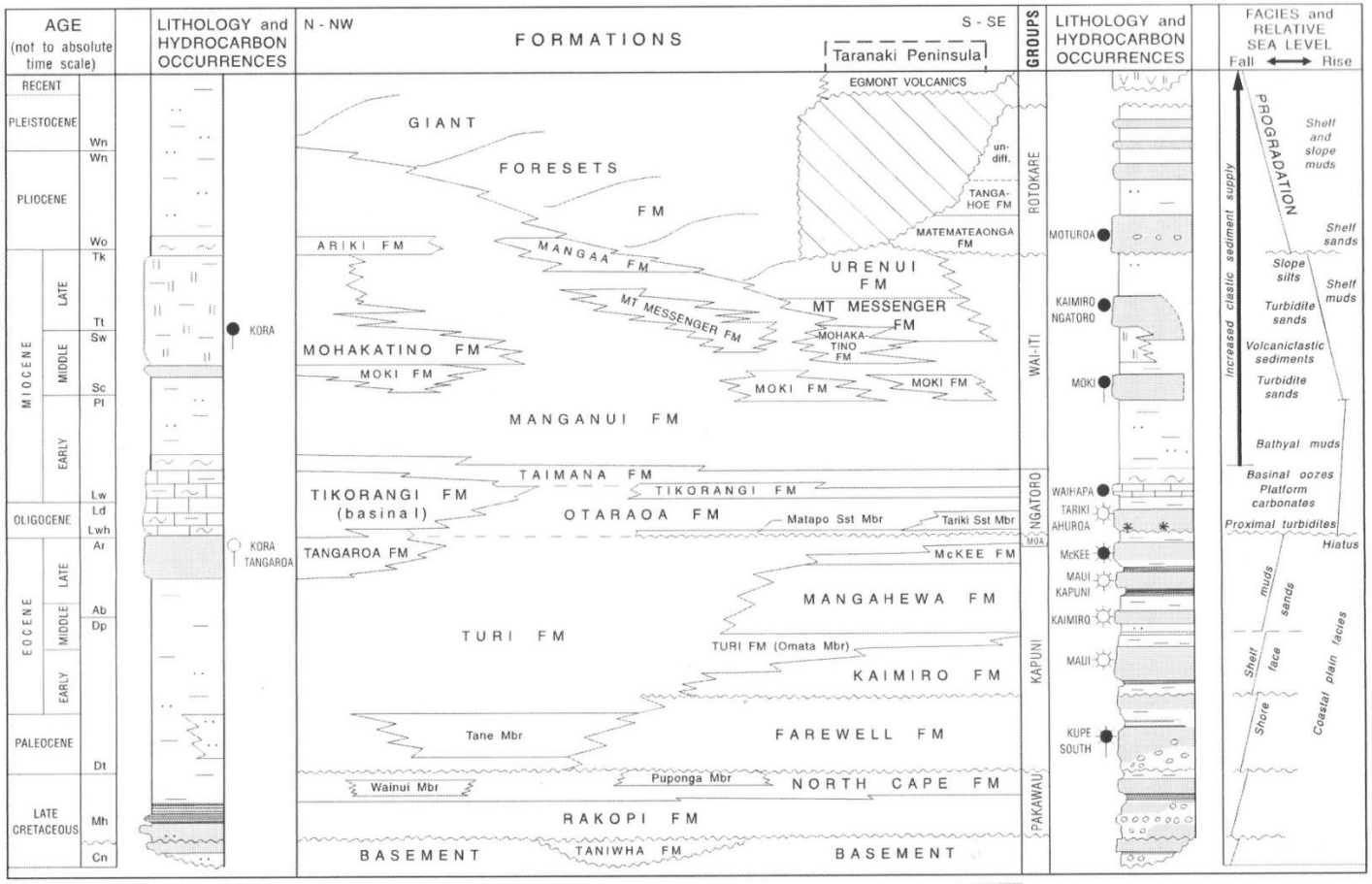

Figure 2.7. Cretaceous - Cenozoic sediment fill and stratigraphic architecture for Taranaki Basin. Not to scale. (From: King and Thrasher, 1996: Fig. 4.1).

3. Data and Methods

3.1 Introduction

The seismic mapping undertaken in thi ect was completed using Kingdom SMT software (2D/3D EarthPAK version 8.5), a program that was provided to the University of Waikato under an Academic License in 2010. The seismic data used in this study, comprised of extensive 2D and 3D surveys, was made available to the University of Waikato by New Zealand Petroleum and Minerals (NZPAM) in the 2015 New Zealand Petroleum Exploration data pack. In this study, 175 2D seismic lines and one 3D seismic survey (Parihaka-3D) were utilized.

Fifteen drill holes/wells were used in this thesis to tie the stratigraphy to the seismic data. These included Arawa-1, Ariki-1, Awatea-1, Kanuka-1, Kora-1, Kora-2, Kora-3, Kora-4, Taimana-1, Tangaroa-1, Te-Kumi-1, and Witiora-1, all of which lie inside the confinements of the study area, as well as Kahawai-1, Mangaa-1, and Wainui-1, which lie outside of the boundaries of the study area. The main biostratigraphic control for this study was provided by three of these wells (Arawa-1, Ariki-1, and Kora-1), which, along with the other afore-mentioned wells, enabled ties to be made to the seismic data. These three wells were the main ones analysed biostratigraphically by Hansen (2003) as reported in Hansen and Kamp (2004). Biostratigraphy for other wells was entered into Kingdom™ manually from various open file petroleum reports, which are listed in the references section of this thesis and illustrated in Enclosure 1.

Figure 3.1 depicts a map of the study area studied in relation to the New Zealand coastline. This map includes a polygon showing the boundaries of the study area, the distribution of both the 2D seismic lines and a 3D seismic survey, as well as the physical location of the fourteen wells inside the study area; Kahawai-1 and Mangaa-1 lie just to the east of the study area boundary. The other wells displayed are not utilized in this study.

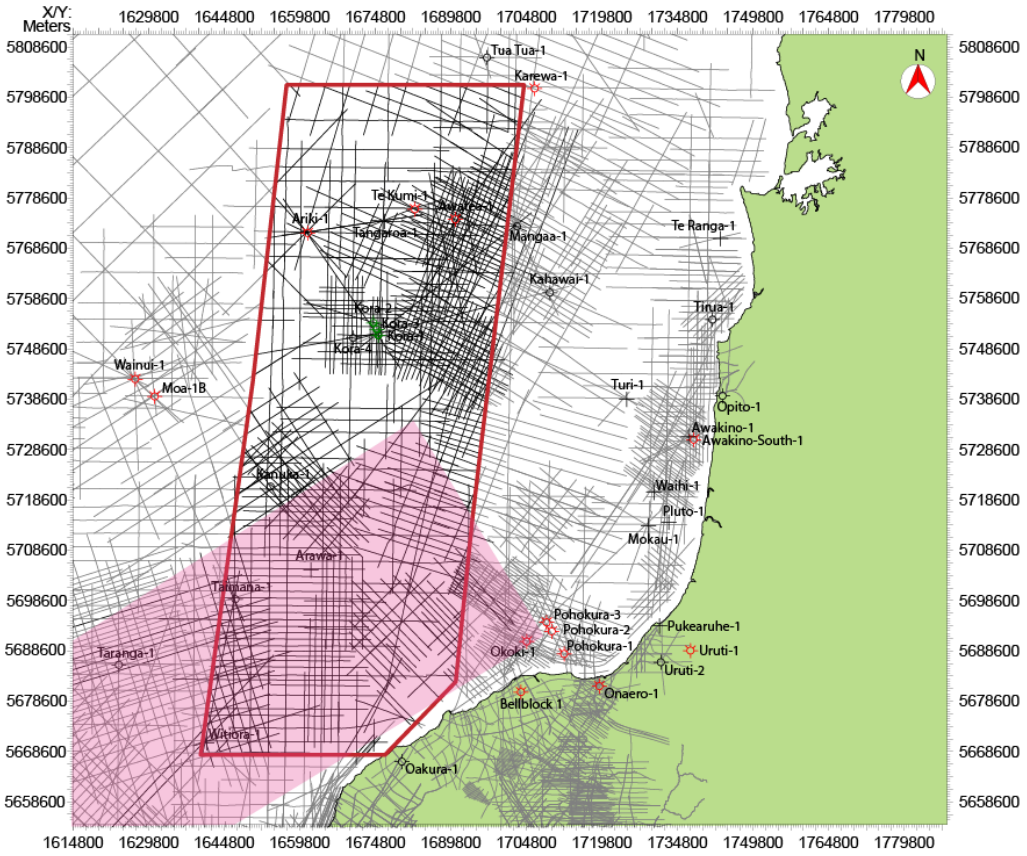

Figure 3.1 Locations of 2D seismic lines (grey) and single 3D survey (pink) used in this study. Drill holes and their various locations are also shown on the map.

3.2 Introduction to Seismic Reflection Surveying (Data Acquisition)

The main purpose of a seismic reflection survey is to essentially map the subsurface to show both the stratigraphy and structure of a basin, either onshore or offshore, in order to establish potential locations for hydrocarbon exploration wells in an area (Ashcroft, 2011).

In this study, seismic data were acquired by various petroleum companies through both 2D and 3D marine seismic surveys in offshore Taranaki Basin. In a marine seismic reflection survey, long floating cables called 'streamers' are laid off the back of a large vessel and are towed for long distances in a straight line. In 2D surveying, one cable is usually employed; whereas in a 3D survey, multiple streamers are laid down to provide a more detailed output over a greater area (Krohn, 2009). Sensitive receivers called hydrophones are attached to and are evenly spaced along these cables. Acoustic sources, usually in the form of airguns, are towed in front of these streamers, which release compressed air into the water every 15-20 seconds creating numerous sound wavelets. These wavelets travel down through the water and into the subsurface, where they can

penetrate the rock up to several thousand kilometres deep. As these waves reach the various boundaries between different sedimentary rock layers in the earth, the waves are reflected back to the surface as echoes where they are captured by the recording sensors (see figure 3.2). The time it takes for the wave to travel from the source and return to the hydrophone is recorded in two way travel time (TWT), and it is from this information that a seismic image is then produced, in which it is possible to depict the various layers, structures and potential hydrocarbon prospects in the rock (Ashcroft, 2011)

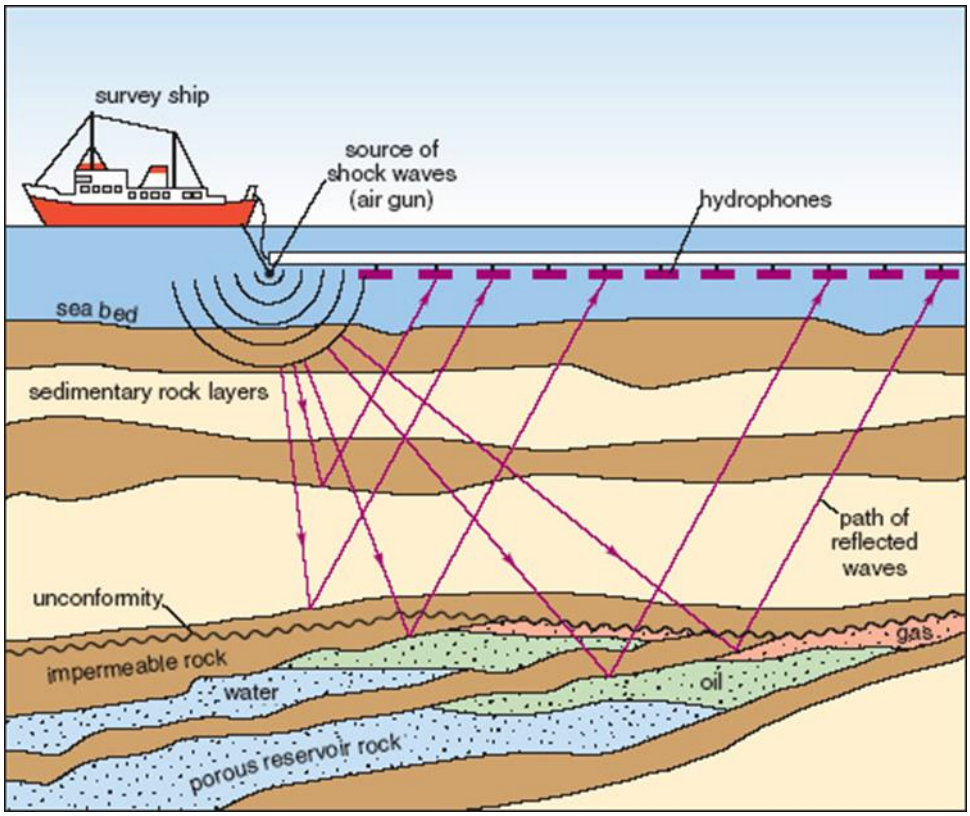

Figure 3.2 Image depicting the methods of a marine seismic survey (Sourced from EPA, 2011).

3.3 Data Processing

Seismic data processing involves the manipulation of measured raw data, so that errors are reduced, subsurface structures and reflection geometries become more apparent, and therefore a more enhanced and accurate seismic image can be produced for later interpretation. There are a series of steps that are carried out to process seismic data both on land as well as offshore, which include Velocity Analysis, Common Mid-Point (CMP) sorting/stacking and Normal Move-Out correction (NMO).

3.3.1 Velocity analysis

Velocity is determined as the rate at which a wave travels through a medium (Schlumberger, 2016). It is an important measurement that is used in data processing, as both stacking and time/depth migration require accurate velocity measurements. However, velocity does not remain constant with increasing depth. Sediment compaction and increasing pressures cause velocities to increase when passing through the deeper subsurface, as opposed to travelling slower nearer the surface. Velocity also varies with the changing densities of different lithologies. Velocity analysis is therefore the process of calculating these changes in velocity, which occurs commonly through Common Mid-Point sorting (CMP) and Normal Move Out corrections (NMO) (Schlumberger, 2016).

3.3.2 CMP Sorting/Stacking and Normal Move Out Correction

The common mid-point (CMP) is a point which is located halfway between the source and the receiver. When multiple sources and receivers are used and are spaced out correctly, it is likely that more than one trace will share the same midpoint. A trace is Earth's response in time to each individual seismic wave passing from the source, through the subsurface layers, and back to the receiver (Schlumberger, 2016).

The only difference between these traces is the varying distance between source and receiver (offset), which causes a delay in the arrival times of a reflection. This effect is known as 'Normal Moveout', and observed on an offset vs arrival time plot as a hyperbolic shape (see Figure 3.3). In this instance, 'Normal Move Out correction' (NMO) is used to remove the effect of this offset, so that multiple traces can be stacked on top of each other to reduce noise, enhance the signal and improve overall data quality (see Figure 3.3) (Schlumberger, 2016).

The processing of seismic lines for later interpretation is complex, and is completed by a geophysicist. All seismic processing corrections were done prior to receiving the seismic data used in this study.

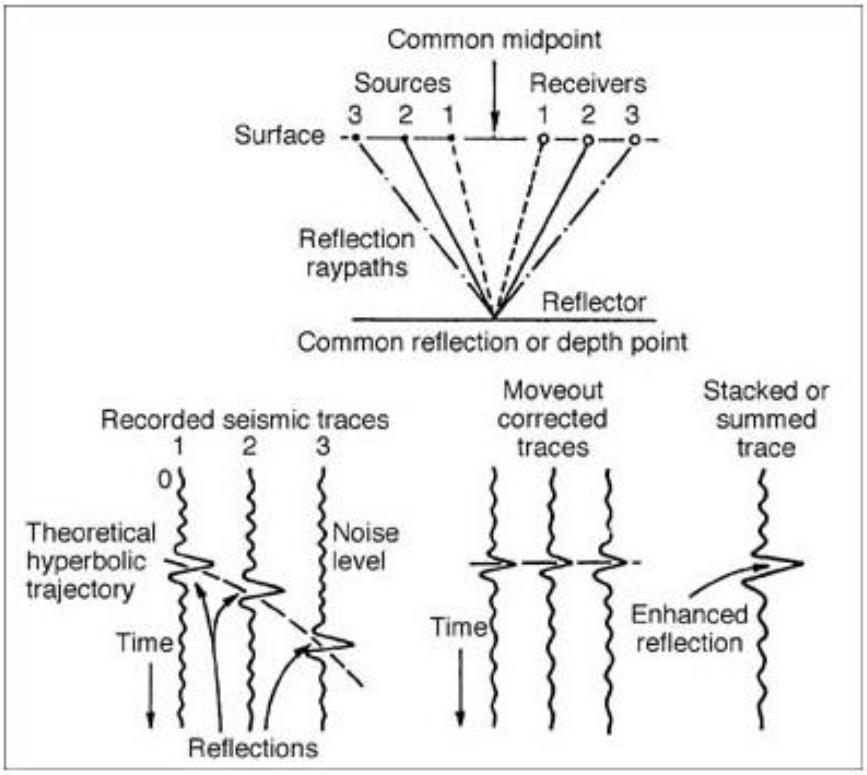

Figure 3.3 Image showing the main steps of data processing (Schlumberger, 2016).

3.4 Principles of Seismic Stratigraphy and Facies Analysis

Seismic reflectors are created due to impedance changes along stratal boundaries (bedding planes) or unconformities within the subsurface rocks. Seismic stratigraphy makes use of the varying patterns of these seismic reflections, in conjunction with other data, to determine stratigraphic interpretations. These include identifying depositional sequences, predicting the lithology and stratification from seismic facies, as well as analysing relative changes in sea level to help determine paleoenvironments (Vail and Mitchum, 1977).

A seismic facies is defined as a constrained group of seismic reflections whose internal structures and physical features are different from others in a sedimentary succession. Seismic facies analysis therefore, involves examining these varying facies in order to assist with overall geological interpretation. The characteristics that can be used to distinguish different seismic facies from each other include reflection configuration, reflection continuity, frequency, amplitude, internal velocity, and external 3D form (Mitchum *et al.*, 1977).

Reflection configuration signifies the type of stratification and therefore helps to provide a basic geological interpretation of depositional energies and processes, as well as paleoenvironments. Reflection continuity is indicative of lateral continuity and analogous depositional processes. Seismic amplitude looks at the differences in impedance between reflectors, usually resulting from a change in lithology or cementation. Used in conjunction with frequency, fluid content, bed thickness and the type of lithology change in the facies package is able to be inferred (Schroeder, 2004). A change in density causes variation with internal velocities and therefore provides information on both lithology and porosity of strata. External geometries can be worked out by mapping the boundaries of the stratal packages and producing isopach maps, which can also provide information about the source of sediment and the overall geological setting (Mitchum *et al*., 1977)

It is this method that has been used to help describe the geometry of the basin in the study area, in a later chapter of this thesis.

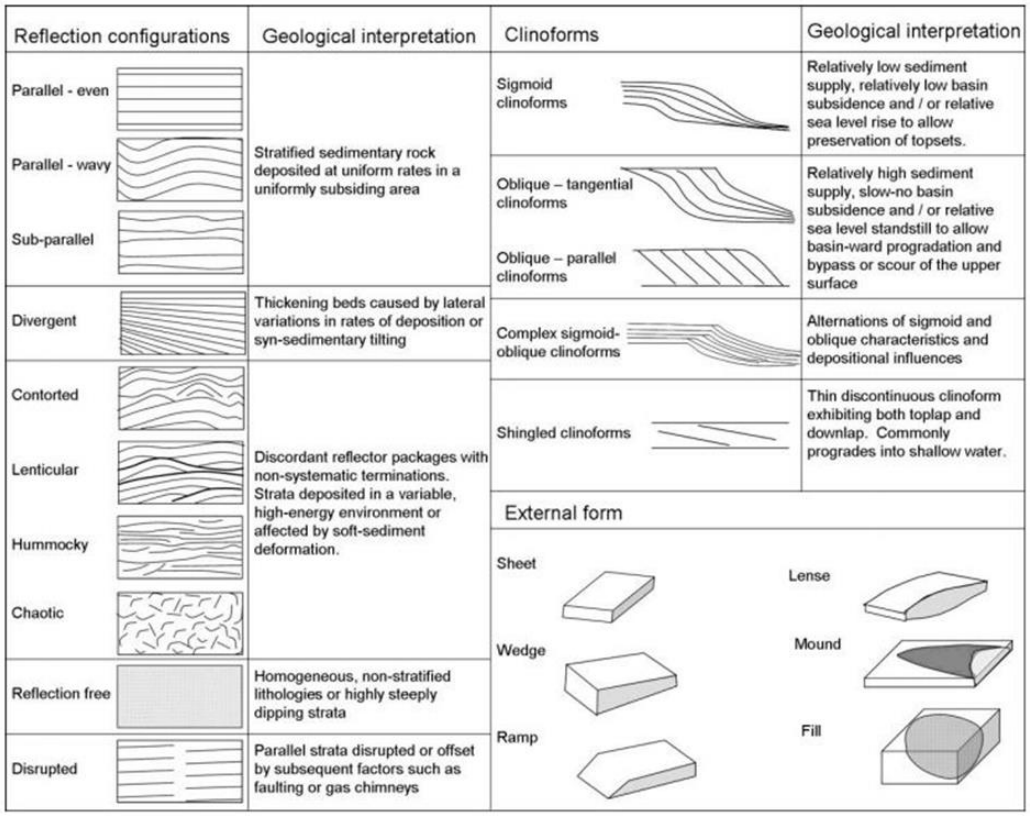

Figure 3.4 Configuration of typical reflection patterns and associated geological interpretations and 3D external forms (From Grain, 2008. Figure 4.2, after Mitchum et al., 1977. Figures 4, 6, 9, 11 and 12).

3.5 Seismic Interpretation of the Study Area, Late Miocene-Pleistocene

Seismic interpretation in this study involved the mapping of several seismic reflectors, each reflector selected on the basis of biostratigraphic (NZ stage boundary) control, across the area of interest, in order to create several maps that show deposition over time. The fundamental objective of these maps is to help establish the geological development of North Taranaki Graben and the deposition patterns of the sediment in the surrounding areas from the Late Kapitean stage through to the Present Day. Detailed methods and procedures for the creation of these maps in Kingdom™ software, including time grids, structure contour maps, velocity maps, and isopach maps, with their manipulation in both ArcGIS and Adobe Illustrator, are included in Appendix D.

The following section lists the basic steps that were taken to interpret the seismic grid in the study area:

- Drill hole data, primarily biostratigraphic stage boundary determinations and their corresponding depths, were gathered from several sources and then entered into relevant wells in Kingdom™. Time depth curves for each of the relevant wells, along with formation tops, had been loaded into Kingdom software beforehand through previous seismic work completed by Lyon (2015).

- Horizon interpretation was initially undertaken between wells for which there was confident biostratigraphic control. Standard seismic line interpretation techniques of intersecting ties and loop ties were used to extend this horizon mapping across the entire study area. Any faults observed were also defined.

- Structure contour maps of each stage boundary were created in TWT time using an in-built gridding function. The maps were constrained via a predefined polygon (study area boundary), and maps were then contoured using suitable contour spacing, of either 50 or 100m, depending on the detail required.

- Fault polygons were constructed to illustrate areas of faulting along with the nature (primarily relative size and orientation) of said faults. The width of the polygon essentially shows the width of the fault offset.

- Velocity maps were constructed for each stage, again by means of an in-built function. The velocity maps were then used to convert the TWT structure contour maps into depth structure contour maps.

- Isopach maps of each biostratigraphic stage were similarly created using an in-built mapping function in Kingdom™ software. The function generated an internal velocity map between stages which allowed the difference between structure maps to be determined, thus resulting in a map depicting the thickness of the deposited sediment through a specific stage.

The geological time scale used to determine the most recent/current numerical age for each Stage boundary is given in Appendix A, and the utilized drill hole data used for this determination is shown in Appendix B. All of the seismic lines interpreted in this study can be found in Appendix C, and further detailed methods and data manipulation are outlined in Appendix D

3.6 Summary

Seismic data is dealt with in three main steps: Firstly, the raw seismic data are acquired through numerous seismic reflection surveys. Secondly, the raw data are processed though several methods so that a more enhanced seismic image can be generated. Finally, the images produced are interpreted, dependent of the requirements of the study.

In this study, seismic data were acquired by various petroleum companies through both 2D and 3D marine seismic reflection surveys in offshore Taranaki Basin; the processing of the data had been completed prior to the data being available for this study. The interpretation of the data involved the mapping of several seismic reflectors, each reflector selected on the basis of biostratigraphic control, in order to create several maps that show deposition of sediment over time. These maps include time grids, structure contour maps, velocity maps, and isopach maps. The seismic mapping undertaken in this project was completed using Kingdom SMT software, utilizing 175 2D seismic lines, and one 3D seismic survey (Parihaka-3D).

DISCLAIMER: The purpose of this study was to use seismic data to attempt to understand the formation and stratigraphy of the Northern Taranaki Graben and its subsequent sedimentary patterns through time. This research required only a simple understanding of seismic processing and interpretation, as well as a basic knowledge of how the Kingdom software works. Consequently, the maps and figures produced in this thesis, along with their interpretations, are conceptual, and should not be used in carrying out in depth basin analysis or to assist in the search for hydrocarbons.

4. Stratigraphy and Biostratigraphy

4.1. Formational Stratigraphy

4.1.1 Manganui Formation

The Manganui Formation is a widespread calcareous mudstone that dominated Miocene deposition within Taranaki Basin (King and Thrasher, 1996). The Early Miocene was a period of substantial subsidence within the basin, and as a result, a large amount of accommodation space was generated. The Manganui Formation was deposited into this newly-created space, mostly at bathyal depths (Hansen and Kamp, 2004). Within the study area, the Manganui Formation is predominantly seen in the south west, in the vicinity of Arawa-1 and Taimana-1. It is depicted on wireline logs by a relatively featureless GR and SP signal (typical of mud-dominated lithologies), and is, on average, approximately 700 m thick in well holes (Enclosure 1). However, in the northwest, (Ariki-1), the Manganui Formation interfingers with the volcaniclastic sediments of the Mohakatino Formation, and these two formations are difficult to distinguish from each other in seismic profiles. This composite formation is referred to as the Upper Manganui/Mohakatino Formation (King and Thrasher, 1996), and is overlain in the study area by either the Ariki Formation or the Giant Foresets Formation (Enclosure 1 and Figure 4.1).

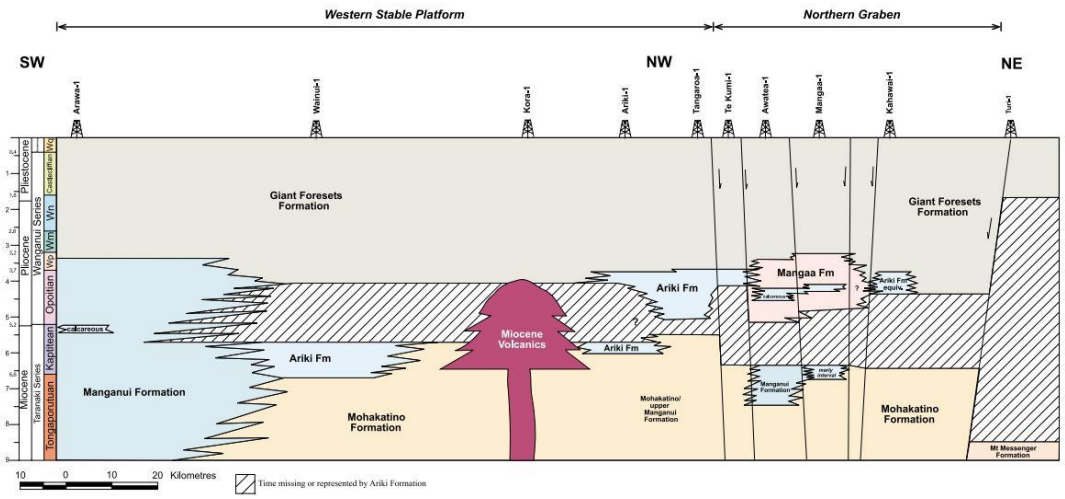

Figure 4.1 Chronostratigraphic panel representing Northern Taranaki Basin. Stage abbreviations; Wq – Haweran, Wn – Nukumaruan, Wm – Mangapanian, Wp – Waipipian (from Hansen and Kamp, 2002).

4.1.2 Urenui Formation:

The Urenui Formation is an upper slope to bathyal fine-grained siltstone facies (Vonk and Kamp, 2008). It is a lateral correlative of Upper Manganui Formation slope deposits, and it is therefore often hard to differentiate between the two (King and Thrasher, 1996). In the study area, the Urenui Formation is only found in the south west (Kanuka-1). On the wireline logs, it is depicted by a similar wireline facies to the Manganui Formation and is approximately 300 m thick in Kanuka-1 (Enclosure 1). It is overlain by the Ariki Formation.

4.1.3 Mohakatino Formation:

The Mohakatino Formation is composed of volcaniclastic (andesitic) siltstone, mudstone and sandstone. This formation is also inclusive of the now buried andesitic volcanic edifices (Mohakatino Volcanic Centre) from which the volcaniclastic material was sourced (King and Thrasher, 1996). In the study area, the Mohakatino Formation is found in the northern and north eastern regions, proximal to the volcanic centres, as well as on the flanks of the volcanic structures. The formation is present in Tangaroa-1 and Te Kumi-1, but is also present in Ariki-1 as the Upper Manganui/Mohakatino Formation. In Kora-1, it is largely represented as andesitic volcanics (volcanic edifice) or Mohakatino Formation equivalent. It is overlain by either the Ariki Formation or the Giant Foresets Formation, and underlain by the Manganui Formation. On wireline logs, this formation displays varying thicknesses, ranging from approximately 50 m at Te Kumi-1, to 150 m at Ariki-1 and 300m at Tangaroa-1, which is the closest well of these three wells to the central volcanic massifs in the Northern Graben (i.e. Kora volcanic massif) (Enclosure 1 and Figure 4.1).

4.1.4 Ariki Formation:

The Ariki Formation is a Late Miocene to Early Pliocene calcareous marl that is characterised by its rich planktic foraminifera content, up to and greater than 90% (Hansen and Kamp, 2008). The high percentage of foraminifera reflects the relatively deep (fully oceanic) environment in which the marl was deposited. Deposition of this condensed formation is associated with a substantial period of terrigenous sediment starvation within the northern Taranaki Basin during this time (Hansen and Kamp, 2004). The uppermost boundary of the Ariki Formation is easily recognised by an abrupt decrease in planktic foraminiferal abundance, dropping from 90% to less than 50 % in the basal part of the overlying Giant Foresets Formation. This drop is often used to help locate the base of the Giant Foresets Formation in wireline log interpretation, which can be later

transferred onto seismic reflection profiles allowing the base of the Giant Foresets Formation to be physically mapped (Hansen and Kamp, 2002). The Ariki Formation is relatively extensive over the northern part of the Western Platform and within the Northern Graben; in the northern half of the study area it appears in Ariki-1, Tangaroa-1 and Te-Kumi-1, as well as in Wainui-1 (immediately outside of the study area). In the south west, it is intersected in Kanuka-1, and is also expressed as a thin marl horizon in Taimana-1 (Enclosure 1 and Figure 4.1.). The Ariki Formation is overlain by the Giant Foresets Formation and underlain by either Mohakatino Formation or Manganui Formation. The thickness of this formation ranges from 25m in Taimana-1, to approximately 100 m in Ariki-1 (Enclosure 1).

4.1.5 Mangaa Formation:

The Mangaa Formation is interpreted as packages of fine-grained turbidite sandstone which were deposited as basin floor fan lobes within the Northern Graben. The formation was named after the well where it is most prominent (Mangaa-1), and is used to differentiate from the lithologically similar, but older, Mount Messenger Formation. The Mangaa Formation began depositing in the Early Pliocene (Opoitian Stage) and comprises the initial sedimentary fill in the Northern Graben. The formation is overlain by the Giant Foresets Formation and underlain by the Manganui Formation (See Enclosure 1 and Figure 4.1). Evidence from seismic reflection profiles show that the path of sediment transport was dominantly from south to north. The individual sandstone beds within the formation are approximately 10 m thick, and were deposited on top of one another, creating multiple amalgamated packages of sediment up to 40 m thick. These are separated by thinner mudstone intervals that are 10-20 m thick. Overall, this formation is thickest along the axis of the Northern Graben, oriented NNE/SSW (King and Thrasher, 1996). In the study area, the Mangaa Formation is only present in Awatea-1, where the numerous sandstone packages have a total thickness of approximately 500 m (Enclosure 1).

4.1.6 Giant Foresets Formation:

The Giant Foresets Formation (GFF) is mainly composed of siltstone and mudstone with interbedded sandstone beds, which were continuously deposited throughout the entire Plio-Pleistocene interval (approximately 5 Ma – present day) (King and Thrasher, 1996). It is the uppermost stratigraphic unit in the northern half of Taranaki Basin, and is inclusive of the recent seafloor surficial sediments (Hansen and Kamp, 2002). The Giant Foresets Formation is very extensive, occurring across offshore Taranaki Basin (Figure 4.1 and

Enclosure 1). It is also a very thick succession of sediment, in places reaching thicknesses of up to 3000 m (e.g. in the Arawa sub basin) (Hansen and Kamp, 2004). The Giant Foresets Formation is present in all of the wells within in the study area. This formation is underlain by either Manganui Formation, Ariki Formation, Mangaa Formation or by Mohakatino Formation age equivalent volcanic massifs (i.e. in Kora-1) (Hansen and Kamp 2002).

The Giant Foresets Formation is characterised by a stacked succession of off-lapping clinoforms prograding toward the north west, which are easily recognizable on seismic reflection profiles. Each individual clinoform reflector is representative of the short-lived position of the shelf-slope break and slope through geological time (King and Thrasher, 1996). The Giant Foresets Formation can be further subdivided into four separate parts, which are identified based on their different seismic characteristics. These include (i) topsets which are sub-parallel, sub-horizontal, moderately continuous reflectors; (ii) progradational foresets, which are (usually) moderately continuous reflectors that prograde in a basinward direction; (iii) degradational foresets, representative of mass movement downslope and are steeply dipping and more chaotic, not showing any regular pattern; and (iv) bottomsets, which are sub-horizontal to slightly inclined reflectors with variable continuity (Figure 4.2). These seismically defined parts of the Giant Foresets Formation are representative of various depositional environments and their associated lithologies. Topsets are deposited on the shelf, and are composed of sandstone and muddy siltstone beds which contain the odd shelly or pebbly interval, forests are deposited on the slope, where the lithologies are highly variable (sandstones, mudstones) and bottomsets are deposited on the basin floor, and are comprised of mudstones with the occasional sandstone (Hansen and Kamp, 2002).

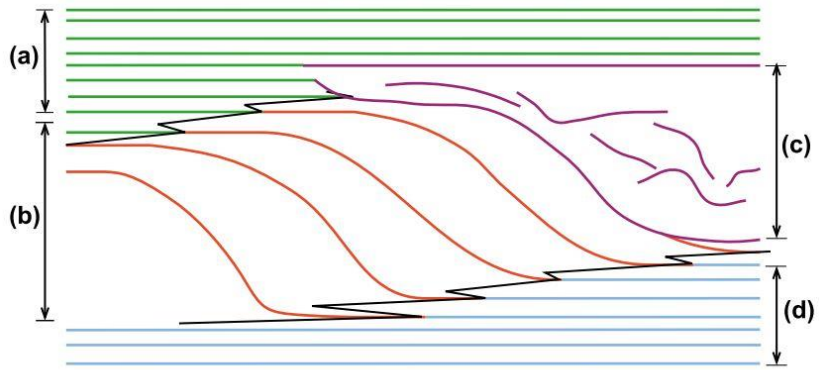

Figure 4.2 Schematic illustration of foreset divisions (Taken from Hansen and Kamp, 2002).

4.2. Biostratigraphy

Biostratigraphy is a branch of stratigraphy which uses fossil content and index fossils to subdivide strata in a sedimentary succession based on relative geological time, and involves the assignment of biostratigraphically determined stages to sedimentary horizons (Cooper et al, 2001). Index fossils are utilized because they are easy to identify, are abundant and geographically widespread, and evolved rapidly, only being present across certain defined biozones and are therefore representative of age (Jones, 2006).

Biostratigraphy is commonly used as a tool to analyse the subsurface of marine basins, and as a means of correlation across an area of interest. Different types of microfossils (foraminifera (commonly used), radiolarians and calcareous nanofossils) are recovered from drill cuttings and core from a wellbore, and examined. By studying the placement and ranges of certain key microfossils (index fossils) within a drill hole, the relative ages of horizons (seismic reflectors) at different depths can be established. These age horizons can then be correlated across other boreholes at depth within a field of study, by means of seismic mapping (Nichols, 2009).

However, a significant problem with biostratigraphy that is frequently encountered is the fact that this method is not capable of yielding a fully complete and reliable data set. This can be due to both natural and artificial factors (Jones, 2006). In a marine basin, there are many different depositional environments which change throughout both space and geological time. Considering the conditions between each environment are so variable (i.e. temperature, the amount of terrestrial sediment input, water depth, varying energies), it is to be expected that no single species, genus or family could live in all of the environments across a basin at any given time (Nichols, 2009). This could be why index fossils of certain stages are not preserved across an entire area. Preservation of fossils is also a causative factor of incomplete biostratigraphic data sets. For example, the preservation potential of foraminifera is favoured in low energy environments over high energy environments. This is why fewer fossils are preserved on the shelf in shallower water depths with higher energy conditions than in the deeper ocean. The diagenetic history of an area is also important as it can cause alteration (e.g., partial dissolution, re-calcification), making the foraminifera harder to identify or even result in complete removal of fossils. For example, slow sedimentation rates cause the remains of foraminifera to lie exposed on the seafloor for long periods of time where they are subject to biogenic degradation and reworking (Nichols, 2009).

The usefulness of fossils can also be reduced by artificial factors such as sample acquisition and processing. For instance, samples collected from wellbores may not be suitable to identify foraminifera (e.g. wrong lithology or depth of acquisition, or other factors such as the presence of juvenile foraminifera which have similar forms and are difficult to distinguish), or could be subject to downhole contamination. There is also a degree of subjectivity in specific species identification (Cooper *et al*., 2001).

To overcome this problem of an incomplete biostratigraphic data set in this study, depths based off previously determined biostratigraphic boundaries (well reports, other studies) were used to choose appropriate seismic reflectors, which were then mapped around the basin. Seismic reflectors are, for the most part, continuous to semi continuous around the Taranaki Basin, and therefore have become the primary data set for constraining stage boundaries within the study area. For this project, it is considered that this is the optimal way to illustrate the relationship between the biostratigraphy and the physical seismic reflectors and their assigned ages within the study area (Enclosure 1).

In order to assign ages/stage boundaries to specific seismic reflectors, the most recent biostratigraphy for five NZ stages (Kapitean, Opoitian, Waipipian, Mangapanian and Nukumaruan) were gathered from several sources for all the wells within the study area. This study mainly follows the biostratigraphy from Hansen (2003, 2006), as well as recent edits by Hansen (pers. comm; 2016), based on the latest ages and the most current calibration of the New Zealand geological time scale from Raine *et al* (2015). Relevant biostratigraphy from the New Zealand Petroleum and Minerals (NZPAM) exploration data pack from well completion reports, as well as the most current biostratigraphy from GNS from 2002, have also been utilized. Table 1 presents a comparison of all the biostratigraphy gathered from the various data sources. Depths of biostratigraphic stage boundaries were loaded into all the relevant wells in the study area using Kingdom™ software (Ariki-1, Arawa-1, Kora-1, Taimana-1, Tangaroa-1, Te Kumi-1, Awatea-1, Kanuka-1 and Witiora-1).

The horizons finally selected for structure contour mapping were initially based on the biostratigraphic data and depths from two of the wells examined in the detailed biostratigraphic analysis by Hansen (2006); Ariki-1 and Arawa-1. These two wells have a higher degree of confidence on their biostratigraphic stage boundary positions within the hole (Hansen, 2006). From the Waipipian onwards, most of the well sites utilised in this study were sitting at shelfal depths, as a result of rapid northward shelf migration.

However, at Ariki-1 well site, conditions remained fully oceanic through to the Mangapanian Stage. As there are more planktic foraminifera in the deep ocean than on the shelf, the foraminifera are more likely to be preserved and hence the biostratigraphic analysis in this well is enhanced. As seen on Table 1, the three different sources of biostratigraphic data for Arawa-1 list similar downhole depths for each of the stage boundaries, which supports the high confidence given to the downhole position of these stage boundaries. Although this well section was shelfal for the majority of the period of interest, the well lies on the edge of the Arawa sub-basin, which remained deep and potentially open to oceanic currents until the start of the Mangapanian. Thus there is a higher proportion of age-diagnostic planktonic foraminifera in the Opoitian through to the Mangapanian, which translates to a higher degree of accuracy with stage boundary placement.

After the biostratigraphy (relative to seismic reflectors) was defined, two large loop ties (one in the northern half of the study area, and another in the south) was completed between these control wells, using Kora-1 as a connection point. The Opoitian Stage was completed first, and then the following stages through to the Nukumaruan Stage. Loop-tying proved to be difficult as the lower reflectors (Kapitean – Waipipian) did not match up. When using the biostratigraphy from Kora-1 as a linking control point, the area to the east of Kora-1 became too shallow (high level in the section) after following the inclining reflectors that tied into the well biostratigraphy. Coming from the northern part of the study area (using Ariki-1 and Tangaroa-1 as biostratigraphic tie-in points, the same reflectors mapped out much lower in the seismic section and did not match with the biostratigraphically-defined horizons. This was also the case when trying to tie in the southern part of the study area (using Arawa-1 as the control). Consequently, the constraints of the biostratigraphy in Kora-1 had to be relaxed and essentially ignored for the Waipipian and Opoitian stage boundaries, in order for the loop tie in the top half of the study area to link with the loop tie in the lower half. The biostratigraphy for the Nukumaruan and Mangapanian stage boundaries (Kora-1) was still used however, as these retained a reasonable fit with the selected seismic reflectors. With some adjustment to find the closest match for the loop ties, this study aimed for no more than 100 m difference overall between the well biostratigraphy and the seismic reflector selected to represent a specific stage boundary. Once satisfied the loops were precise enough, the seismic interpretation was then expanded across the entire study area, using the other wells as control points.

Table 1. Comparison of biostratigraphy.

		Various biostratigraphic depths (MD Measured Depth)				
		NZPAM Data Pack (2015)	Petroleum Report PR2938 (Hansen, 2006)	GNS Updated Biostrat Report (2002)	Depth entered into Kingdom Software	Two way travel time equivalent
Arawa-1	Nukumaruan	668-980?	670-800?		670	580
	Mangapanian	980-1525?	800-1117.5?		800	730
	Waipipian	1525	1540		1540	1390
	Opoitian	1560	1557.5		1557.5	1410
	Kapitean	1760	1760		1760	1550
Ariki-1	Nukumaruan		1315-1815?	1450	1450	1460
	Mangapanian		1815-1995?	unrecognised (1700-1900?)	1890	1810
	Waipipian		1995	unrecognised (1910-2000?)	1995	1885
	Opoitian		2015	2000	2015	1960
Awatea-1	Nukumaruan	670/720 -1730/1760			700	520
	Mangapanian	1730/1760 - 1970/1980			1745	1500
	Waipipian	1970/1980-2270/2280			1970	1670
	Opoitian	2270/2280 - 2690/2700			2270	1870
	Kapitean	2690			2690	2150
Kahawai-1	Nukumaruan	<590 - 1250			590	660
	Mangapanian	1250-1950?			1250	1270
	Waipipian	1250-1950?			1620 (positive evidence)	1750
	Opoitian	1905-1930			1905	1770
Kora-1	Nukumaruan	630-1300?	638-815	1000-1300?	638	700
	Mangapanian	1300?	1125-1350?	1000-1300?	Both 1125 + 1300	1180 - 1320
	Waipipian	1390	1350	1360	1350	1350
	Opoitian	1767	1710	1700	1710	1610
Tangaroa-1	Nukumaruan			1210-1830?	1210	1260
	Mangapanian			1910	1910	1820
	Waipipian			2010-2040	2010	1885
	Opoitian			2040	2040	1905
Te Kumi-1	Nukumaruan	800			800	800
	Mangapanian					
	Waipipian					
	Opoitian	2065			2065	1900
Wainui-1	Nukumaruan		480-1700	810	480	360
	Mangapanian		1700	unrecognised (1410?)	1700	1530
	Waipipian		2015	1510	2015	1750
	Opoitian		2115	2000-2210	2115	1800
	Kapitean		2215	2218	2215	1890
Witiora-1	Nukumaruan	150-550			450	
	Mangapanian	550-750			600	
	Waipipian	750-950			800	
	Opoitian	950-1250			1000	
	Kapitean	1250-1337			1250	

4.3. Comparison of Seismic Stage Boundaries with Biostratigraphic Stage Boundaries

In Hansen (2003), stage boundaries were mapped across several holes in the northern part of Taranaki Basin based on an in depth analysis of the biostratigraphy found in each bore. Each of these boundaries in every well section analysed were qualitatively assigned a confidence level (high, medium, or low) (refer to Enclosure 1). High to moderate confidence levels were assigned to the boundaries that were defined by good age-diagnostic criteria, whereas low confidence levels were assigned to the stage boundaries that had poor age-diagnostic criteria (Hansen, 2003). Other authors placed confidence levels on their own biostratigraphy, at various boundaries or at certain depths, and these are similarly illustrated on Enclosure 1.

The seismic reflectors and their assigned biostratigraphy are as follows; The top Kapitean (Tk) mapped in this study is equivalent to the Opoitian (Wo) Stage boundary; the top of the Opoitian (Wo) stage boundary mapped in this study is equivalent of the Waipipian (Wp) Stage boundary; the top of the Waipipian (Wp) mapped in this study is equivalent to the Mangapanian (Wm) Stage boundary; and the top of the Mangapanian (Wm) Stage boundary mapped in this study is equivalent to the Nukumaruan (Wn) Stage boundary.

4.3.1 Arawa-1

The top of the Wn Stage boundary has not been defined by Hansen (2003) due to a lack of age-diagnostic foraminifera, but it has been defined in this study at 668 m, based on the biostratigraphy from NZPAM, as well as back-tying from other nearby control wells (i.e. Taimana-1)

Hansen's (2003) top Wm Stage boundary is placed at 800 m depth, observed with low confidence. This study has mapped the top of the Wm at 840m depth, giving a 40 m difference. The first downhole appearance (FDHA) of the Wm planktic foraminifera *Globorotalia i triangulata* is observed with high confidence at 805 m (Crundwell *et al*., 1992). Both the biostratigraphically-defined and the seismically defined boundaries lie within topsets (shelfal facies).

The top Wp Stage boundary is placed at 1540 m in Hansen (2003), and is assigned moderate confidence. This study has seismically mapped the top of the Wp only slightly lower at 1553 m, resulting in a 13 m difference. The FDHA of *Truncorotalia oceanica* (S) (Wo - Wm) is placed at 1542 m with high confidence (Crundwell et al., 1992), as well as *Truncorotalia crassaconica* (Wo -Wp) at 1545 m, placed with low confidence and

Globoconella pliozea (Early Wo) placed at 1555 m with a moderate confidence (Hansen, 2003). Both these boundaries lie within the foresets (slope facies).

The top Wo Stage boundary of Hansen (2003) is placed at 1555 m, and assigned moderate confidence. This study has mapped the top of the Wo deeper than this at 1605 m, resulting in a 50 m difference. This is still in the foresets (slope facies).

Hansen's (2003) top Tk Stage boundary is placed 1760 m, observed with moderate confidence. The boundary lies just within the bounds of the foresets (slope facies). This study has mapped the top of the Tk at 1789 m, giving a 29 m difference. This boundary marks the division between the bottom sets (basin floor facies) and the foresets (slope floor).

Overall, the biostratigraphic boundaries in Arawa-1 mapped in this study line up accurately with the stage boundaries investigated in Hansen (2003), with a maximum difference of only 50 m (Enclosure 1).

4.3.2 Ariki-1

Due to a lack of age-diagnostic criteria, the top of the Wn Stage boundary has not been defined in this well. However, Hansen (2003) divided the Wn into an upper and lower stage, with the boundary placed with high confidence at 1310 m. The high confidence on this subdivision is due to the presence of the Wn planktic foraminifera *Truncorotalia truncatulinoides* (Wc-Rec) at 1310m and *Truncorotalia crassula* (Wn-Rec) at 1330 m, both observed with high confidence. This study has mapped the top of the Wn at 1497 m, which on comparison gives a difference of 187 m. Hansen (2004) placed the last downhole appearance (LDHA) of *Tr. truncatulinoides* at 1390 m, but this is ranked with low confidence and could be a result of possible cavings. However, this depth is closer to the top of the mapped Wn Stage boundary of this study at 1497m, making a smaller difference of 117 m. This is part of the foresets (slope facies).

Hansen (2003) placed the top Wm Stage boundary at 1810 m, assigned with moderate confidence. This study has seismically mapped the top of the Wm at 1839 m, resulting in a 29 m difference. The last common occurrence (LCO) of *Tr. crassula*, and the LDHA of *Truncorotalia crassiformis* (?Wm - Wc) are placed at 1770 m, observed with high confidence (Hansen 2004). The FDHA of *Tr. oceanica* is placed at 1830 m, observed with low confidence (Hansen 2003). It is noted that in the down-hole depth range from 1800-

2050 m, there were sparse foraminifera and the Wm interval is therefore poorly defined. Both these boundaries lie within the bottomsets (basin floor facies).

The top Wp Stage boundary is placed by Hansen (2003) at 1995 m. There is no confidence placed on this boundary. This study has mapped the top Waipipian at 1975 m, giving a difference of 20 m. The LDHA of *Truncorotalia tosaensis* (Wm - Wn) is placed at 1990 m, observed with high confidence (Hansen, 2003), and the FDHA of *Globoconella subconomiozea* (Late Wo) is identified at 1990 m, also observed with high confidence (Hayward, 1986). This interval is based on (foraminiferal) absence criteria. Both these boundaries lie within the bottomsets (basin floor facies).

The top Wo Stage boundary is placed at 2105 m, observed with moderate confidence. This study has mapped the top of the Wo at 2101 m, resulting in a minimal a difference of only 4 m. This is based predominantly on the FDHA of the Late Tk to Wo planktic foraminifera *Globoconella pliozea*. Both these boundaries lie within bottomsets (basin floor facies).

The top Tk Stage boundary is placed by Hansen (2003) at 2150 m, observed with high confidence. This study has seismically mapped the top of the Tk at 2210 m, giving a difference of 60 m. The FDHA of *Truncorotalia crassaconica* (Wo - ?Wp) and the LDHA of *Globoconella inflata* (Late Wo - Recent) are placed at 2150 m (Hansen, 2003; Hayward,1986), the FDHA of *Globoconella miotumida* (Tl - Tk; Hansen, 2003) and *Globoconella conomiozea* (Tk; Hansen 2003; Hayward, 1986), and the LDHA of *Tr. oceanica* (S) are identified at 2170 m, all observed with high confidence (Hansen 2003). Both these boundaries lie within bottom sets (basin floor facies).

Overall, the biostratigraphic boundaries in Ariki-1 seismically mapped in this study align closely with the Wm, Wp and Wo stage boundaries identified in Hansen (2003), with a maximum difference of only 30 m (the Wo only differs by 4 m). The Wn and Tk Stage boundaries vary from Hansen's boundaries by a greater amount (117 m and 60 m respectively) (Enclosure 1). However, during the Wn, this well site was shelfal, being located on the edge of the shelf break, suggesting less oceanic conditions and less planktonic foraminifera. This could be why the foraminiferal analysis during this stage does not have the same level of accuracy as the older stages, and is why the chosen reflector for the Nukumaruan Stage in this study is contradictory with that observed in Hansen (2003).

4.3.3 Kora-1

Due to a lack of diagnostic criteria, the top of the Wn has not been defined by Hansen (2003) in this well. The upper Nukumaruan/Castlecliffian Stage has however been differentiated from the lower Wn Stage, at 810 m, observed with moderate confidence. This is based on the LDHA of *Tr. truncatulinoides* at 810 m (Hansen 2003), while the LCO of *Tr. truncatulinoides* is placed at 750 m, both with high confidence (Hansen, 2003). This study has mapped the top of the Wn at 630 m, giving a difference of 180 m. Both these boundaries lie within the topsets (shelf facies). Within the depth range between 630 m-1080 m, there are few planktic foraminifera to be analysed, which contributes to the variation between seismic and biostratigraphic placement of the stage boundary.

The top Wm Stage boundary of Hansen (2003) is placed with low confidence at 1125 m. This study has mapped the top Wm at 1109 m, giving a small difference of 14 m. However, this interval is poorly defined as a result of only rare planktic foraminifera. Both these boundaries lie within foresets (slope facies).

The top Wp Stage boundary of Hansen (2003) is placed at 1350 m. This is observed with moderate confidence. This is based on the FDHA of *Hirsutella aff. praehirsuta* (Wp) and *Tr. tosaensis* at 1360 m. This boundary lies within the foresets (slope facies). This study has mapped the top Wp into Kora-1 at 1625 m, based on the loop-tie method from the two control wells (Arawa-1 and Ariki-1). Near this depth, the LCO of *Hr. aff. praehirsuta* is placed at 1650 m with high confidence (Hansen 2003), indicating Waipipian-aged strata. Comparison of these two boundaries gives a large difference of 275 m, which can be partly accounted for by the lack of biostratigraphic control within Kora-1.

Hansen's (2003) top Wo Stage boundary is placed at 1715 m with moderate confidence. This is based on the identification of the FDHA of *Globoconella subconomiozea* (Late Wo) and *Gc. cf. pliozea* at 1730 m (Waghorn et al 1996), and 1740 m (Hansen, 2003) respectively. This study has seismically placed the top Wo boundary at 1827 m, with a difference of 112 m observed. These boundaries are placed within bottomsets (basin floor facies).

The top Tk Stage is not recognised in this well in Hansen (2003). In this study it has been placed at 2324 m based on loop-tying, and falls within the undifferentiated (and undated) volcanic interval in Kora-1.

Overall, the seismic boundaries in mapped in this study do not match the biostratigraphic boundaries of Hansen (2003), with differences in depth downhole ranging from 112-275 m (Enclosure 1). This is a result of both the biostratigraphic control in this study for Kora-1 having to be relaxed in order for the loop ties to match up across the study area, as well as the sparse foraminifera throughout the well strata, with ages within the well assigned with less confidence.

4.3.4 Taimana-1

The top of the Wn Stage has not been defined in this well by Scott (1989) or Crundwell *et al* (1994), although the lower Wn is differentiated from the upper Nukumaruan/Castlecliffian at 420 m (placed with low confidence; Hansen, 2003). This study has mapped the top of the Nukumaruan at 655 m. These boundaries both lie within the topsets (shelfal facies).

The top Wm Stage boundary has been identified at 880 m (PR1026), although with low confidence. This study has seismically mapped the top of the Wm at 818 m, a difference of 62 m. The LCO of the benthic foraminifera, *Notorotalia zealandica* (Wn to Recent) is placed at 820 m with high confidence (Scott 1989). *Truncorotalia oceanica* is observed at 860 m with low confidence (Scott, 1989). These boundaries both lie within the topsets (shelfal facies).

The top Wp Stage boundary is placed at 1180 m, observed with moderate confidence. This is based on the observation of the LDHA of *Tr. cf. oceanica* at 1130 m Hoskins and Raine, 1984), and the FDHA of the benthic foraminifera *Cibicides molestus* (Tt-Wp) at 1190 m (Crundwell et al., 1994). This study has placed the top of the Wp at 1461 m, with a large difference of 271 m between the biostratigraphically and seismically determined boundaries.

The top Wo Stage boundary is placed by Scott et al., (2004) at 1435 m observed with moderate confidence. This study has mapped the top of the Wo stage boundary at 1564 m, with a difference between the two of 129 m. While Crundwell et al (1994) place the FDHA of the Kapitean-Opoitian planktic Gc. Pliozea at 1490m, Hoskins and Raine (1994) identify the FDHA of *Gc. pliozea* and *Globoconella puncticulata*, and the LDHA of *Tr. crassaconica* at 1530 m with high confidence. The FDHA of *Globoconella mons* (Tk-Early Wo) is placed at 1550 m, also with high confidence (Crundwell *et al*., 1994). These all indicate that the seismic placement is within Opoitian-aged strata. Both these boundaries lie within the foresets (slope facies).

The top Kapitean Stage boundary equivalent is placed at 1695 m by Scott *et al.,* (2004) with moderate confidence (Hansen, 2003). This study has mapped the top Kapitean at 1727 m, a difference of just 32 m. Both these boundaries lie within the bottomsets (basin floor facies).

Overall, the seismically defined boundaries mapped into Taimana-1 in this study do not always match the biostratigraphic boundaries presented in Hansen (2003), with differences in depth ranging from 30-271 m (Enclosure 1).

4.3.5 Tangaroa-1

The top of the Wn Stage has not been defined in Hansen (2003) in this well, although the upper Wn/Wc stage has been differentiated from the lower Wn Stage. This boundary has been placed by Waghorn *et al* (1994) at 1045 m with low confidence. This study has seismically mapped the top of the Wn Stage boundary at 1189 m. The presence of both *Tr. crassaformis* (FDHA placed with high confidence at 1210 m (Hayward, 1985b) and *Tr. oceanica* (Waghorn *et al*., 1996) within close proximity to the seismic stage boundary position confirm a Wn age. When comparing the biostratigraphic vs seismic boundaries, a difference of 144 m is observed. Both these boundaries lie within the foresets (slope facies).

The top Wm Stage boundary equivalent is placed at 1840 m (Waghorn *et al*., 1996) with low confidence (Hansen, 2003). The top of the Wm is mapped in this study at 1908 m, resulting in a difference of 58 m. Both of these boundaries lie within bottomsets (basin floor facies)

In Hansen (2003), the top Wp Stage boundary is placed at 1980 m, with low confidence. The LDHA of *Tr. tosaensis* is placed at 1960 m, and the LDHA of *Tr. crassula* is observed at 2010 m with high confidence (Hayward, 1985b), supporting entry into Wp-aged strata. This study has mapped the top of the Wp at 2012 m, close to the LDHA of *Tr. crassula*. On comparison of these two boundaries, a difference of 32 m is observed. Both these boundaries lie within bottomsets (basin floor facies).

The top Wo Stage boundary has been placed at 2025 m by Waghorn *et al* (1996), with moderate confidence. This study has mapped the top of the Wo Stage boundary at 2046 m, resulting in a minimal difference of only 13 m. Rare occurrences of *Tr. oceanica* (S) observed at 2040 m (Scott, pers. comm., 2001; Hansen 2003), as well as the FDHA of *Gc. pliozea* observed with moderate confidence at the same depth by Waghorn *et al*., (1996)

confirm entry into the Opoitian Stage. Both these boundaries lie within bottomsets (basin floor facies).

The top Tk Stage boundary equivalent has been placed by Waghorn *et al* (1996) at 2070 m, with moderate confidence. This is confirmed by the FDHA of *Gc. mons* (Waghorn *et al*., 1996), the observation of *Gc. puncticulata* and *Tr. crassaconica* (Hayward, 1985b), and the LDHA of *Gc. inflata* and *Tr. oceanica* (S) at 2060 m. This study has mapped the top of the Tk at 2094 m. The FDHA of *Gc. miotumida* at 2100 m (observed with high confidence; Waghorn *et al*., 1996) confirms entry into the Tk Stage. Comparison of the seismic vs biostratigraphic boundaries reveals a difference of 24 m. Both these boundaries lie within bottomsets (basin floor facies).

Overall, the biostratigraphic boundaries in Tangaroa-1 mapped in this study closely line up with the all the stage boundaries considered in Hansen (2003) except for the Wn Stage boundary. The Tk through to the Wn stages show minor differences in boundary depths ranging from only 13 m to 60 m. The difference in projected depth of the mapped vs biostratigraphic Wn Stage boundary is 147 m (Enclosure 1). However, because of a lack of foraminifera for analysis and definition of the top Wn Stage (potentially because the well site was sitting at shelfal depths at this time), some discrepancy is to be expected.

4.3.6 Te Kumi-1

The top of the Wn Stage is poorly resolved in this well (Waghorn et al., 1996), with only the upper Nukumaruan/Castlecliffian stage being differentiated from the lower Wn Stage with low confidence (Hansen, 2003) at 1170 m. This study has seismically mapped the top of the Wn at 1206 m, which on comparison gives a difference of 36 m. Both of these boundaries lie within the foresets (slope facies).

The top of the Wm Stage boundary is identified at 1870 m. This is observed with low confidence and is also poorly resolved (Waghorn *et al*., 1996). This study has mapped the top of the Wm at 1890 m, resulting in a small difference of 20 m only. The top or near top Wm Stage is confirmed by the LO of *Tr. crassiformis* placed at 1850 m with high confidence (Waghorn et al., 1996). Both of these boundaries lie within the bottomsets (basin floor facies).

The top Wp Stage boundary is identified at 1960 m, although is given a low confidence rating (Hansen, 2003). The LDHA of *Tr. crassula* at 1950 m (Waghorn et al., 1996) indicates that below this depth strata are older than Wm, supporting the stage boundary

placement. This study has mapped the top Wp at 1956 m, with a minor difference of 4 m noted. Both of these boundaries lie within the bottomsets (basin floor facies).

Waghorn et al., (1996) identified the FDHA of *Gc. pliozea, Gc. puncticulata, Tr. crassaconica* and *Gc. subconomiozea* at 2026 m, with moderate confidence placed on the top Wo Stage boundary (2070 m) as a result (Hansen, 2003). This study has mapped the top of the Wo lower than this at 2189 m, a moderately large difference of 119 m. Both these boundaries lie in the bottomsets (basin floor facies).

The top Tk Stage is not recognised in this well in Hansen 2003. In this study it is mapped as 2200 m, but is deeper than the lowest point measured on the well log in the enclosure, and is therefore not included.

Overall, the seismic stages for Te Kumi-1 mapped by this study closely match the Wn, Wm and Wp biostratigraphic stage boundaries presented in Hansen (2003) and illustrated in Enclosure 1. Differences in depth (of boundary placement) range from only 4 m to 36 m. The Wo Stage boundary has a greater difference of 119 m (Enclosure 1).

4.3.7 Awatea-1

The top Wn Stage boundary is identified in Hansen (2003), at 695 m, and is observed with moderate conference between 670-720 m in Strong *et al*., (1996). This boundary lies within the topsets (shelf facies). This study has seismically mapped the top Wn stage boundary at 1092 m which has resulted in a substantial difference of 397 m, and pushed the boundary into the foresets (slope facies).

The Wm Stage boundary is placed with moderate confidence at 1740 m (Hansen, 2003). Strong *et al*., (1996) placed the LDHA of *Tr. crassaformis* at 1730 m with high confidence, supporting strata no older than Wm above this interval. This study has mapped the top Wm Stage boundary at 2051 m. On comparison between the two techniques, there is a large difference of a 310 m. Both these boundaries lie within the bottomsets (basin floor facies).

The LDHA of *Tr. crassula* at 1950 m, and the FDHA of *Hr. praehirsuta* and *Tr. crassaconica* at 1980 m, (Strong *et al*., 1996) supports the placement of the Wp Stage boundary equivalent at 1976 m (with high confidence; Hansen 2003). This study has mapped the top Wp Stage boundary at 2355 m. Again, there is a difference (in this instance of 405 m), between the biostratigraphically and seismically assigned stage boundaries. However, both these boundaries lie within the bottomsets (basin floor facies).

Top Wo Stage boundary is placed at 2275 m in Hansen (2003), observed with moderate to high confidence. This is likely to do with the FDHA appearance of *Gc. subconomiozea* placed at 2280 m, and *Gc. puncticulata* at 2290 m, both Wo foraminifera, and noticed with high confidence (Strong *et al*., 1996). This study has mapped the top Wo stage boundary at 2470 m. This is a lesser, but still significant, difference of 195 m. Both these boundaries lie within the bottomsets (basin floor facies).

Strong et al., (1996) note the FDHA of *Gc. miotumida* and LDHA of *Gc. mons* at 2690 m, which supports the placement of the top Tk Stage boundary equivalent at 2670 m (Hansen, 2003, with high confidence). This study has seismically mapped the top Tk stage boundary at 2585 m, resulting in a much smaller difference of 85 m between the seismic and biostratigraphic boundaries. Both these boundaries lie within the bottomsets (basin floor facies).

Overall, the seismically mapped boundaries in Awatea-1 in this study illustrate the greatest inconsistencies in boundary depths when compared with those the biostratigraphically determined boundaries in Hansen (2003) and other studies. The seismic boundaries are significantly deeper, with differences from 85 m to the greatest variance of 405 m (Enclosure 1).

4.3.8 Kanuka-1 and Witiora-1

Kanuka-1 and Witiora-1 wells were not analysed in Hansen (2003), but seismically defined boundaries have been mapped in these wells in this study.

In Kanuka-1, the top of the Wn Stage boundary has been mapped at 535 m, the top of the Wm Stage at 785 m, the top Wp Stage at 1623 m, the top Wo Stage at 1687 m, and the top Tk Stage at 1835 m.

In Witiora-1, the top of the Wn Stage boundary has been mapped at 466 m, the top Wm Stage at 575 m, the top Wp Stage at 776 m, the top Wo at 920 m, and the top Tk Stage at 1100 m.

5. Basin Geology and Geometry

5.1 Introduction

This chapter outlines the framework for basin development in the North Taranaki Basin from the latest Miocene until the Present Day. Five horizons were mapped through seismic lines across the north Taranaki Basin area/Northern Graben area [area delineated in Figure 5.1.1]. These horizons are: top of the Kapitean Stage (5.3 Ma), top of the Opoitian Stage (3.6 Ma), top of the Waipipian Stage (3.0 Ma), top of the Mangapanian Stage (2.4 Ma), and top of the Nukumaruan Stage (1.63 Ma) (presented in detail in Figure 5.1.2). The set of seismic lines mapped in this investigation are illustrated on Figure 5.1.1. This figure also shows the location of wells used for biostratigraphy and formation ties interpreted. Seismic lines are presented in Enclosure 1 and on separate figures in this chapter and in other parts of the thesis. Enclosure 1 also shows structure contour and isopach maps, used to describe and illustrate the basin's evolution from the Late Miocene to the Present day.

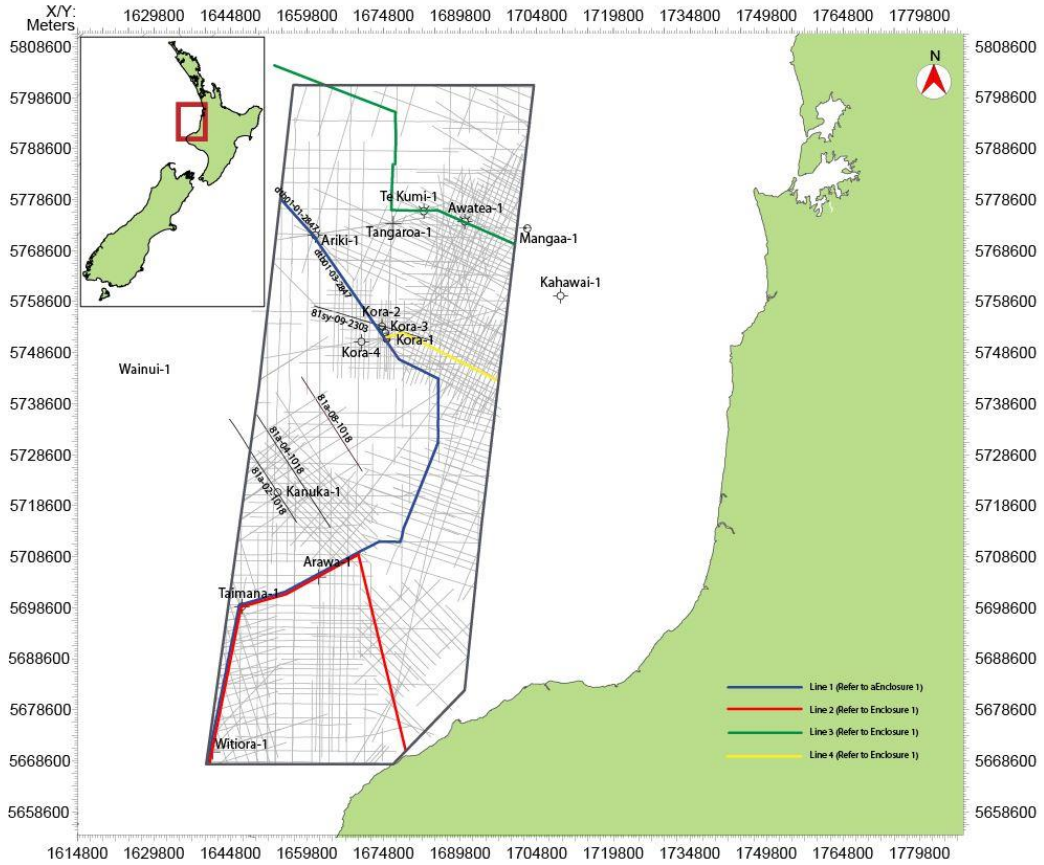

Figure 5.1.1 Location Map of the study area in North Taranaki Basin. The location and distribution of seismic lines and drill holes are also represented.

5.2 Top Kapitean Stage Boundary (5.3 Ma)

5.2.1 Structure Contour Map

The structure contour map of the top Kapitean Stage boundary (5.3 Ma) is presented in Figure 5.2.1. The general pattern shows an increase in depth of this surface towards the north east with a structural low aligned along the approximate position of the Northern Graben. The deepest parts of this structural low range approximately between 2500 m and 2700 m. The top Kapitean surface is shallowest in the south-west of the study area in the vicinity of Witiora-1 (approximately 1000 m depth at this location). A structural high on which Kora-1 is located on the flanks of, is likely a result of the emerging Kora volcanic massif. Normal faults (oriented SW-NE) clearly offset the top Kapitean surface, which suggest that the faults were active while the underlying sediments were accumulating. The largest offset is that of the Parihaka Fault, located in the centre of the study area, adjacent to (and forming the western boundary of) the Arawa sub basin, offsetting strata by approximately 600 m. In contrast, sediment onlaps the flanks of the volcanic massifs (part of the Mohakatino Volcanic Centre) which were still visible during this time. This indicates that the volcanoes were formed before the sediment was deposited (refer to later Figure 5.3.3)

5.2.2 Seismic Facies Analysis and Sediment Distribution

During the Kapitean Stage, Manganui Formation/Urenui Formation sediments were accumulating in the southern half of the study area (Kanuka-1, Arawa-1, Taimana-1), and the Mohakatino Formation was being deposited in the northern half (Ariki-1, Tangaroa-1, Te-Kumi-1, and Awatea-1). The Ariki Formation was beginning to accumulate near the end of this stage as seen in Ariki-1 well (Refer to Enclosure 1).

Manganui Formation can be distinguished in this seismic package by its low amplitude reflectors, indicative of a bathyal mudstone (Figure 5.2.2); in the north, these low amplitude reflectors are contrasted by high amplitude reflectors of the overlying Mohakatino Formation

The Kapitean Stage sedimentation is therefore characterised by sub parallel and in some places wavy, seismic reflectors (Figure 5.2.2, refer to Lines 1, 2 and 4 on Enclosure 1). This type of reflection configuration is indicative of consistent rates of suspension deposition in a uniformly subsiding area (Mitchum *et al*., 1977, Grain, 2008)

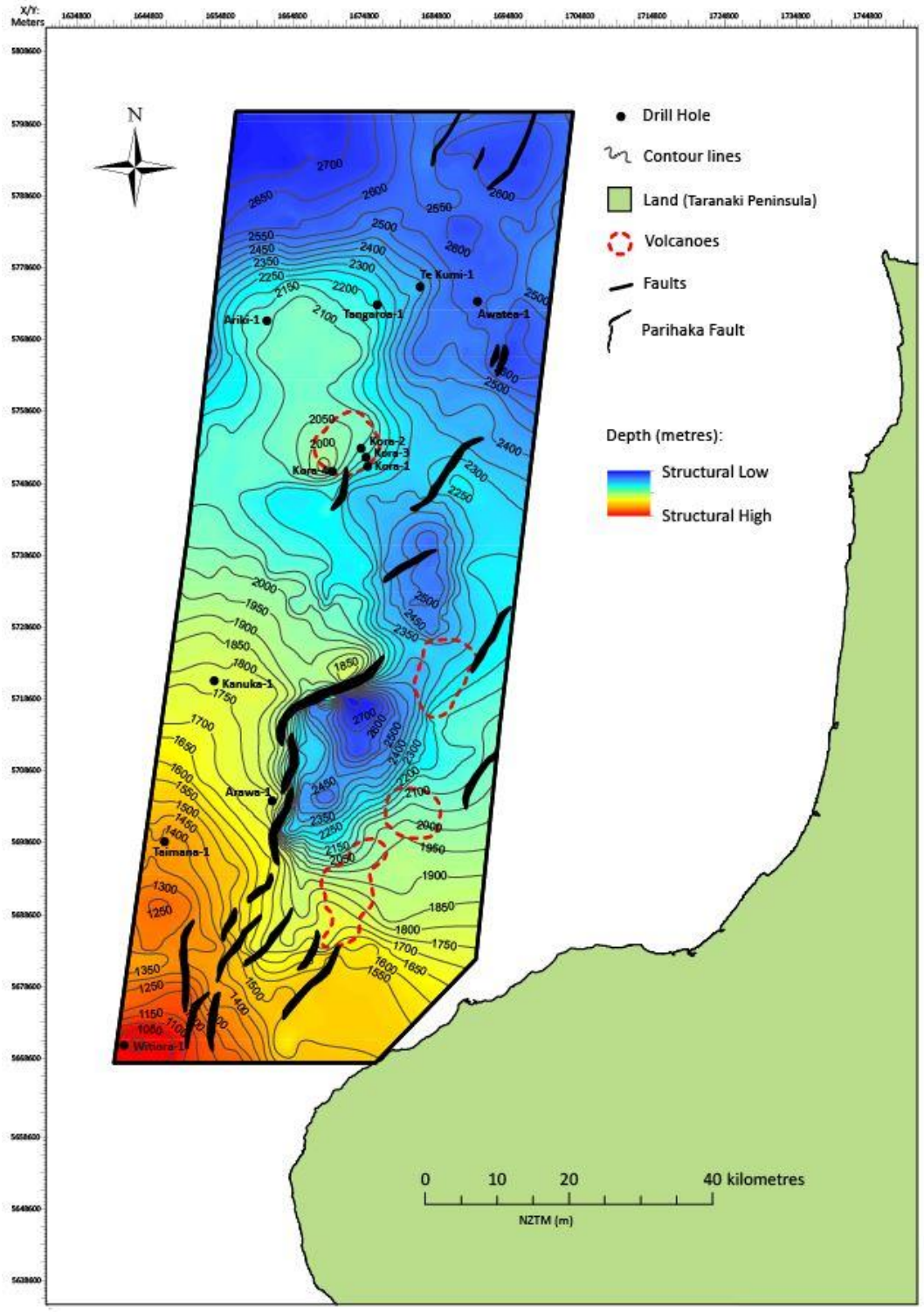

Figure 5.2.1 Structure contour map of the top of the Kapitean Stage Boundary (5.3 Ma).

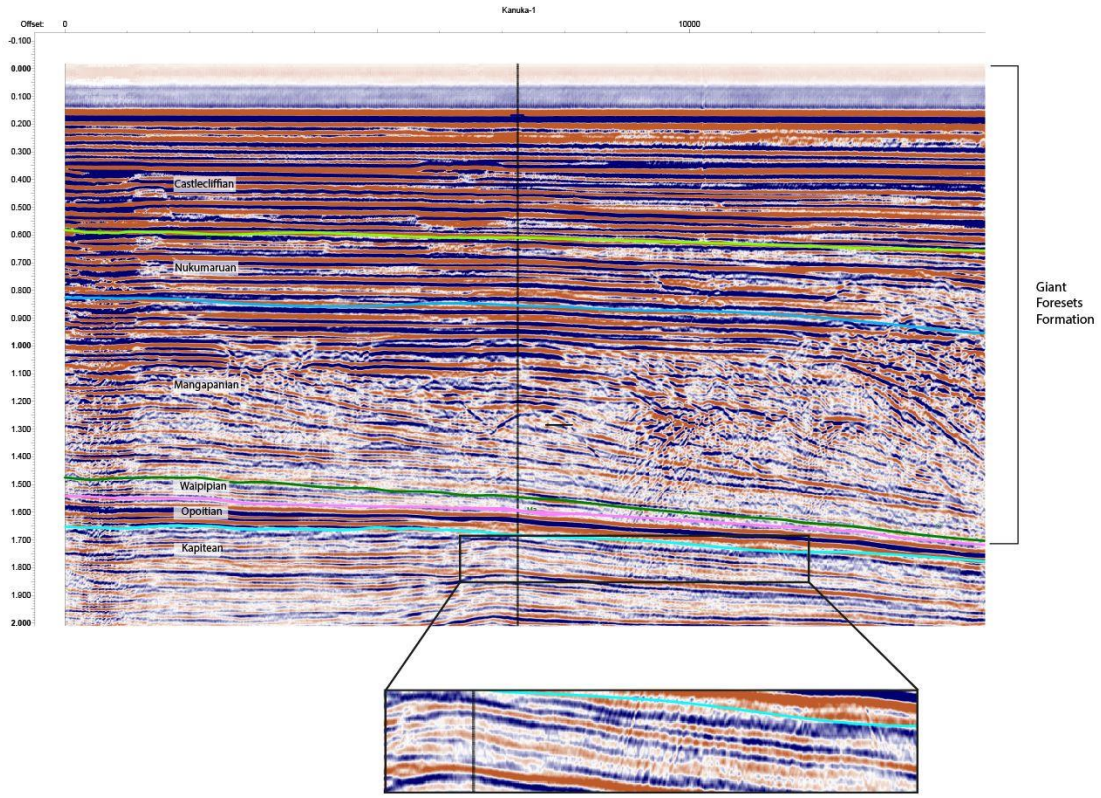

Figure 5.2.2 Image depicting the characteristics of the Manganui Formation in seismic profile (Line 81a-02-1018).

5.3 Top Opoitian Stage Boundary (3.6 Ma):

5.3.1 Structure Contour Map

The structure contour map for the top of the Opoitian Stage boundary (3.6 Ma) is presented in Figure 5.3.1. By the end of this stage, the entire study area had shallowed by approximately 150m. The structure contour pattern in Figure 5.3.1 mirrors that of the underlying Kapitean stage boundary depicted in Fig 5.2.1. The Arawa sub basin has become the most prominent depocentre by this time and the Opoitian Stage boundary below KB lies at 2450 m at its deepest point. During this time, the Arawa sub basin remained open to the north east. The structural high in the vicinity of Witiora-1 well site is still present (900m below KB). A low structural high continues to delineate the Kora volcanic massif, and a new, although low, structural high has formed towards the central and eastern region of the study area between two volcanic massifs. Normal fault activity is still a feature during the Opoitian and sediments continue to onlap the volcanic massifs.

5.3.2 Seismic Facies Analysis and Sediment Distribution

During the Opoitian Stage, several formations were accumulating in various locations simultaneously across the basin. In the south, deposition was similar to the Kapitean Stage, with Manganui Formation/Urenui Formation mudstones being deposited (Arawa-1/Taimana-1 and Kanuka-1 respectively). Approximately 50m of Ariki Formation marl was also deposited during this stage, in the vicinity of Kanuka-1 well. In the north, the Ariki Formation had also begun accumulating, with the marl intersected in the Ariki-1, Tangaroa-1, Te Kumi-1, and Awatea-1 wells. Beneath the Ariki Formation in Kora-1 and Te Kumi-1, andesitic volcanics (or Mohakatino Formation equivalent) are present. Importantly, initiation of the deposition of the Mangaa Formation occurred during this interval of time in the north eastern part of the study area (intersected in Awatea-1 well; Refer to Enclosure 1).

On high quality seismic reflection lines, the Ariki Formation can be distinguished in the seismic package a pair of bold, high amplitude reflectors (Figure 5.3.2). This formation is generally expressed as sub parallel to parallel reflector patterns. The andesitic volcanic massifs are easily recognised on seismic lines by the chaotic reflection patterns, which show poor internal seismic characteristics, but have obvious high reflective outer boundaries (Figure 5.3.3, refer to Lines 1 and 2 on Enclosure 2). This pattern is indicative of sediment deposited in a high energy variable environment or deposits affected by soft sediment deformation (i.e. when magma cuts through previously deposited sediments as

volcanoes are formed). The Mangaa Formation is represented by high amplitude sub parallel reflector patterns, which are indicative of submarine fan deposition (King and Thrasher, 1996).

The observed thickness of the sediment deposited during the Opoitian ranges from 0 – 1120 m (Figure 5.3.4). The sediment distribution pattern for the most part correlates to the location of depocentres that were available to fill at the end of the Kapitean with the greatest deposition during this time occurring in the north east. This is depicted by the numerous sediment clusters in the north east of the study area (Northern Graben), which is directly related to Mangaa Formation fan deposition (Figure 5.3.4). The decreasing thickness over the north western half of the study area is reflective of little terrigenous sediment input and consequently the calcareous Ariki Formation deposits accumulated.

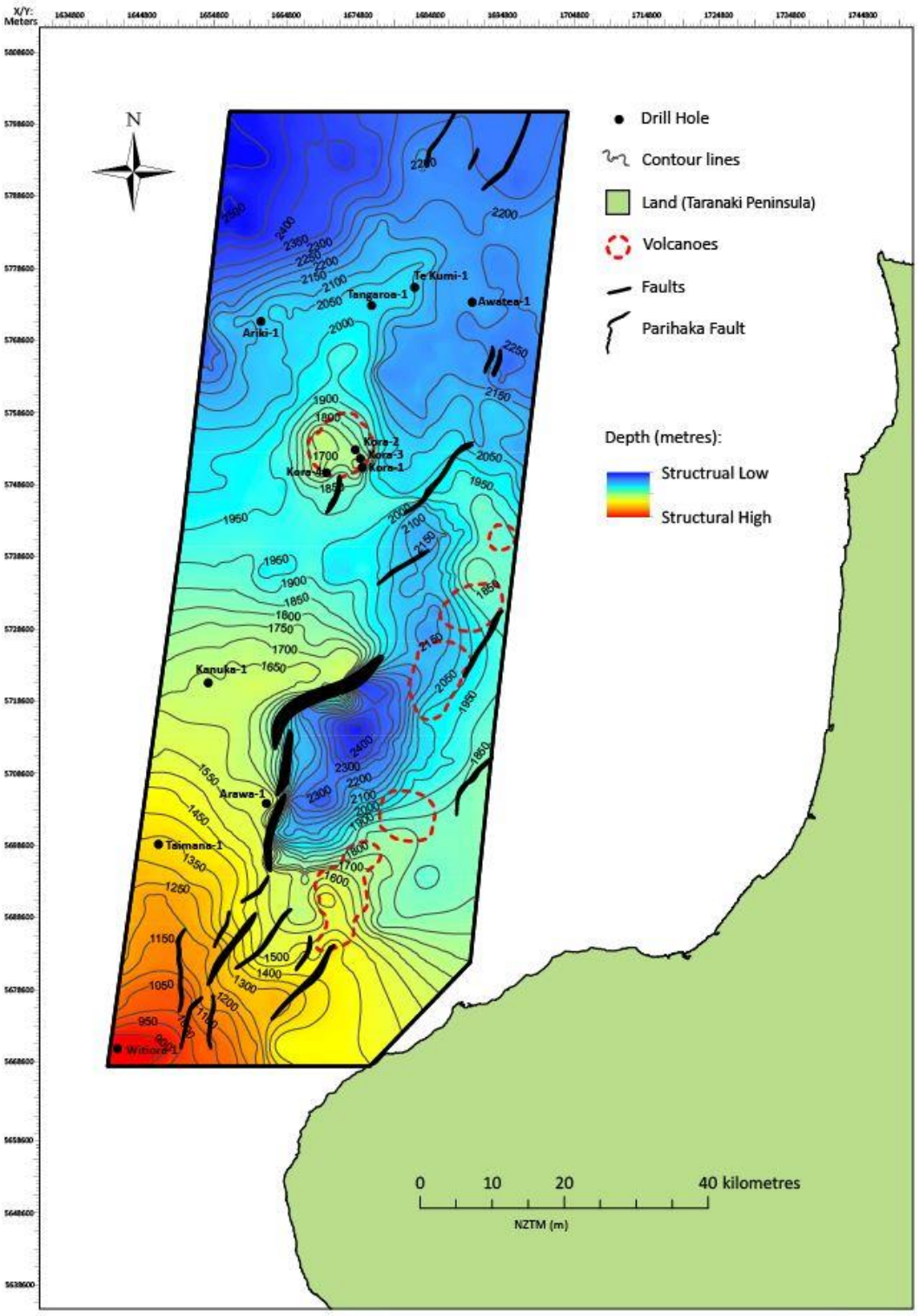

Figure 5.3.1 Structure contour map of the top of the Opoitian Stage Boundary (3.6 Ma).

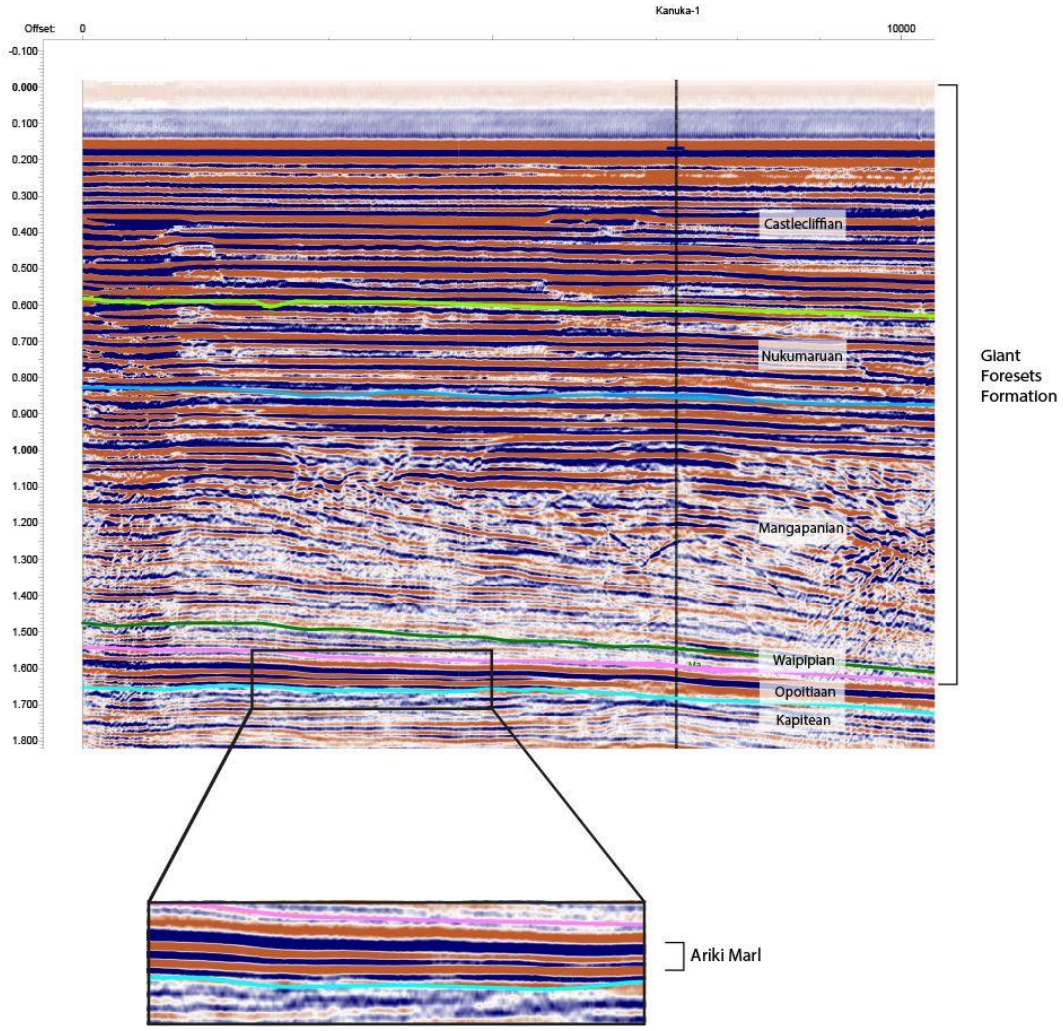

Figure 5.3.2 Image depicting the characteristics of the Ariki Marl in seismic profile (Line 81a-02-1018).

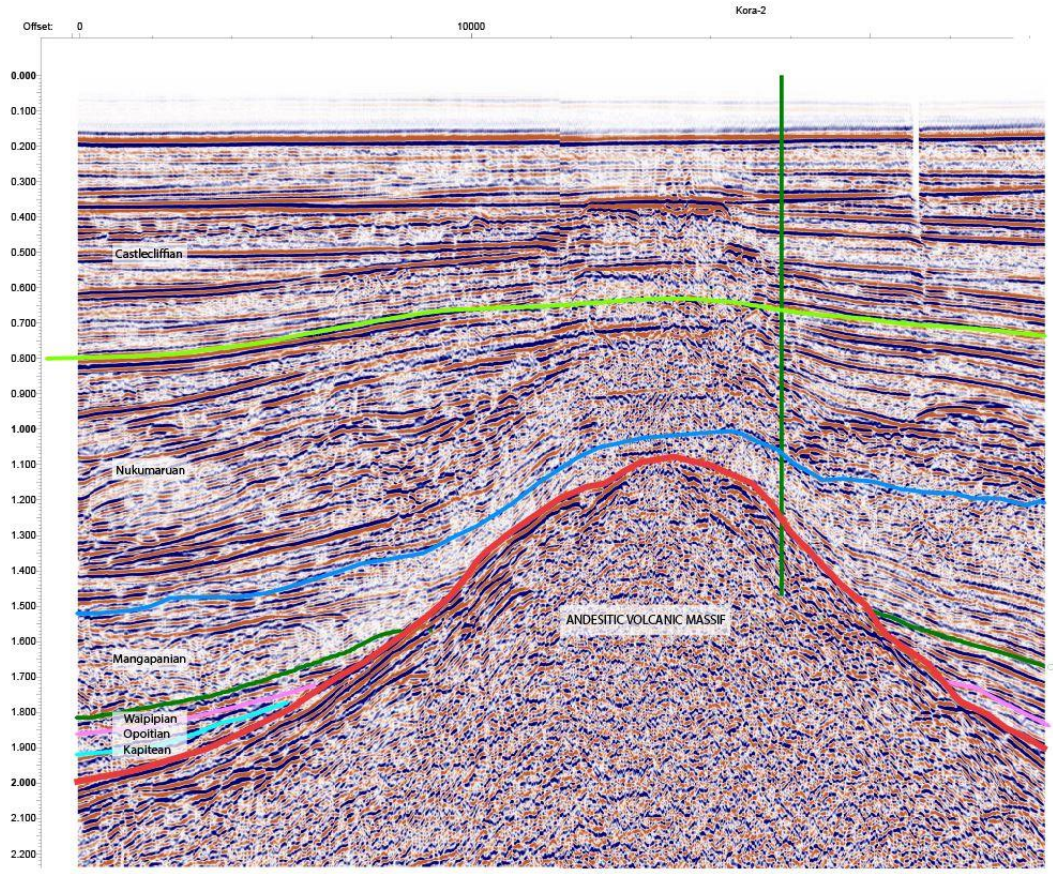

Figure 5.3.3 Image depicting the characteristics of an andesitic volcanic massif (Mohakatino formation age equivalent) in seismic profile (Line 81sy-09-2303). Note how the Kapitean to early part of the Mangapanian-aged sediments on lap the flanks of the massif

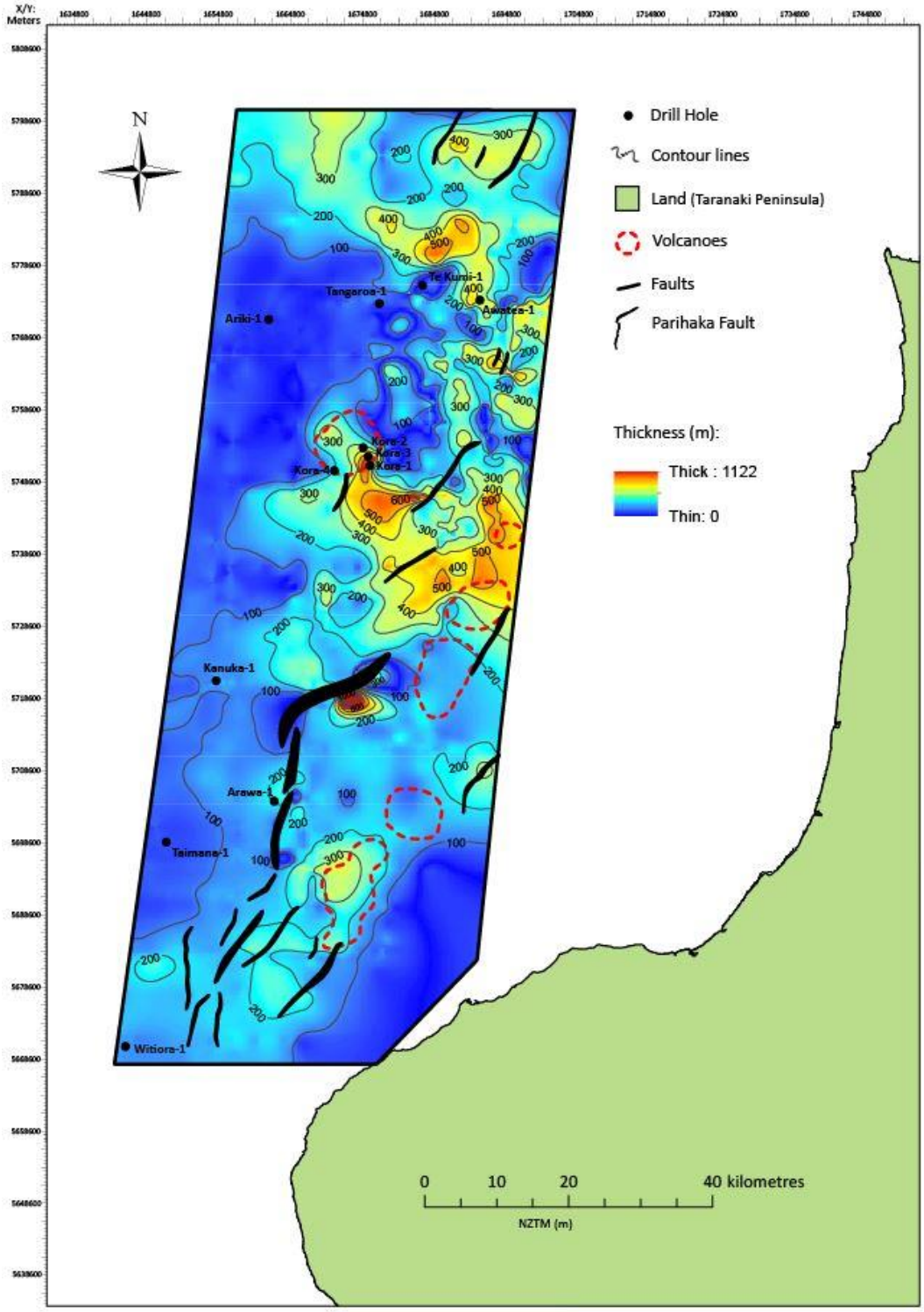

Figure 5.3.4 Isopach map of the sediment deposited during the Opoitian Stage (5.3-3.6 Ma).

5.4 Top Waipipian Stage Boundary (3.0 Ma):

5.4.1 Structure Contour Map

The structure contour map of the top of the Waipipian Stage boundary (3.0 Ma) is presented in Figure 5.4.1. By the end of the Waipipian Stage, the structural low forming the Arawa sub basin was still present, only shallowing by approximately 50-100 m bkb when compared with the seismically mapped surface presented in the Opoitian structure contour map. However, as shown in figure 5.4.1, by this time it had become an enclosed stand-alone depocentre, no longer contiguous with the Northern Graben. The main structural high had moved northward from Witiora-1 to the vicinity of the Taimana-1, and a new structural high had formed in the south east corner of the study area. The Mohakatino volcanics have had a strong influence on the structure of this horizon, evident by the minor structural highs which have become more prominent over the locations of the volcanic massifs. The structural high delineating the top of Kora volcanic massif became more prominent by the end of this stage, although the exposed tops of these massifs had decreased, due to the continued deposition of sediment on the flanks of these structures, burying them further. Normal fault activity is still a feature during the Opoitian and sediments continue to onlap the volcanic massifs.

5.4.2 Seismic Facies Analysis and Sediment Distribution

During the Waipipian Stage, deposition continued to vary across the basin. Manganui Formation sediments were still being deposited in the south (identified in both Arawa-1 and Taimana-1). A thin marl also accumulated in several places, being identified in Taimana-1 in the south, as well as in Tangaroa-1 in the north (in the latter well, likely an extension of the Ariki Formation marl). In the vicinity of Awatea-1, Mangaa Formation continued to accumulate. It was during this stage that the Giant Foresets Formation (GFF), which now dominates the sedimentary succession in northern Taranaki Basin, began to accumulate, being intersected in numerous wells (Kanuka-1, Taimana-1, Ariki-1, Tangaroa-1, Te-Kumi-1, and Kora-1;Refer to Enclosure 1) during this time period.

The GFF is made up of four parts, which show varying characteristics in seismic reflection (refer to section 4.1.6 in the Stratigraphy and Biostratigraphy chapter). In this time interval, the GFF was deposited as mud-dominated bottomsets, i.e., deposited on the basin floor. The bottomset reflectors are presented in literature as showing sub-horizontal

to slightly inclined reflectors, which may have variable continuity (Hansen and Kamp, 2002). However, due to the fact the amount of sediment that was deposited during the Waipipian is very thin across the study area, the bottomsets are difficult to distinguish in seismic profile and these patterns are unable to be observed in this data set.

The Waipipian Stage is relatively thin in terms of sediment thickness, with approximately 0 – 300 m only deposited across the study area. Several small areas of increased thickness are noted however, and when comparing with the top Waipipian structure contour map, they are related to high points rather than depocentres (Compare Figures 5.4.1 and 5.4.2). The overall low deposition rates and thin accumulation of Waipipian-aged strata is a manifestation of the low sediment input to the entire area.

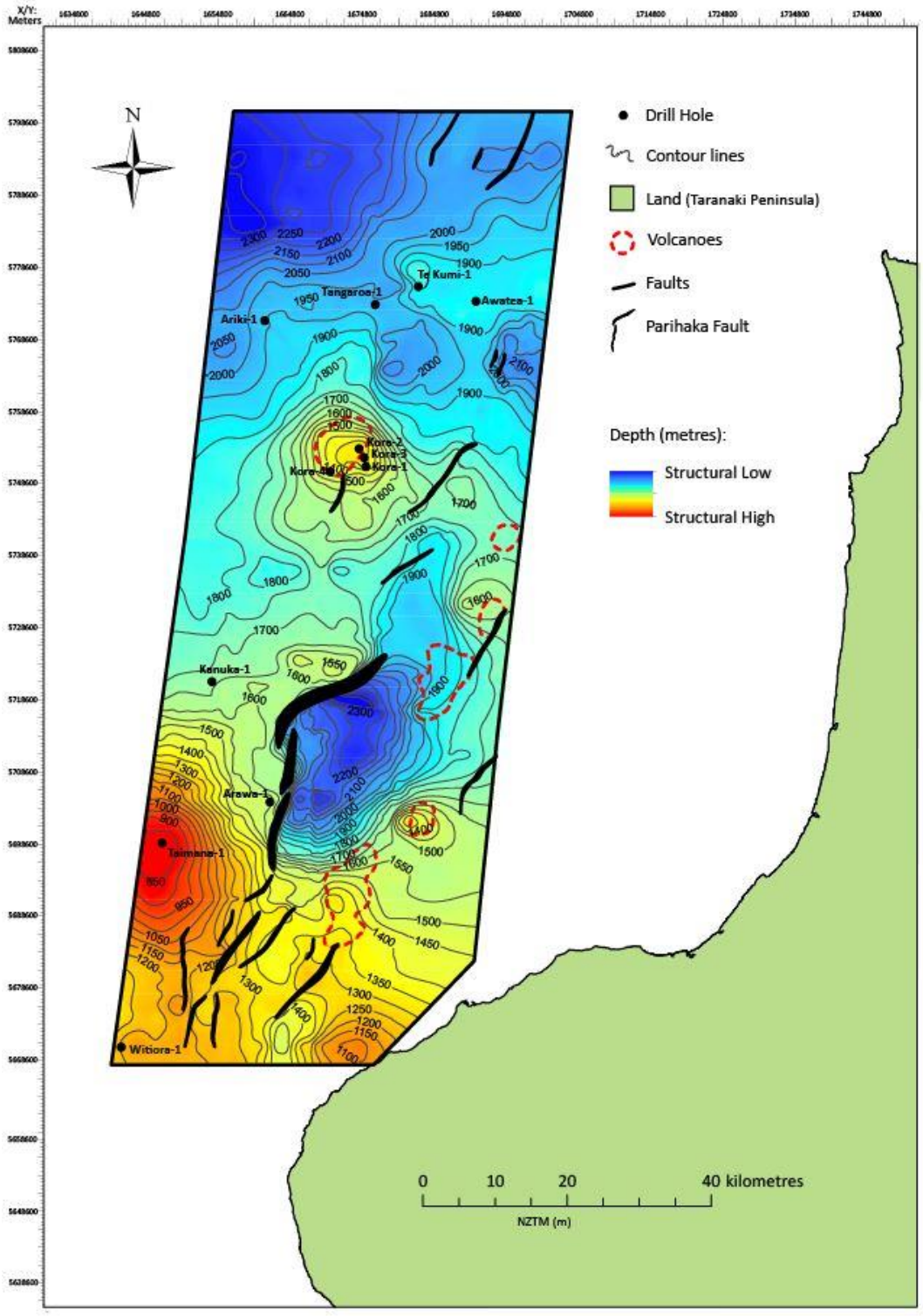

Figure 5.4.1 Structure contour map of the top of the Waipipian Stage boundary (3.0 Ma).

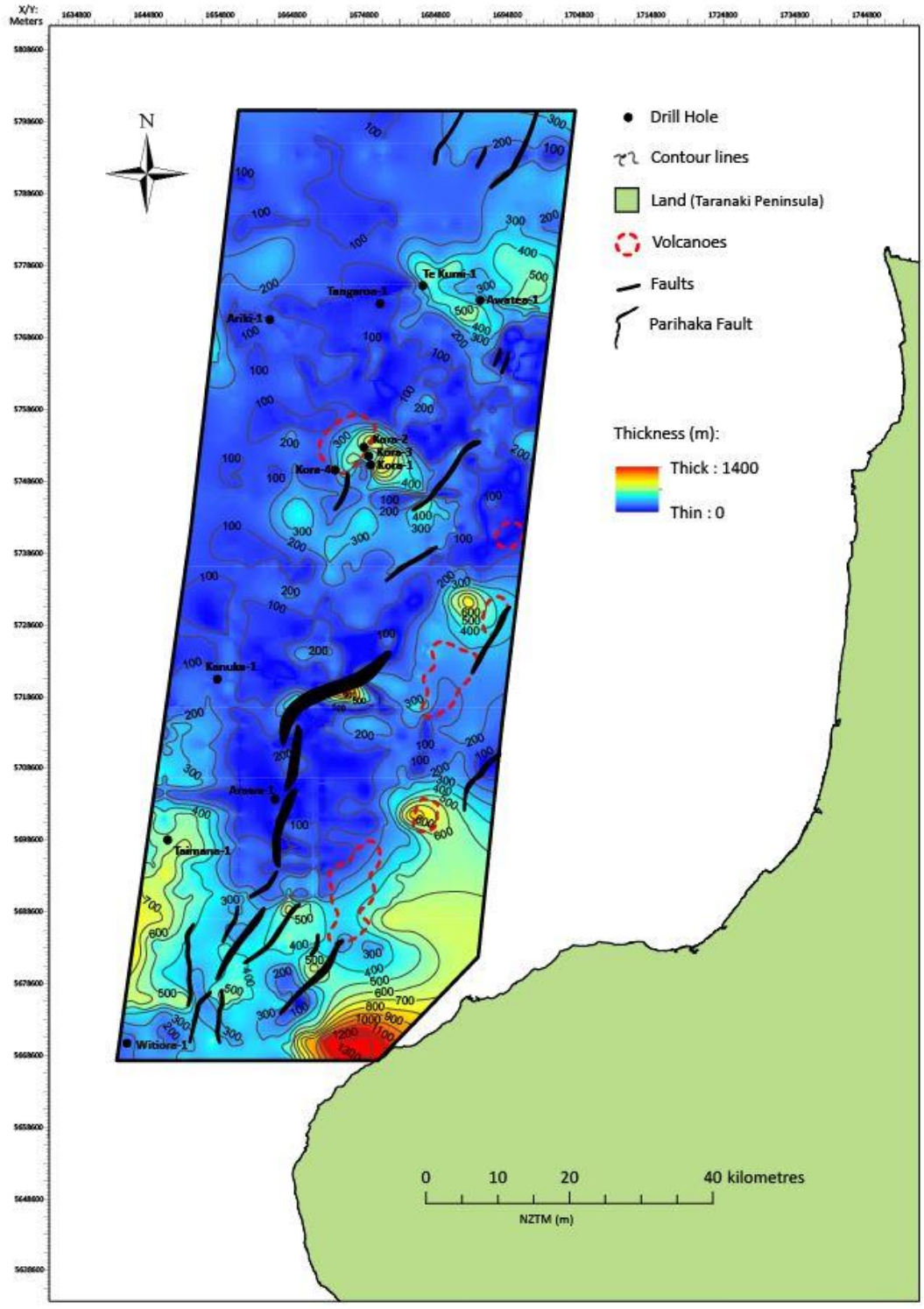

Figure 5.4.2 Isopach of the sediment deposited during the Waipipian Stage (3.6 – 3.0 Ma)

5.5 Top Mangapanian Stage Boundary (2.4 Ma):

5.5.1 Structure Contour Map

The structure contour map of the top of the Mangapanian Stage boundary (2.4 Ma) is presented in Figure 5.5.1. By the end of the Mangapanian Stage, the entire lower half of the study area, including the once prominent Arawa sub basin depocentre, had been infilled by approximately 600-1000 m. The seismically mapped surface presented by the structure contour map shows that a well-defined shelf break had developed oriented WSW/ENE, which deepened rapidly from 1250 m bkb to 1500 m bkb across a steep shelf-slope margin. The structural highs observed at the top Waipipian Stage have largely disappeared and the general pattern shown in Figure 5.5.1 depicts the outbuilding of the continental shelf, and a progression from a shallow shelfal environment in the south east, through a shelf slope break to a deeper basin floor environment in the north west. Offset on the Parihaka Fault is not as significant as seen in previous structure contour maps, with a maximum of ~100-150 m indicated. This is indicative of a decrease in the amount of movement observed on this fault. The few volcanic structures that were still discernible at the top of the Waipipian are no longer visible on this horizon as they have been overtopped with sediment and buried.

5.5.2 Seismic Facies Analysis and Sediment Distribution

During the Mangapanian Stage, sediment deposition was dominated by the GFF prograding across the study area, with the only exception being in the Awatea-1 area, where Mangaa Formation sediments are intersected at this interval (Enclosure 1).

Figure 5.5.2 shows that, although the shelf had prograded rapidly to the north during the Mangapanian, the thickest accumulation of sediment during this time was mainly in the south east, in the area surrounding and including the Arawa sub basin. This sediment pile ranges from 500 to 1200 m thick. This indicates a very large sediment input to the area during the Mangapanian, the rapid infilling of the Arawa sub basin, and subsequent progradation across the shelf towards the northwest, infilling the available accommodation space

In the Mangapanian seismic package, the GFF shows varying characteristics depending on where it was deposited. In the northern half of the study area (Ariki-1, Tangaroa-1, Te Kumi-1, Kora-1), where there was less deposition, the seismic reflection patterns show slightly inclined to sub-horizontal reflectors with variable continuity, likely bottomsets

(Refer to Enclosure 1). In the southern half of study area, bottomsets, progradational reflectors and topsets are all observed. Prograding reflectors are representative of continental slope outgrowth and the inflection point in each clinoform represents the location of the shelf-slope break through time. The different clinoform patterns related to progradation are indicative of varying rates of deposition and overall water depth (Miall, 2013, Mitchum et al., 1977). In the Mangapanian seismic package, a mix of sigmoid and oblique tangential clinoform patterns (complex sigmoid oblique clinoforms) are interpreted (shown in Figure 5.5.3. and on Enclosure 2); Sigmoid clinoforms tend to develop in a shallower environment with a lower sediment supply and relatively low basin subsidence and/or relative sea level rise to allow for the preservation of topsets, whereas tangential clinoforms develop when there is a high sediment supply with rapid deposition, with little to slow basin subsidence and/or a sea level standstill (Mitchum et al., 1977). Topsets are reflector patterns made up of sub-parallel, sub-horizontal, moderately continuous reflectors that were deposited in a shelfal environment. These are illustrated in Figure 5.5.4.

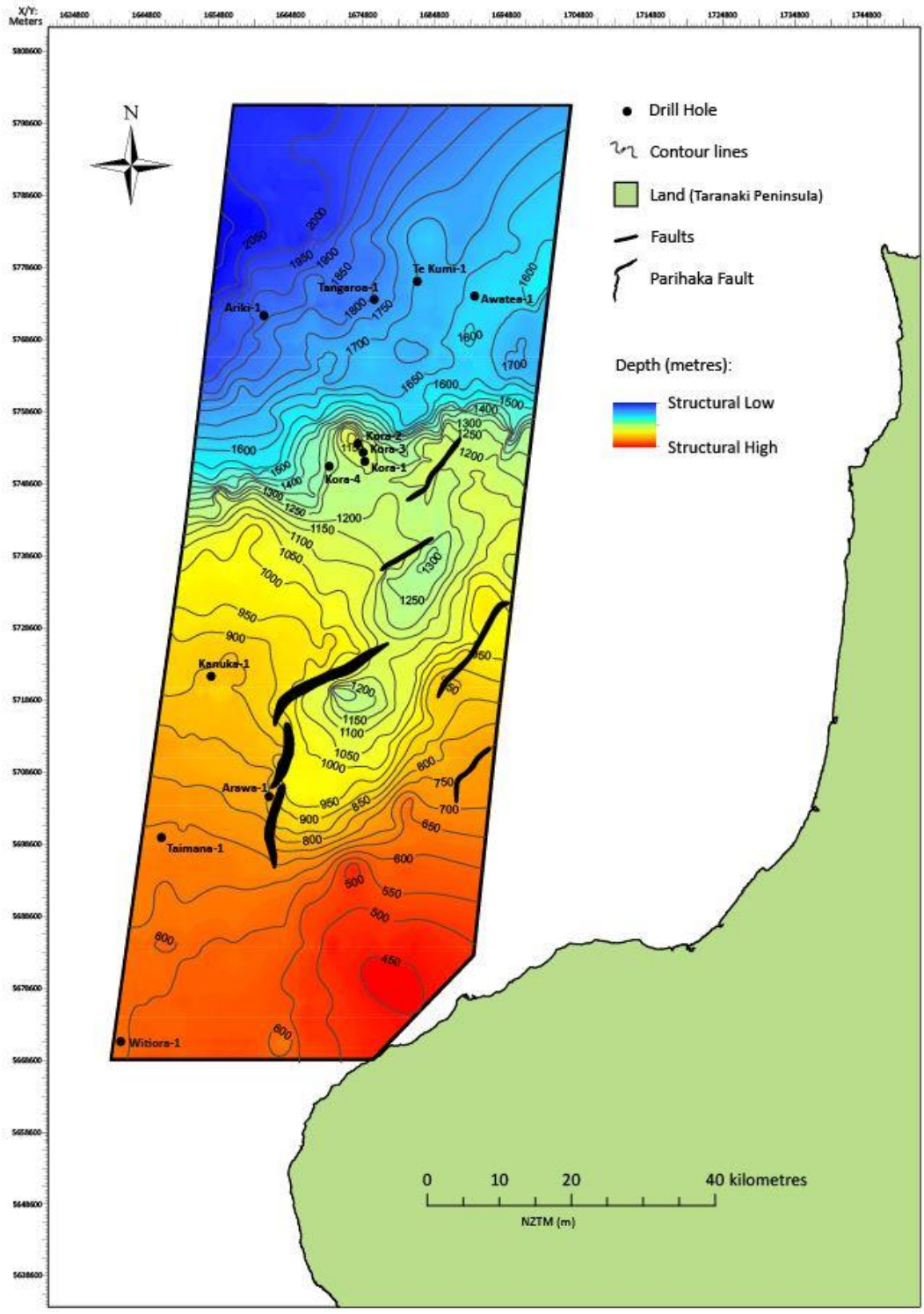

Figure 5.5.1 Structure contour map of the top of the Mangapanian Stage Boundary (2.4 Ma).

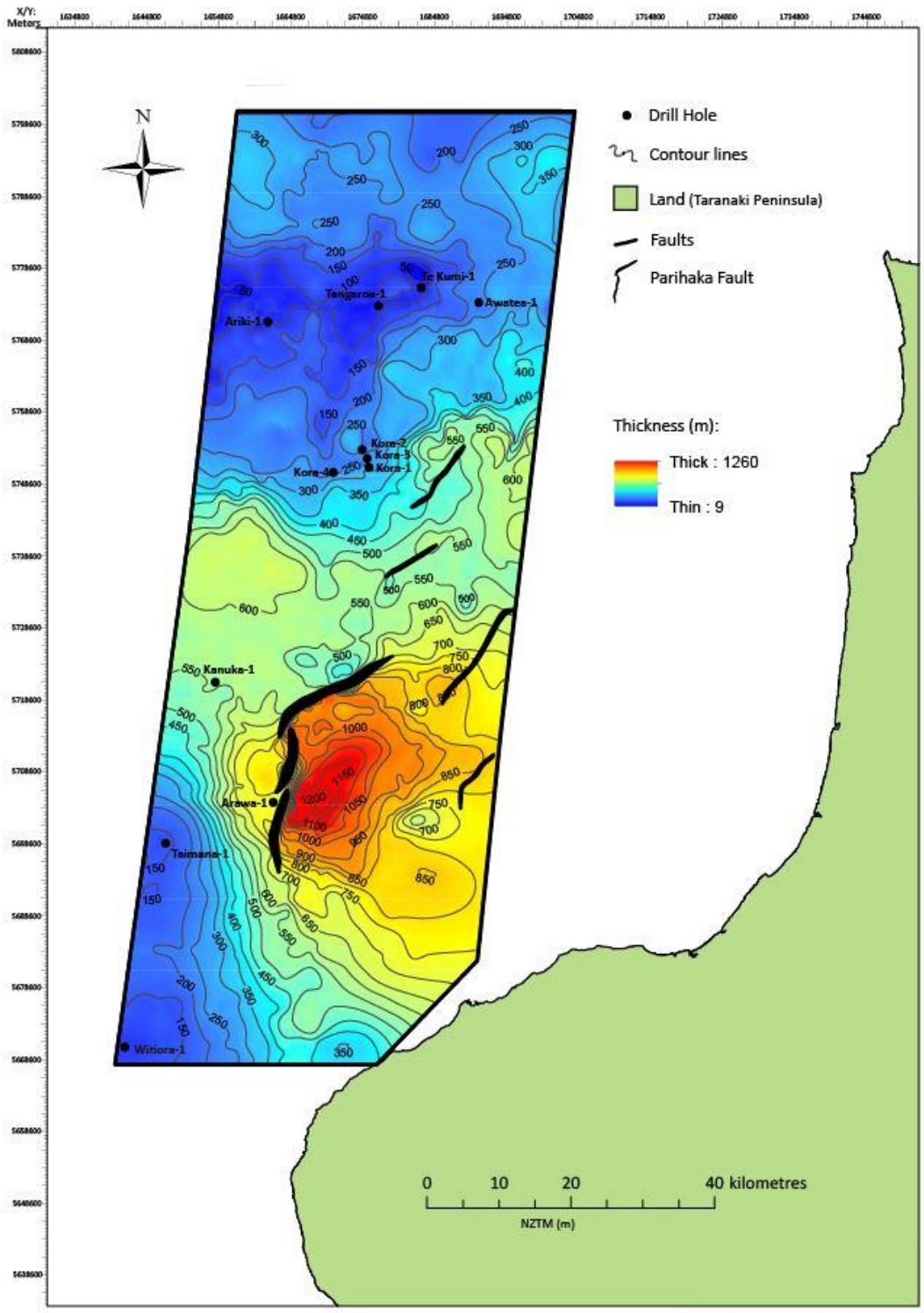

Figure 5.5.2 Isopach map of the sediment deposited during the Mangapanian Stage (3.0 – 2.4 Ma).

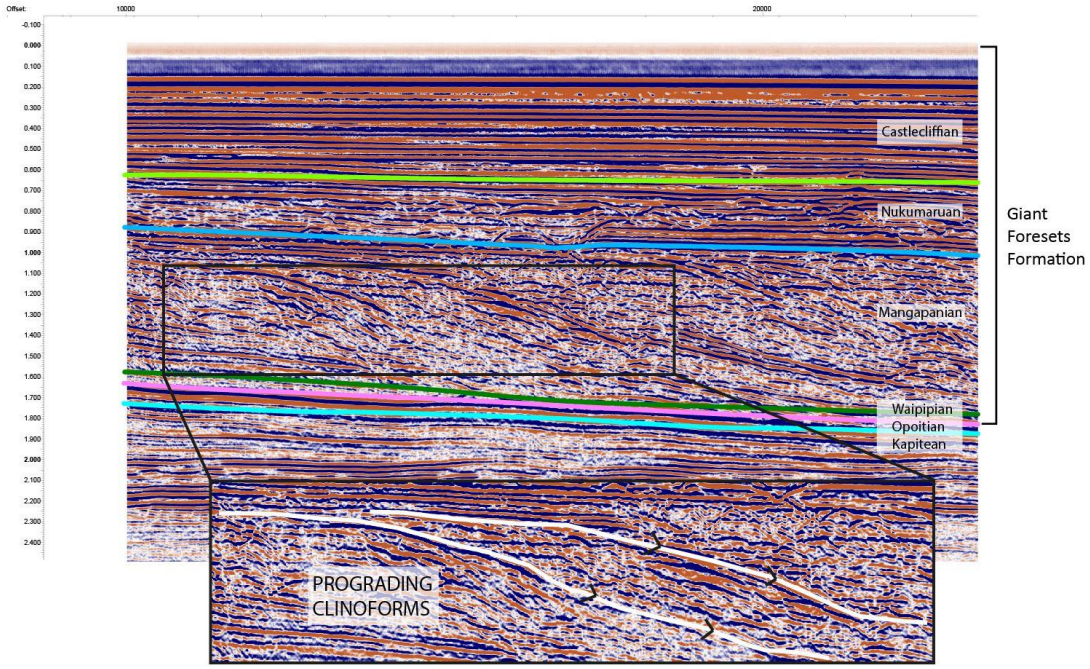

Figure 5.5.3 Image depicting prograding clinoforms of the GFF in seismic profile (Line 81a-04-1018) (Mangapanian Stage).

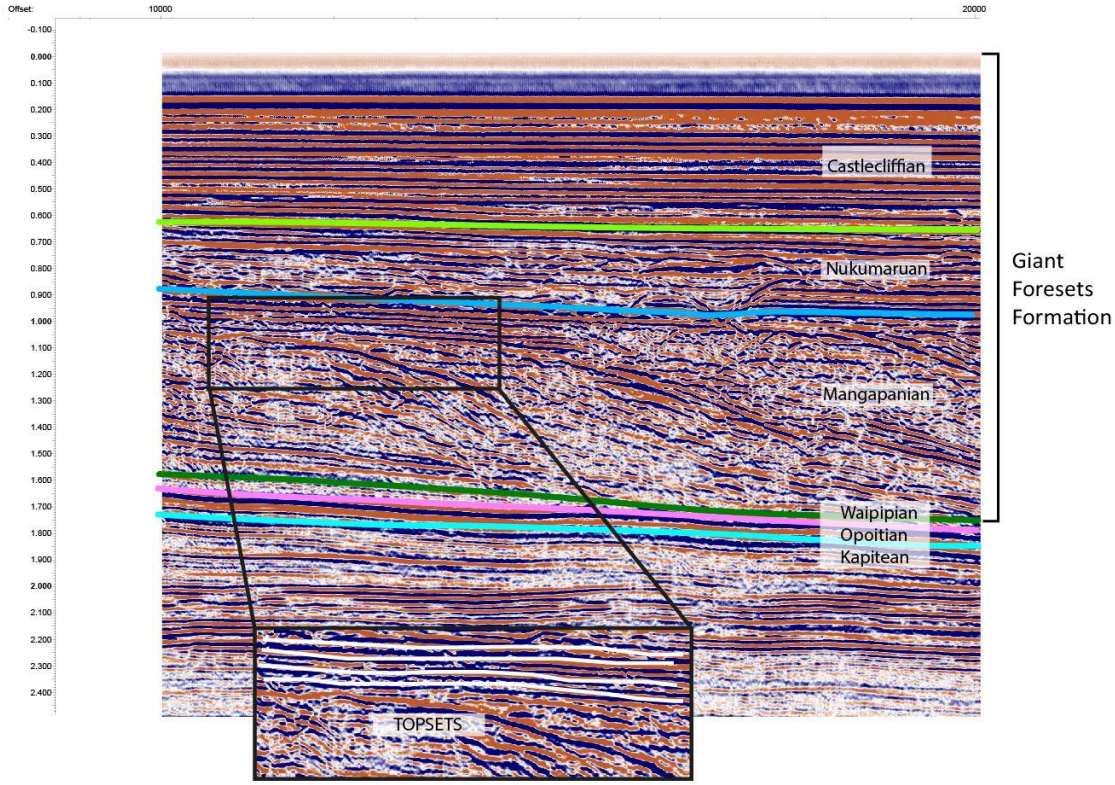

Figure 5.5.4 Image depicting the Mangapanian topsets of the GFF in seismic profile (Line 81a-04-1018).

5.6 Top Nukumaruan Stage Boundary (1.63 Ma)

5.6.1 Structure Contour Map

The structure contour map of the top of the Nukumaruan Stage boundary (1.63 Ma) is presented in Figure 5.6.1. By the end of the Nukumaruan Stage, the northern Taranaki Basin had shallowed considerably, with a 200-700 m bkb difference across the study area when compared with the top Mangapanian Stage horizon observed. The well-developed shelf break continued to move north westward during this time, although its orientation swung to SW/NE direction. The shelf break deepens from 850 m bkb to 1250 m bkb across a steep shelf-slope margin to the west, and a less steep shelf-slope break to the east. A new structural high formed over Taimana-1 well in the south west during this interval. Fault structures are no longer visible on this horizon as they are no longer offsetting the deposited sediment. The general pattern of the top Nukumaruan Stage horizon mirrors the top Mangapanian Stage horizon, progressing from a shallow shelfal environment in the south east, through a shelf slope break to a deeper basin floor environment in the north west.

5.6.2 Seismic Facies Analysis and Sediment Distribution

During the Nukumaruan Stage, the GFF was being deposited over the entire study area (See Enclosure 1).

On seismic lines, progradational foresets (slope deposition) and topsets (shelf deposition) dominate the GFF sedimentary package (Figures 5.6.2 and 5.6.3). Sediment accumulation was concentrated mainly in the slope progradational front (progradational forests), clearly seen in Figure 5.6.4, where sediment thickness ranges from 600 to 1300 m. Much thinner deposits are found on the shelf (topsets) to the south during this time (100-450 m).

In the central part of the study area, immediately south of the Kora holes, is a region of slightly thicker sediment accumulation (550-650 m; Figure 5.6.4). This is in the region of the northern part of the Arawa sub basin/southern part of the Northern Graben, and indicates that these depocentres still had accommodation space at this time.

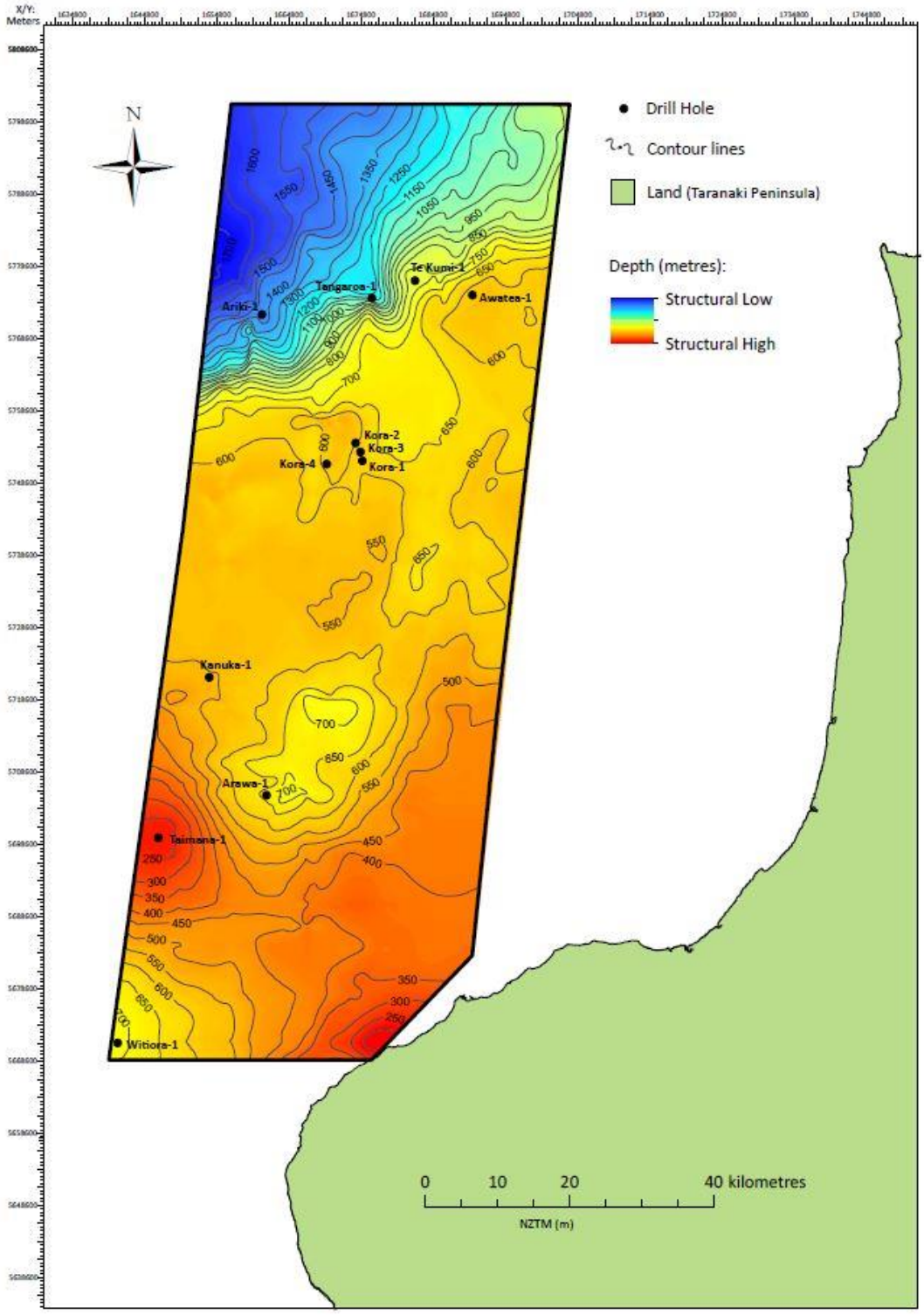

Figure 5.6.1 Structure contour map of the top of the Nukumaruan Stage Boundary (1.63 Ma).

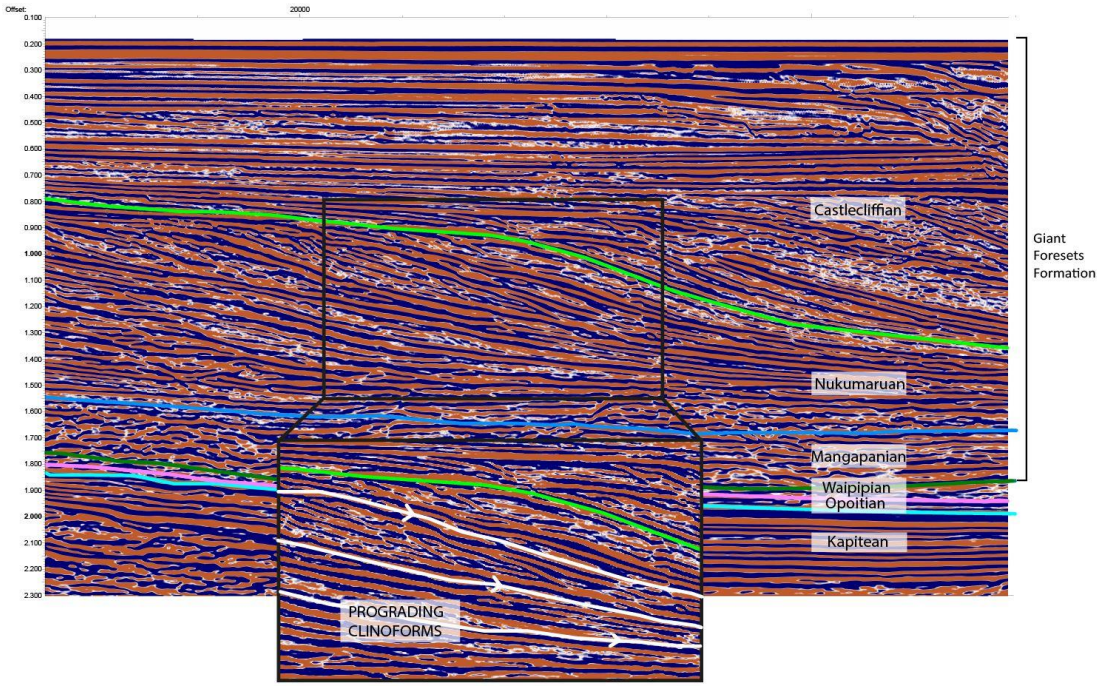

Figure 5.6.2 Image depicting the Nukumaruan prograding clinoforms of the GFF in seismic profile (Line dtb01-03-2847).

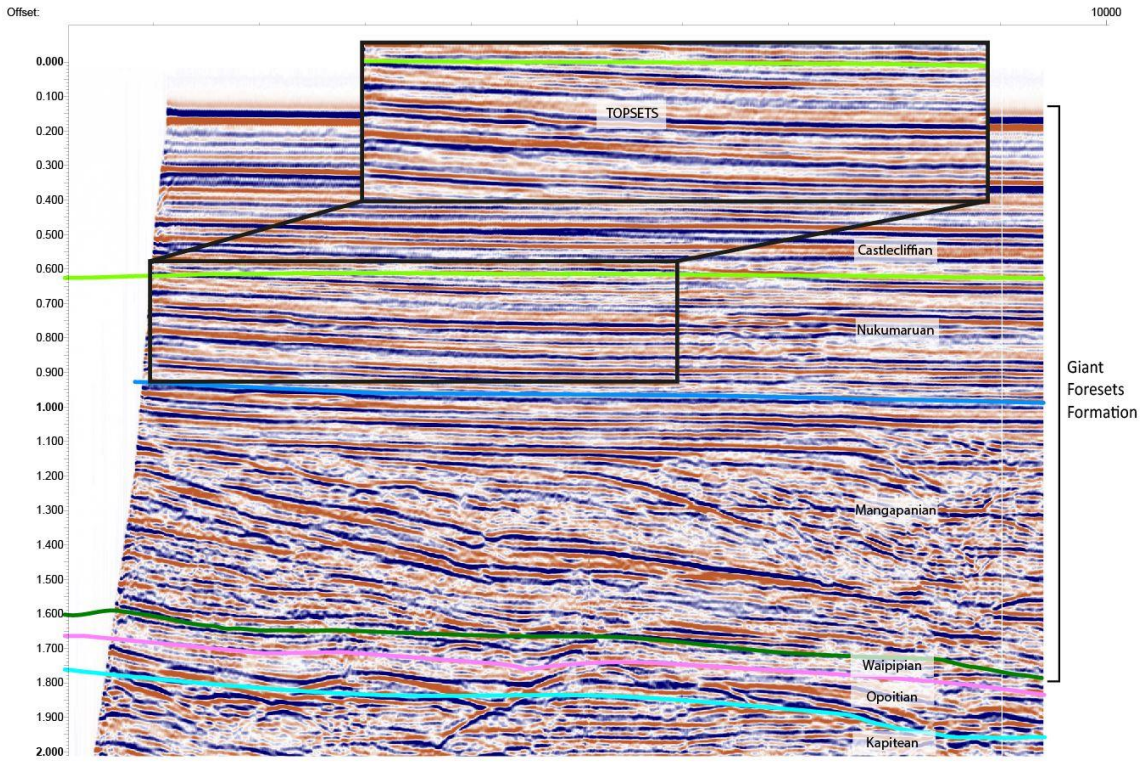

Figure 5.6.3 Image depicting the Nukumaruan prograding clinoforms of the GFF in seismic profile (Line 81a-08-1018).

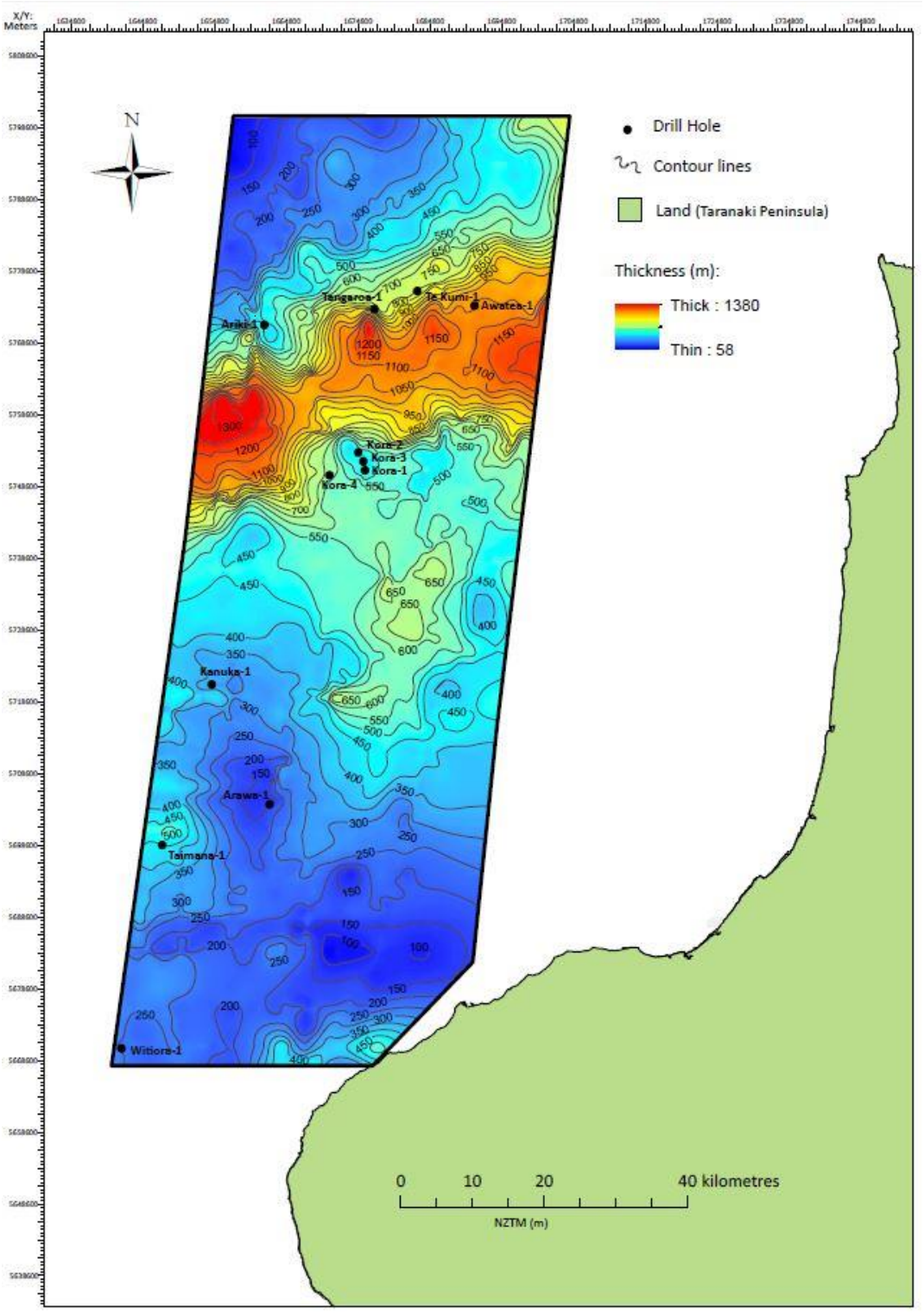

Figure 5.6.4 Isopach map of the sediment deposited during the Nukumaruan Stage (2.4 – 1.63 Ma).

5.7 Top Nukumaruan to Present day Deposition (1.63 Ma – 0 Ma)

5.7.1 Seismic Facies Analysis and Sediment Distribution

From the end of the Nukumaruan Stage to the Present day (Castlecliffian and Haweran Stages), GFF continued to be deposited over the entire study area (Enclosure 1).

In the Nukumaruan-Recent seismic package, the GFF is represented by topsets in the study area, with the occasional degradational foresets (slumped and hummocky slope deposits) identified. Degradational foresets (Figure 5.7.1) have lower amplitude reflectors than that of typical progradational foresets, and are more steeply dipping and show chaotic and irregular internal patterns.

The accumulation of sediment during this period is concentrated across the migrating outer shelf and slope (across Ariki-1, Tangaroa-1 and Te-Kumi-1 holes; See Figure 5.7.2). When comparing the (top) Nukumaruan to Recent isopach map with that of the Nukumaruan isopach (Figure 5.6.4), the shelf break has continued to move in a north west direction, with the most recent isopach map depicting its current position at present. This sediment thickness of the slope package ranges between 600 and 1300 m. Thinner deposits of sediment (200 - 500 m) occur across the broad shelf during this period. A slightly thicker accumulation is oriented along the axis of the Arawa sub basin-Northern Graben alignment (Figure 5.7.2), representative of the continued infilling of these depocentres. Thickness of sediment in this region ranges from 550 to 600 m.

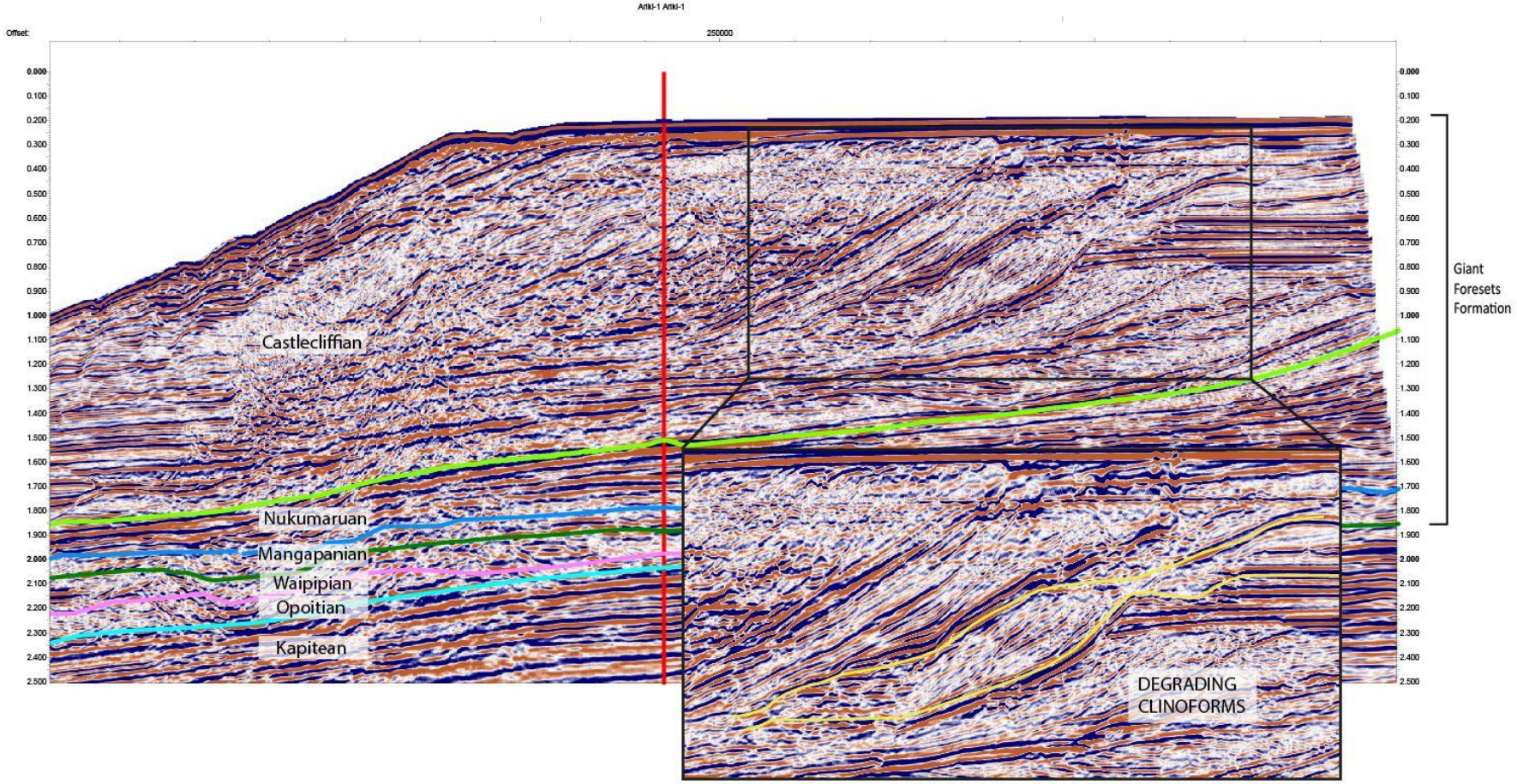

Figure 5.7.1 Image depicting the Nukumaruan prograding clinoforms of the GFF in seismic profile.

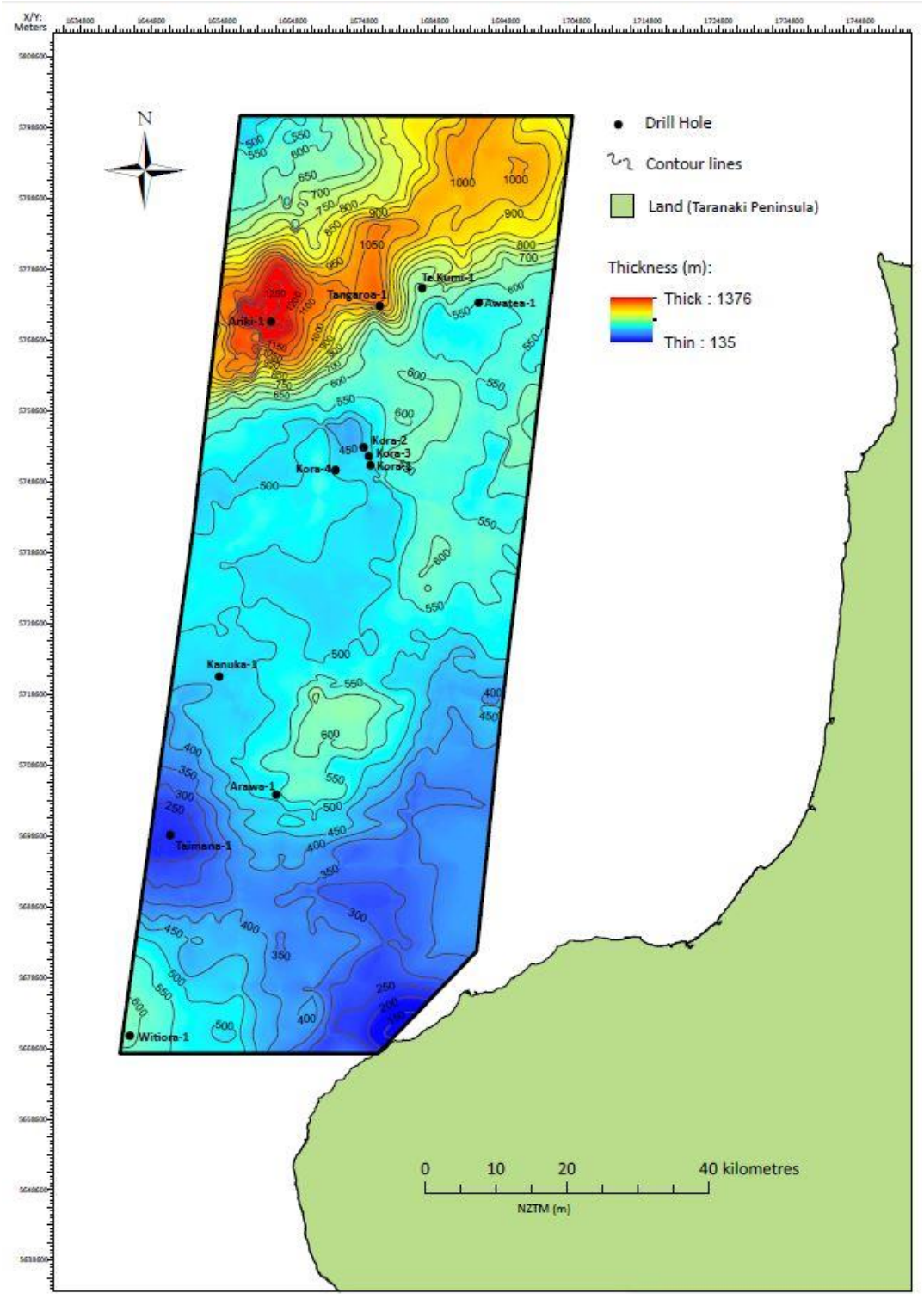

Figure 5.7.2 Isopach map of the sediment deposited from the end of the Nukumaruan Stage to the present day 1.63 – 0 Ma).

6. Synthesis

This chapter sets out to apply the new results obtained from this study to a wider geological setting and pre-existing knowledge base. Objectives presented at the beginning of this thesis will be revisited and addressed in this chapter. The focus is on the evolution of the study area (basin geometry and sedimentation patterns) through time. It will also briefly address the apparent differences between biostratigraphy of the sections in the drill holes and the mapping of seismic reflection horizons between the holes.

6.1 Biostratigraphy versus Seismic Mapping of Horizons between Holes

Biostratigraphy is commonly used as a tool to establish the age of stratigraphic sections and as a means of correlation across an area of interest. By studying the placement and ranges of key index fossils down a borehole, the relative ages of horizons at different depths can be established. These horizons can then be correlated between boreholes within a field of study. In parallel with biostratigraphy, in many cases correlation between these sections in holes can be achieved by the mapping of seismic reflection horizons. However, a significant problem with biostratigraphy is that there is a lack of coherency in inter-bore correlations between these two methods. This can be due to both natural and artificial factors (See Chapter 4). This issue has been recognised in the past and specifically for North Taranaki Basin in the PhD work by Hansen (2003) and reported in papers (e.g. Hansen and Kamp 2004, 2006).

In the PhD work completed by Hansen (2003), seismic horizons representative of Late Miocene to Pleistocene New Zealand stage boundaries, were mapped across 11 wells in the northern part of Taranaki Basin via a grid of 32 seismic reflection profiles, based on an in-depth analysis of the biostratigraphy found in each borehole. The boundaries mapped in every well section were qualitatively assigned a confidence level (high, medium, or low). High to moderate confidence levels were assigned to the boundaries that were defined by good age-diagnostic criteria, whereas low confidence levels were assigned to the stage boundaries that had poor age-diagnostic criteria (Hansen, 2003). Other authors placed confidence levels on their own biostratigraphy, at various stage boundaries or at certain depths. This pre-existing information is illustrated on Enclosure 1.

This study took advantage of this biostratigraphic analysis, which identified that Ariki-1 gave the best quality determination of New Zealand stage boundaries of all the holes in North Taranaki Basin. This was followed by the quality of biostratigraphy in Arawa-1. The

reasons for the better quality biostratigraphy in these two holes is probably associated with their more western and hence oceanic water mass conditions and hence the better representation of planktic foraminiferal content upon which the New Zealand stage classification is based. The other holes in this part of Taranaki Basin give variable levels of biostratigraphic resolution and confidence, but were used as a supplementary control in the seismic mapping. This study employed a similar technique to Hansen, but instead utilized 175 2D seismic reflection profiles and one 3D seismic survey (Parihaka-3D), in order to 'seismically' map the NZ stage boundaries between 15 well sections. This provided a more extensive data set, and thus the ability to more accurately document the distribution and progradation of the sediment fill through the defined stages. The depth of the newly mapped key seismic horizons between holes in this study is illustrated as a comparison with prior biostratigraphic studies on Enclosure 1, and effectively summarises the age model for the Pliocene-Pleistocene section in the basin.

In comparing the biostratigraphically defined stage boundaries (Hansen, 2003/2006) with the seismically placed stage boundaries of this study, a number of discrepancies were identified (Chapter 4). In some cases, the biostratigraphy matched well with the seismic horizons; for example, the seismically mapped boundaries in Arawa-1 in this study line up accurately with the biostratigraphic stage boundaries investigated in Hansen (2003), with a maximum difference of only 50 m. The seismic boundaries interpreted in Ariki-1 and Tangaroa-1 align closely with the Tk, Wo, Wp and Wm (seismic) stage boundaries identified in Enclosure 1, but the top Wn Stage seismic horizon is not well defined biostratigraphically, generally as a result of a lack of age-diagnostic criteria in this interval. Some wells have stages which align closely with the biostratigraphy and others that do not. For example, the differences in Taimana-1 well range from only 30 m (top Tk boundary) to a significant difference of 271 m (top Wp boundary). Other wells in the study area have very poor correlation between the biostratigraphically and seismically-determined boundaries; none of the seismically mapped boundaries in Kora-1 match the biostratigraphic boundaries of Hansen (2003), with differences in depth downhole ranging from 112-275 m (Enclosure 1). This is a result of both the biostratigraphic control in this study for Kora-1 having to be relaxed in order for the loop ties to match up across the field area, as well as the sparse foraminifera throughout the well strata causing the ages within the well to be assigned with less confidence (Chapter 4). Awatea-1 shows the greatest inconsistencies in boundary depths when compared with the biostratigraphically-determined boundaries outlined in Hansen (2003). The seismic boundaries are

significantly deeper downhole than their correlative biostratigraphic boundaries, with differences ranging from 85 m to 405 m. This is likely a result of the complications of faulting in the area and the volcanics on the eastern side of the study area, which make loop-tying more difficult.

While there are inconsistencies when comparing the biostratigraphically defined boundaries with seismically mapped boundaries, the real uncertainty comes from the inability to place the initial biostratigraphic boundaries with confidence, due to a paucity of age-diagnostic foraminifera.

In the context of seismic reflection mapping, these uncertainties and inconsistences are not an issue, so long as the reflection horizons can be mapped throughout the basin, the age of those horizons can chiefly rely upon the best quality biostratigraphy, even if that is limited to one or two records. This is effectively the approach taken in this thesis mapping.

6.2 Northern Taranaki Basin Evolution

Taranaki Basin initially formed during the Late Cretaceous (Haumurian) as an oblique rift concurrent with sea floor spreading in Tasman Sea. During the Late Palaeocene, and following the end of sea floor spreading in Tasman Sea (57 Ma), Taranaki Basin became tectonically quiescent, with slow regional subsidence and marine onlap, which continued through to the Early Oligocene. The earliest part of the Oligocene (Lower Whaingaroan) was characterised by paraconformity development over significant parts of Taranaki Peninsula and South Taranaki Basin, and minimal sediment accumulation. At the beginning of the Late Oligocene (Upper Whaingaroan) plate motions across New Zealand changed from transtensional to transpressional, causing the initiation of Hikurangi subduction in eastern Northland and Bay of Plenty areas. Alpine Fault offset also started at this time, reflecting early development of the Australia-Pacific plate boundary zone.

6.2.1 Mid-Late Miocene (Waiauan – Kapitean)

This study has been focused on evolution of North Taranaki Basin from mid-Late Miocene (Waiauan – Kapitean Stages) to present day. Taranaki Basin formed as a foreland basin through the Late Oligocene and Miocene and during the latest Miocene, extension developed in North Taranaki Basin, expressed in the development of normal fault offset and in the depocentres created that are traced along an axis oriented from south west to north east. Giba *et al*., (2010) places the timing of the initiation of normal faulting (coinciding with the creation of the extensional features) at approximately 12 Ma,

although Hansen and Kamp (2004) place the development of the extensional Northern Graben around the Late Miocene- Early Pliocene (6.5 – 5.3 Ma) as marked by offset on Kahawai Fault. This study, through the top Kapitean structure contour map, illustrates that several depocentres were present in the study area, including the prominent Arawa sub basin, by this time. This is indicative that the Northern Graben had already started developing before the end of the Kapitean Stage (5.3 Ma), and therefore supports the ages presented in other studies.

Sediment deposited during the Kapitean has been offset by as much as 600 m on Parihaka Fault, a prominent structural feature making up the western flank of the Arawa sub basin (see Lines 1 and 2, Enclosure 2). Giba *et al.,* (2012) express that although the initial displacement on Parihaka Fault occurred during the Cretaceous to Paleocene in response to west-east extension, the fault was obliquely reactivated around 3.7 Ma during the early Pliocene.

During the Kapitean, both Manganui/Urenui formations and Mohakatino Formation were deposited in different parts of the basin. This is shown by the well logs on Enclosure 1; Manganui /Urenui Formations (both bathyal mudstone) are intersected in several holes in the south west (Arawa-1, Taimana-1), and Mohakatino Formation (volcaniclastic siltstone, mudstone and some sandstone) is intersected in several wells in the north western half of the study area (Ariki-1, Tangaroa-1, Te Kumi-1, Awatea-1). The deposition of the mud-dominated Manganui/Urenui formations is indicative of a basinal environment that existed in northern Taranaki Basin during this period. A basin floor environment is evident in the Kapitean structure contour map (Figure 5.2.1), which shows that the majority of the study area resided at a lower bathymetry bkb. An exception to this is the structural high depicted in the vicinity of Witiora-1. In Strogen et al 2011 (Figure 2.4), the paleogeographic map for 5.0 Ma illustrates the presence of a large fan lobe in this area as a result of significant amounts of sediment being fed to this site, and thus explaining the presence of the structural high at Witiora-1.

6.2.2 Opoitian-Waipipian

The development of the Northern Graben caused local changes in basin physiography, with sediment funnelled into, and being trapped within, this depocentre. Consequently, sediment was unable to reach the areas beyond the graben. The continuing subsidence of the graben in the early Pliocene (Opoitian) focused sediment dispersal along the axis of the structure (Salazar *et al.,* 2015). The volcanic massifs which were extinct (for the

most part) during this time, also played a role in directing sediments to the north, due to a series of paleohighs that had been created during their active phase (Hansen and Kamp, 2002). This idea of focused sedimentation is represented through the deposition of the Mangaa Formation, which accumulated as sandy basin floor fans in the north east of the study area. The isopach map for the Opoitian Stage (5.3-3.6 Ma) illustrates a concentration of sediment along the axis of the graben, which supports this concept (Figure 5.3.4). The sediment was most likely sourced from uplift and erosion of the landmass to the east in the King Country (Hansen and Kamp, 2002). By the end of the Opoitian stage (3.6), the Arawa sub basin had become fully enclosed, due to the deposition of these lobes. This can be observed when comparing the top Kapitean structure contour map (Figure 5.2.1), which has several linked depocentres, and the top Opoitian structure contour map (Figure 5.3.2), which illustrates the enclosed Arawa sub basin as the prominent depositional low.

During the Opoitian, numerous formations were being deposited simultaneously. Manganui Formation (bathyal mudstone) was still being deposited in the southern half of the study area. In the north west and in distal parts of the study area relative to Taranaki Peninsula, the Ariki Formation (calcareous marl) had begun to accumulate. Both Manganui Formation and Ariki Formation were deposited in a basin floor depositional environment, evidenced by the top Opoitian structure contour map (Figure 5.3.2), which shows structural lows across the majority of the study area. The thicker areas of sediment deposition on the isopach map (Figure 5.3.2), within the Northern Graben, represent deposits of Mangaa Formation basin floor fans.

The majority of wells located in the study area record only a very thin Opoitian to Waipipian succession (Enclosure 1). This hiatus from sediment deposition is clearly observed on the Waipipian isopach map (Figure 5.4.2) as well as on seismic (Lines 1-4, Enclosure 2). This thin Wo-Wp succession provides evidence that sediment was being deposited somewhere else during this time; although there was large sediment input from the erosion of the Southern Alps at this time, this sediment was isolated from North Taranaki Basin due to rapid subsidence in Wanganui Basin and in Central Graben. Sediment was funnelled into these depocentres, resulting in sediment starvation in northern Taranaki Basin (Hansen and Kamp, 2004). The cessation of active andesitic volcanism around this time also diminished the local supply of volcaniclastic sediments to the basin floor (Hansen and Kamp 2004). However, sedimentation towards the end of the Waipipian began to outpace accommodation created by subsidence, and the shelf-slope

wedge slowly started to prograde northward into the study area (Hansen and Kamp, 2002). Despite the sediment hiatus across the majority of the northern Taranaki Basin during this time, this idea of the initiation of progradation into the northern basin is supported by both the top Waipipian structure contour map (Figure 5.4.1) which shows structural highs in the bottom of the study area in the vicinity of Taimana-1, and the Waipipian isopach map (Figure 5.4.2), which shows patches of thicker sediment in the same area.

From the Waipipian isopach map (Figure 5.4.2), the approximate location of the (top Waipipian) shelf slope break was determined in Figure 6.1. To confirm the approximate location of the shelf break at this time, the depositional environment as determined by biostratigraphic analysis for Taimana-1, was examined. In the well report (Diamond Shamrock Exploration Oil Co (NZ), 1984), by the end of the Waipipian, Taimana-1 well site was shelfal, with the shelf break being north of this point.

While volcanic massifs had mostly been buried by accumulating sediment by the end of this period, they still formed positive relief on the sea floor, and likely continued to influence the direction of sediment flow, as well as sediment onlapping onto the flanks of the volcanoes themselves. The Parihaka Fault continued to offset Waipipian sediment (Figure 5.4.1 and Enclosure 2), which indicates that this fault was still active during this period.

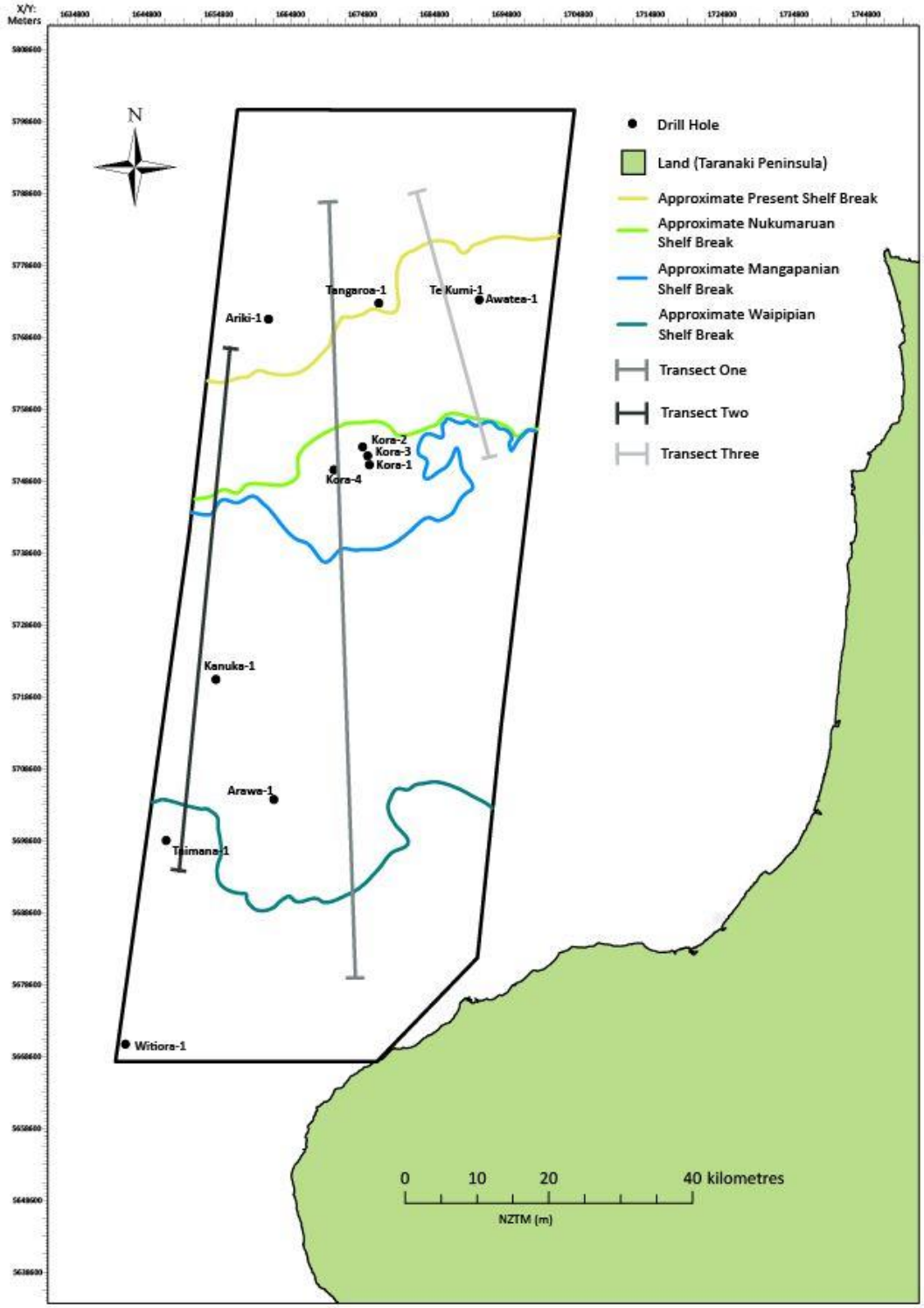

Figure 6.2. Approximate locations of the shelf slope break through the Pliocene and Pleistocene.

6.2.3 Mangapanian

Driven by Late Cenozoic convergence between the Australian and Pacific plates, rapid uplift of the Southern Alps triggered an influx of sediment into Taranaki Basin at this time (Tippett and Kamp, 1995). Amongst other affects, this caused the Arawa sub basin to be rapidly infilled, and by the end of the Mangapanian Stage (2.4 Ma), it was almost entirely infilled. Thick accumulations of sediment also occur in other parts of Northern Taranaki Basin as evident on the Mangapanian isopach map (Figure 5.5.2)**,** with the sedimentary pile ranging from 500 to 1200 m thick. This compares with much lesser thicknesses that accumulated during the Waipipian (Figure 5.4.2).

The increased sediment supply to the basin during the Mangapanian caused sedimentation to exceed subsidence. Infilling and overtopping of the Wo-Wp depocentres led to progradation of the shelf-slope margin towards the northwest, formation of a defined shelf-slope break that is clearly imaged on the structure contour map (Figure 5.5.1) and internal progradational stacking patterns (clinoforms) that are indicative of steady progradation into a deep basin (Hansen and Kamp, 2004; Hansen and Kamp, 2006; Salazar *et al*., 2015;).

The position of the top Mangapanian shelf break can be observed on Figure 6.1 by the bright blue line. Comparison of the location of the Waipipian shelf break with the Mangapanian shelf break illustrates that it prograded a large distance (approximately 55 km) relatively quickly (in 0.77 m.y.). This idea is further explored by looking at the rate of progradation across different biostratigraphic stages on Transect 1 (Figure 6.1), represented graphically in Figure 6.2. Progradation through the Mangapanian (blue line) is more rapid (55 km/0.6 m.y. = 91 mm/k.y.) than the Nukumaruan (17 km/0.77 m.y. = 22 mm/k.y.) (green line) and the Recent propagation (12 km/1.63 m.y. = 7.3 mm/k.y.) (yellow line) (Figure 6.2).

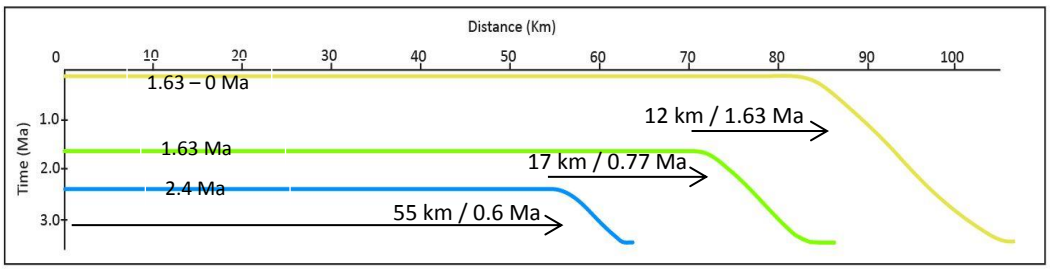

Figure 6.3 Progradation rates, Mangapanian-Recent, Transect 1 (see Figure 6.1). The end Mangapanian is represented by the blue line, the end Nukumaruan by the green line, and Recent progradation by the yellow line.

The indent in the progradational front of the Mangapanian shelf break, illustrated in Figure 6.1, is indicative of the fact sediment was still accumulating in the Arawa sub basin at this time. However, whilst the shelf-slope break was still prograding north westward, it was not doing so at a constant rate in the centre of the study area when compared with the progradational rates either side of this depocentre. This is depicted by comparison of Transect 1 with Transect 2. On Transect 1, the shelf break migrated at a rate of 91 mm/k.y. However, on Transect 2, a rate of 70 mm/k.y. has been calculated. This suggests that even though the Arawa sub basin depocentre had to be infilled and essentially overtopped in order for the progradation of the shelf front to occur through the central region of the study, progradation was actually faster in this area than on the sides of the depocentre.

During the Mangapanian Stage, the Giant Foresets Formation was being deposited across the entire study area (Enclosure 1). The Giant Foresets Formation is illustrated in seismic reflection lines during this time as bottomsets in the northwest, topsets on the shelf (Figure 5.5.4) but more importantly as prograding clinoforms across the slope (Figure 5.5.3). When sediment supply exceeds the accommodation space available on the continental shelf, sediment is transported to deeper water beyond the shelf break, producing the foreset and bottom-set packages. Beggs (1990) suggests that sea level lowstands are likely to produce foresets and bottom-sets due to the lack of accommodation space on the shelf. The different clinoform patterns observed are indicative of varying rates of deposition and overall water depth (Miall, 2013, Mitchum et al., 1977). Sigmoid clinoforms tend to develop in a low bathymetry setting with a low sediment supply and relatively low basin subsidence and/or relative sea level rise to allow for the accumulation of topsets, whereas tangential clinoforms develop when there is a high sediment supply with rapid deposition, with no to slow basin subsidence and/or a sea level standstill. In the Mangapanian section, this study shows a mix of sigmoid and

oblique tangential clinoform patterns (complex sigmoid oblique clinoforms) (Figure 5.5.3, Enclosure 2). This is due to a combination of these two scenarios. During this time, the North Taranaki Basin continued to uniformly subside at a slow rate (King and Thrasher, 1996), which corresponds to the development of sigmoidal clinoforms; however there was a very high sediment supply from the Southern Alps (Tippett and Kamp, 1995) and likely the eastern hinterland, which corresponds to the growth of tangential clinoform patterns.

Normal faults within the study area do not show great offset in the Mangapanian. This is evidenced on Lines 1 and 2 on Enclosure 2 on the major Parihaka Fault structure, with a maximum of ~100-150 m offset, as opposed to approximately 600 m offset during the Kapitean - Waipipian. This is indicative of a decrease in the amount of movement observed on this fault during this interval. Giba et al., 2010, state that from 4 Ma, the displacement rates of the normal faults in northern Taranaki Basin slowed significantly and then had completely ceased at 2 Ma. The evidence found in this study supports this conclusion.

By the end of the Mangapanian Stage, volcanoes no longer interfered with sediment patterns. This is evident on the top Mangapanian structure contour map, where the volcanic massifs are no longer observed as they have been overtopped and buried by the prograding continental wedge (Figure 5.5.1). The burial of these volcanic massifs coincides with cessation of active volcanism in the northern half of the study area, with volcanism shifting eastward onto Taranaki Peninsula during the Pleistocene, and thus no longer affecting the sediment distribution in the basin (King and Thrasher, 1996).

6.2.4 Nukumaruan

Progradation of the shelf-slope break toward the north west continued through the Nukumaruan Stage, however at a slower rate. This is shown clearly on Figure 6.1 (green line), with the Nukumaruan shelf break located just basinward of the Mangapanian shelf break. The Arawa sub basin at this time had been infilled and hence sediment prograded to the shelf edge and beyond. On Transect 1, the rate of progradation is calculated to be 17 km/0.77 m.y. (22 mm/k.y.). On Transect 2, it is 5 km/0.77 m.y. (6.4 mm/k.y.) and in Transect 3 it is 2 km/0.77 m.y. (2.5 mm/k.y.). These variable progradation rates clearly show that during the Nukumaruan, the Arawa sub basin was less significant as a depocentre that it had previously been.

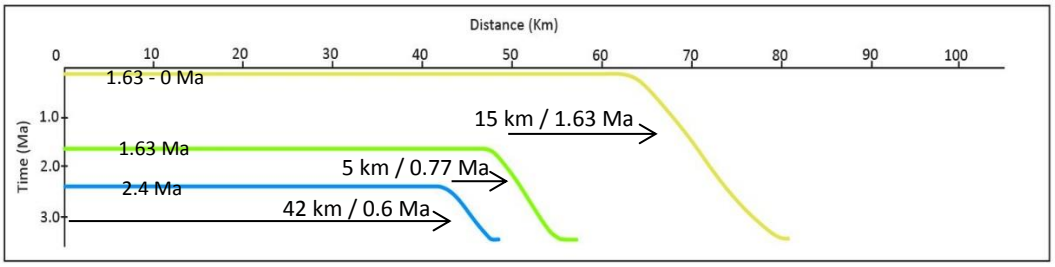

Figure 6.3 Progradation rates, Mangapanian-Recent, Transect 2 (see Figure 6.1). The Mangapanian is represented by the blue line, the Nukumaruan by the green line, and Recent progradation by the yellow line.

Normal faults do not visibly offset strata within the study area at the end of the Nukumaruan Stage. This is evidenced on the top Nukumaruan structure contour map (Figure 5.6.1), as well as on the seismic lines interpreted in Enclosure 2. This is supported by studies completed by Giba et al., 2010, who state that movement along the normal faults in the northern Taranaki Basin had completely ceased by 2 Ma.

6.2.5 End of the Nukumaruan - Present Day

From the end of the Nukumaruan Stage to the Present Day (Castlecliffian and Haweran Stages), the shelf break has continued to prograde in a north westward direction. The isopach map depicting sediment thickness for this interval (Figure 5.7.2), was used to confirm the present day shelf break. This is represented by the yellow line on Figure 6.1. This figure also illustrates that the shelf break re-oriented to a more SW/NE trend, compared with the WSW/ENE orientation of the Nukumaruan shelf slope break. This is indicates that the rates of progradation across the recent shelf-slope break were faster on the eastern side of the study area than those across the central and western sides. The idea of uneven progradation rates is visually represented when comparing the rates of progradation for the Nukumaruan to Recent on Transects 1 and 2 (Figures 6.2 and 6.3) with those on Transect 3 (Figure 6.4). Figure 6.2 illustrates that the shelf slope break prograded towards the north west along transect 1 at 12 km /1.63 m.y, and Figure 6.3 illustrates that the shelf slope break prograded towards the north west along Transect 2 at a similar rate of approximately 15 km/ 1.63 m.y. However, Figure 6.4 illustrates that the shelf slope break prograded towards the north west along transect 3 at 25 km /1.63 m.y. almost double the rate of the progradation across Transects 1 and 2.

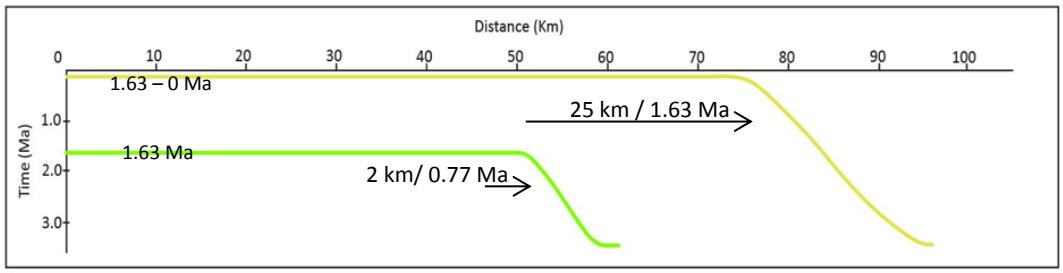

Figure 6.4 Progradation rates, Nukumaruan-Recent, Transect 3 (see Figure 6.1). The Nukumaruan is represented by the green line, and Recent progradation by the yellow line.

In the Nukumaruan-Recent section, the Giant Forests Formation is mainly represented by topsets across most of the study area, with some thick degradational foresets across the shelf slope break (Figure 5.7.1). Degradational foresets are differentiated from progradational foresets on the steepness of the slope. Where the slope angle exceeds ~3°, slope instability causes mass failures and secondary movements of sediment to greater water depths, creating distinctive degradational features (Beggs, 1990). These are characterised by steeply dipping, low amplitude reflectors which show chaotic and irregular internal patterns. The seismically distinct chaotic character of these upper units compared with those of Mangapanian and Nukumaruan age, as well as the increased thickness of this sediment package (Figures 5.7.1 and 5.7.2, Enclosure 2), is suggestive of an increased input of sediment from the contemporary shelf (Hansen and Kamp, 2002). Studies completed by Anell and Midtkandal (2015) support the concept that a lowering of sea level causes the shoreline to migrate out to or near the shelf edge, resulting in an increased input of coarser grained siliciclastic material and a greater chance of over steepening and overall shelf collapse. With the shoreline more proximal to the shelf slope break, this results in higher shoaling wave energy, causing scouring and general erosion of the foresets. These ideas provide a reason why the degradational patterns are observed during this time. Progradation of the shelf slope break is continuing in the present day.

7. Summary and Conclusions

7.1 Overview

This thesis explored the development of the Late Miocene to Recent part of a portion of North Taranaki Basin. In particular, focus was given to the basin geometry and sedimentation patterns for the Late Cenozoic section, primarily through seismic reflection profile mapping. The age model appeals to biostratigraphic data reported in petroleum reports and in papers. This study aimed to improve on prior investigations that were based on paper-based seismic reflection mapping (Hansen, 2003). The seismic reflection mapping used Kingdom ™ industry-standard software, made available to the research group via an academic licence.

This chapter begins by re-stating the objectives for this study, followed by a brief overview of Taranaki Basin. The following sections present a chapter by chapter summary with conclusions from each chapter identifying the key findings.

7.2 Project objectives

This thesis had 3 main objectives:

- To seismically map a series of horizons within part of Northern Taranaki Basin to better understand the structural and sedimentation history of the basin, using existing biostratigraphy to select and date the mapped horizons.
- From these new data, create a suite of structure contour and isopach maps that illustrate the basin evolution and structure.
- Compare the results of seismic mapping with the results of previous basin investigations.

7.3 Chapter 2: Geological Setting

Taranaki Basin formed in the Late Cretaceous, initiated by the mid-Cretaceous break-up of New Zealand from Gondwanaland. During the Eocene, Taranaki basin accumulated a non-marine to shelf marine stratigraphic succession, deepening to outer-shelf and slope depths in Northern Taranaki Basin (Turi Formation). The Late Oligocene marked the beginning of the change into a transpressional tectonic regime, with the development of Taranaki Basin as a foreland basin. In the Late Miocene, the development of mild extension in Northern Taranaki Basin caused the formation of the Northern Graben, a significant structural feature, which had a major influence on subsequent sedimentation.

A massive increase in sediment flux from the erosion of the Southern Alps during the Pliocene and Pleistocene infilled and overtopped the subsiding area, and caused the eventual progradation of sediment across the northern basin to form a shelf-slope system.

7.4 Chapter 3: Data and Methods

The data and methods outlined in this chapter detail the types of data used in this study and how it was processed in order to achieve the objectives.

Seismic data were sourced from NZPAM database and uploaded in Kingdom SMT, a software package enabling mapping of seismic lines, with ties to drill hole data such as stratigraphy and biostratigraphy. This chapter outlined the methodology to progress from seismic analysis into gridding and final production of structure contour and isopach maps.

7.5 Chapter 4: Stratigraphy and Biostratigraphy

There are several geological formations that accumulated in the study area between the Kapitean and Present Day, whose lithological characteristics help portray the evolution of the study area. These include the following:

- Manganui Formation: A widespread calcareous mudstone that dominated Miocene deposition within Taranaki Basin. It accumulated mostly at bathyal depths.
- Mohakatino Formation: a series of volcaniclastic (andesitic) siltstone, mudstone and sandstone beds, inclusive of the now buried andesitic volcanic edifices (Mohakatino Volcanic Centre) from which the volcaniclastic material was sourced.
- Ariki Formation: a Late Miocene to Early Pliocene marl characterised by its rich planktic foraminifera content, reflective not only of the relatively deep (fully oceanic) environment in which it accumulated, but also a substantial period of terrigenous sediment starvation within Northern Taranaki Basin during this time.
- Mangaa Formation: Packages of fine-grained turbidite sandstone deposited as basin floor fan lobes, comprising the initial sedimentary fill in the Northern Graben.

- Giant Foresets Formation (GFF): a thick succession mainly composed of siltstone and mudstone with interbedded sandstone beds, which formed the shelf-slope system during the Plio-Pleistocene interval.

Biostratigraphy is commonly used as a tool to determine the age of strata and as a means of correlation across basin. Biostratigraphic data underpin the age model and are used together with seismic stratigraphy to develop an understanding about the evolution of the basin. The development of the age model relied heavily upon the biostratigraphic record in Ariki-1 and Arawa-1 where there is very high confidence in the placement of biostratigraphic stage boundaries. Other wells have more variable quality in the biostratigraphic determinations and this is reflected in stage boundary placements in them with respect to the seismic reflection horizons that have been mapped through all of the well sites. This is an illustration of how seismic reflection mapping provides a real test of biostratigraphic data, which is limited by the occurrence of key planktic taxa and issues to do with down-hole caving. Having loop tied across the study area via Ariki-1 (northern half of the study area) and Arawa-1 (southern half), seismic interpretation was then expanded across the entire study area. These new seismically mapped boundaries have been compared with biostratigraphically defined boundaries from Hansen (2003, 2006) and other studies.

7.6 Chapter 5: Basin Geology and Geometry

This chapter presented structure contour maps and isopach maps, but also reported on the characteristics of seismic packages between the mapped stage boundaries. The following are the main conclusions drawn from the chapter:

- Kapitean Stage: The general pattern shows an increase in depth to this surface towards the north east marked by a structural low. This structural low, which encompasses three clear depocentres, is aligned along the approximate position of the Northern Graben. Well logs show that during this stage, bathyal mudstone/siltstone beds were accumulating in the study area; Manganui Formation/Urenui Formation sediments in the southern half of the study area and Mohakatino Formation in the northern half. Normal faults offset the top Kapitean surface, which suggests that the faults were active during sediment accumulation. The most prominent offset is that of Parihaka Fault, offsetting strata by approximately 600 m, shown in seismic profile and on the structure contour map.

- Opoitian Stage: The Arawa sub basin had become the most prominent depocentre by the end of this stage and it remained open to the north east. Several formations were accumulating in various locations simultaneously across the basin. In the south, the depositional pattern was similar to the Kapitean Stage, with Manganui Formation/Urenui Formation mudstone being deposited. In the north, Ariki Formation had started to accumulate. The sediment distribution pattern for the most part correlates to the location of depocentres that were available to fill at the end of the Kapitean, with the greatest deposition occurring in the north east. This directly relates to Mangaa Formation fan deposition.

- Waipipian Stage: By the end of the Waipipian, the Arawa sub basin had become an enclosed stand-alone depocentre, no longer contiguous with the Northern Graben. Deposition during this stage continued to vary across the basin. Manganui Formation sediments were still being deposited in the south, and Mangaa Formation continued to accumulate in the north east. Notably, the Giant Foresets Formation (GFF) now dominates the sedimentary succession in the northern half of the field area, represented as mud-dominated bottomsets. The thin accumulation of Waipipian-aged strata is an indicator of slow sediment accumulation in the area during this time.

- Mangapanian Stage: The seismically mapped surface presented by the structure contour map depicts the rapid infilling of the Arawa sub basin, the formation and outbuilding of a well-defined continental shelf, and a progression from a shallow shelfal environment in the south east, through a shelf slope break to a deeper basin floor environment in the north west. This is indicative of very large sediment input to the area during this stage. Offset on the Parihaka Fault is not as significant as observed in previous structure contour maps, with a maximum of ~100-150 m indicated, suggestive of a decrease in the amount of movement on this fault. Sediment deposition was dominated by the Giant Foresets Formation prograding across the study area, showing varying lithological and seismic characteristics depending on where it was deposited; bottomsets in the north (basin floor), and progradational clinoforms and topsets in the south (shelf and slope).

- Nukumaruan Stage: The general pattern of the top Nukumaruan Stage horizon mirrors that of the top Mangapanian Stage horizon, progressing from a shallow shelfal environment in the south east, through a shelf-slope break to a deeper

basin floor environment in the north west. The orientation of the shelf slope break shifted to a more SW/NE direction, as it continued to prograde towards the north west. On seismic lines during this stage, the Giant Foresets Formation is presented as progradational foresets (slope deposition) and topsets (shelf deposition). Faults are not observed on either map as they are no longer active during this time.

- End of the Nukumaruan Stage to Recent: The isopach map is indicative that the shelf break continued to move in a north west direction during this stage to its now present day position, where the accumulation of sediment is concentrated. In the Nukumaruan-Recent seismic package, the GFF is represented by topsets in the study area, with the occasional degradational foresets recognized.

7.7 Chapter 6: Synthesis

This chapter integrates all work from the previous chapters and presents the findings on a wider regional scale. It attempts to relate results to current ideas on Northern Taranaki Basin development and evolution

During the latest Miocene, an extensional regime developed in North Taranaki Basin, which is the cause of the development of the main extensional structure in the study area, the Northern Graben. This study places the development of the graben before the end of the Kapitean Stage (5.3 Ma), an age supported by evidence in other studies (6.5-5.3 Ma, Hansen and Kamp, 2004)

The continuing subsidence of the graben structure in the early Pliocene (Opoitian) caused local changes in basin physiography and therefore focused sediment dispersal along the axis of the structure, represented through the deposition of Mangaa Formation.

Thin sedimentary successions observed during the Late Opoitian and the Waipipian across numerous seismic profiles (Enclosure 2), suggest there was slow accumulation of terrigenous sediment within the Northern Basin at this time, despite high sediment supply out of the Southern Alps. Much of this sediment was probably trapped in Wanganui Basin and in the Central Graben of Taranaki Basin.

During the Mangapanian high rates of sediment supply to Northern Taranaki Basin became re-established. This sediment flux began to outpace accommodation created by subsidence and as a result, the shelf-slope wedge began to steadily prograde northward into the study area, rapidly infilling the Arawa sub basin depocentre.

Whilst the shelf-slope break continued to prograde north westward during the Mangapanian, it was not doing so at a constant rate in the centre of the study area, when compared with progradational rates either side of Arawa sub basin. Even though this depocentre captured sediment, progradation of the shelf-slope system was faster to the northwest of it than in flanking areas. Enclosure 2 illustrates that active movement on normal faults within the study area had significantly decreased by the end of the Mangapanian Stage (2.4 Ma).

Progradation of the shelf-slope break toward the north west continued through the Nukumaruan Stage (2.4 - 1.63 Ma), but at a slower rate than in the Mangapanian. The Arawa sub basin at this time had been infilled entirely and hence sediment prograded to the shelf edge and beyond. Maps illustrate that normal faulting in the Northern Taranaki Basin had completely ceased by the end of the Nukumaruan (1.63 Ma).

From the end of the Nukumaruan Stage to the Present Day, the shelf break re-oriented to a more SW/NE trend, indicative that the rates of progradation across the recent shelf-slope break were faster on the eastern side of the study area than those across the central and western sides. Progradation of the shelf slope break is continuing in the present day.

References

Anell, I. & Midtkandal, I. (2015). The quantifiable clinothem – types, shapes and geometric relationships in the Plio-Pleistocene Giant Foresets Formation, Taranaki Basin, New Zealand. *Basin Research*. 1-21.

Ashcroft, W. (2011). *A Petroleum Geologists Guide to Seismic Reflection*, Wiley Blackwell. Hoboken, NJ.

Beggs, J.M. (1990). Seismic Stratigraphy of the Plio-Pleistocene Giant Foresets Formation, Western Platform, Taranaki Basin. 1989 New Zealand Oil Exploration Conference Proceedings, 201-207.

Bergman, S.C., Talbot, J. & Thompson, P.R. (1992). The Kora Miocene submarine andesite stratovolcano hydrocarbon reservoir, Northern Taranaki Basin, New Zealand. 1991 *New Zealand Oil Exploration Conference Proceedings*, 1, 178-206.

Cooper, R.A., Crampton, J.S., Raine, J.I., Gradstein, F.M., Morgans, H.E.G., Sadler, P.M., Strong, P.C., Waghorn, D. & Wilson, G.J. (2001). Quantitative biostratigraphy of the Taranaki Basin, New Zealand: A deterministic and probabilistic approach. *American Association of Petroleum Geologists Bulletin*, 85 (8), 1469–1498.

Crundwell, M.P., Scott, G.H. &Thrasher, G.P. (1994). Calibration of paleobathymetry indicators, integrated seismic and paleontological analysis of foreset sequences, Taranaki Basin, New Zealand. *Proceedings of 1994 New Zealand Petroleum Conference*. 169-178.

Environmental Protection Agency (US). (2011). *Marine Seismic Methods*. Retrieved from: http://www.epa.gov/esf/cmb/GeophysicsWebsite.

Furlong, K.P, & Kamp, P.J.J. (2009). The lithospheric geodynamics of plate boundary transpression in New Zealand: Initiating and emplacing subduction along the Hikurangi margin, and the tectonic evolution of the Alpine Fault system. *Tectonophysics*, 474(3-4), 449-462.

Giba, M., Nicol, A., & Walsh, J. J. (2010). Evolution of faulting and volcanism in a back-arc basin and its implications for subduction processes. *Tectonics*, 1-18.

Giba, M., Walsh, J. J., & Nicol, A. (2012). Segmentation and growth of an obliquely reactivated normal fault. *Journal of Structural Geology*, 39, 253-267

Grain, S.L. (2008). Paleogeography of a mid-Miocene turbidite complex, Moki Formation, Taranaki Basin. *Unpublished MSc Thesis*. University of Victoria. New Zealand.

Hansen, R.J. (2003). Characteristics and evolution of a dynamic prograding continental margin: the late Neogene Giant Foresets Formation, northern Taranaki Basin, New Zealand. *Unpublished PhD Thesis*, University of Waikato. New Zealand

Hansen, R. J. & Kamp, P. J. J. (2002). Evolution of the Giant Foresets Formation, northern Taranaki Basin, New Zealand. *Proceedings of New Zealand Petroleum Conference*, 419-435

Hansen, R. J. & Kamp, P. J. J. (2004). Late Miocene to early Pliocene stratigraphic record in northern Taranaki Basin: Condensed sedimentation ahead of Northern Graben extension and progradation of the modern continental margin. *New Zealand Journal of Geology and Geophysics*, 47(4), 645-662

Hansen, R.J. & Kamp, P.J.J. (2006). Sequence stratigraphy and architectural elements of the Giant Foresets Formation, northern Taranaki Basin, New Zealand. *Proceedings of 2006 New Zealand Petroleum Conference.* 1-13

Hansen, R.J. & Kamp, P.J.J. (2006). An integrated biostratigraphy and seismic stratigraphy for the late Neogene continental margin succession in northern Taranaki Basin, New Zealand. *New Zealand Journal of Geology & Geophysics.* 49. 39–56

Hansen, R.J. & Kamp, P.J.J. (2006). Re-evaluation of the Late Neogene biostratigraphy of Arawa-1, Ariki-1, Kora-1, and Wainui-1, and integrated seismic and biostratigraphic correlation (11 wells), northern Taranaki Basin. *Ministry of Economic Development*. Unpublished Petroleum Report. 2938.

Hansen, R.J. & Kamp, P.J.J. (2008). New insights into the condensed nature and stratigraphic significance of the Late Neogene Ariki Formation, Taranaki Basin. *Proceedings of 2008 New Zealand Petroleum Conference.*

Hayward, B.W. (1985b). Foraminiferal biostratigraphy of Tangaroa-1 offshore well northwest Taranaki. *New Zealand Geological Survey Report* PAL 86.

Hayward, B.W. (1986). Foraminiferal biostratigraphy and paleo bathymetry of Ariki-1 offshore well northwest Taranaki. *New Zealand Geological Report* PAL 110

Hoskins, R.H. & Raine, J.I. (1984). Biostratigraphy of Taimana-1. *New Zealand Geological Survey Report* PAL 74.

Jager, K.G. (2012). Seismic stratigraphy of the Neogene succession in southern Taranaki Basin, New Zealand. *Unpublished MSc thesis*. University of Waikato, New Zealand.

Johnston, A.G. (2014). Interactions between the prograding Giant Foresets Formation and a subsiding depocentre: Insights from the Parihaka 3D and ES89 2D seismic surveys. *Unpublished MSc Thesis*. University of Victoria. New Zealand.

Jones, R.W. (2006). *Applied palaeontology*. Cambridge University Press.

Kamp, P.J.J., Vonk, A.J., Nelson, C.S., Hansen, R.J., Tripathi, A.R., Hood, S.D., Ngatai, M.M. & Hendy, A.J. (2004). Constraints on the evolution of Taranaki Fault from thermochronology and basin analysis: Implications for the Taranaki Fault play. *Proceedings of 2004 New Zealand Petroleum Conference*.

Kamp, P. J. J., Vonk, A. J., Bland, K. J., Hansen, R. J., Hendy, A. J. W., McIntyre, A. P., Ngatai,M., Cartwright, S. J., Hayton, S. & Nelson, C. S. (2004). Neogene stratigraphic architecture and tectonic evolution of Wanganui, King Country, and eastern Taranaki Basins, New Zealand. *New Zealand Journal of Geology and Geophysics*, 47 (4), 625-644.

King, P.R. (1989). Polyphase evolution of the Taranaki Basin, New Zealand: changes in sedimentary and structural style. *Proceedings of 1989 New Zealand Petroleum Conference.*

Knox, G. J. (2012). Taranaki Basin, structural style and tectonic setting. *New Zealand Journal of Geology and Geophysics*, 125-140.

Krohn, C.E. (2008). Seismic Data Acquisition. In: Havelock, D., Kuwano, S and Vorlander, M. (Eds.) Handbook *of Signal Processing in Acoustics*. 1. 1545-1159, New York: Stringer.

Lucas, K.R. (2013). Seismic stratigraphy and foreland basin development of south-eastern Taranaki Basin, New Zealand. *Unpublished MSc Thesis*. University of Waikato, New Zealand.

Lyon, Z. (2015). Seismic mapping of the stratigraphy and structure of the eastern margin of Taranaki Basin, North Taranaki Bight, New Zealand. *Unpublished MSc Thesis*. University of Waikato. New Zealand.

Miall, A. (2013). *Principles of Sedimentary Basin Analysis*. Springer Science & Business Media.

Mitchum, R.M., Vail, P.R. & Sangree, J.B. (1977). Seismic stratigraphy and global changes of sea level, part 6: stratigraphic Interpretation of seismic reflection patterns in depositional sequences. In: Payton, C.E. *ed.* Seismic Stratigraphy - applications to hydrocarbon exploration. *American Association of Petroleum Geologists Memoir* 26, 117-135.

New Zealand Petroleum and Minerals. (2016). Data Retrieved from http://www.nzpam.govt.nz

Nichols, G. (2009). *Sedimentology and Stratigraphy* (2nd Ed). West Sussex, UK. John Wiley & Sons Ltd

Raine, J.I., Beu, A.G., Boyes, A.F., Campbell, H.J., Cooper, R.A., Crampton, J.S., Crundwell, M.P., Hollis, C.J. & Morgans, H.E.G. (2015). Revised calibration of the New Zealand Geological Timescale: NZGT2015/1. *GNS Science Report* 2012/39.

Salazar, M., Moscardelli, L. & Wood, L. (2015). Utilising clinoform architecture to understand the drivers of basin margin evolution: a case study in the Taranaki Basin, New Zealand. *Basin Research*. 1-26

Schlumberger Limited. (2016). Oilfield Glossary – common midpoint. Retrieved from: http://www.glossary.oilfield.slb.com/Terms/c/common_midpoint.aspx

Schlumberger Limited. (2016). Oilfield Glossary – velocity. Retrieved from: http://www.glossary.oilfield.slb.com/Terms/v/velocity.aspx

Schlumberger Limited. (2016). Oilfield Glossary – normal move out. Retrieved from: http://www.glossary.oilfield.slb.com/Terms/n/normal_moveout.aspx

Schroeder, F.W. (2004). Geology and Geophysics Applied to Industry: An Introduction to the Hunt for Oil for Geoscientists not within Industry. Unit 11b: Seismic Facies Analysis. Retrieved from http://www.aapg.org.

Scott, G.H., King, P.R. & Crundwell, M.P. (2004) Recognition and interpretation of depositional units in a late Neogene progradational shelf margin complex, Taranaki Basin, New Zealand: foraminiferal data compared with seismic facies and wireline logs. *Sedimentary Geology* 164. 55-74.

Strogen, D.P., Bland, K.J., Baur, J.R., King, P.R., Vonk, A.J & Kamp, P.J.J. (2011). Neogene: active margin tectonics. In: Strogen, D.P (compiler), Paleogeographic synthesis of the Taranaki Basin and surrounds. *GNS Science Report*. 2010(53), 36-60.

Strong, C.P., Waghorn, D.B., Cooper, R.A., Crampton, J.S., Morgans, H.E.G. & Raine, J.I. (1996). Biostratigraphy of Awatea-1 offshore petroleum exploration drill hole, North Taranaki Basin. *Institute of Geological and Nuclear Sciences Client Report 53652A*. 10. Institute of Geological and Nuclear Sciences, Lower Hutt, New Zealand.

Strong, C.P. & Wilson, G.J. (2002). Biostratigraphic reassessment (foraminiferal & palynology) of key western platform drill holes, Taranaki Basin, *GNS Science Report* 2002/150

Tippett, J.M. & Kamp, P.J.J. (1995). Geomorphic evolution of the Southern Alps, New Zealand. *Earth Surface Processes and Landforms.* 20 (2), 177-192.

Vail, P.R. (1987). Seismic stratigraphy interpretation using sequence stratigraphy Part I: Seismic stratigraphy interpretation procedure. In AAPG Atlas of Seismic Stratigraphy, Bally, A.W., ed. AAPG Studies in Geology No. 27, vol. 1. 1-10

Vonk, A. J., & Kamp, P. J. (2008). The Late Miocene Southern and Central Taranaki Inversion Phase (SCTIP) and related sequence stratigraphy and paleogeography. *New Zealand Petroleum Conference*, 1-18. Hamilton.

Waghorn, D.B., Strong, C.P., Raine, J.I. & Crampton, J.S. (1996). Biostratigraphic review of the Late Miocene and Pliocene of the Mangaa-1, Kahawai-1, Te Kumi-1, Tangaroa-1, and Kora-1 wells, offshore Taranaki Basin. Ministry of Commerce New Zealand. Unpublished Petroleum Report 2417.

Petroleum Reports

PR554 – Hematite Petroleum NZ Ltd. 1970. Mangaa-1 (Offshore). Petroleum Report Series PR554. Ministry of Economic Development.

PR793 – Shell BP & Todd Oil Service Ltd. 1981. Well Resume Tangaroa-1. Petroleum Report Series PR793. Ministry of Economic Development.

PR869 – Shell BP & Todd Oil Services Ltd. 1982. Well Resume Wainui-1. Petroleum Report Series PR869. Ministry of Economic Development.

PR1026 – Diamond Shamrock Exploration Oil Co (NZ). 1984. Final Well Report Taimana-1. Petroleum Report Series PR1026. Ministry of Economic Development.

PR1037 – New Zealand Oil & Gas Ltd (NZOG). 1984. Witiora-1 completion report. Petroleum Report Series PR1037. Ministry of Economic Development.

PR1038 – Shell BP Todd Oil Services Ltd. 1984. Completion Report Ariki-1 Well. Petroleum Report Series PR1038. Ministry of Economic Development.

PR1374 – ARCO Petroleum NZ Inc. 1988. Final well report, Kora-1 Kora-1A. Petroleum Report Series PR1374. Ministry of Economic Development.

PR1386 – Amoco NZ Exploration Co Ltd. 1988. Final well report Te Kumi-1. Petroleum Report Series PR1386. Ministry of Economic Development.

PR1824 – ARCO Petroleum NZ Inc. 1992. Arawa-1 Final Well Report. Petroleum Report Series PR1824. Ministry of Economic Development.

PR1878 – New Zealand Oil & Gas Ltd (NZOG). 1990. Kahawai-1 well completion report. Petroleum Report Series PR1878. Ministry of Economic Development.

PR2262 – Fletcher Challenge Energy Taranaki. 1996. Awatea-1 Well Completion Report. Petroleum Report Series PR2262. Ministry of Economic Development.

PR3843 – Pogo New Zealand. 2007. Kanuka-1 End of Well Completion Report. Petroleum Report Series PR3843. Ministry of Economic Development.

Appendix A – Geological Time Scale (Taken from Raine *et al.*, 2015)

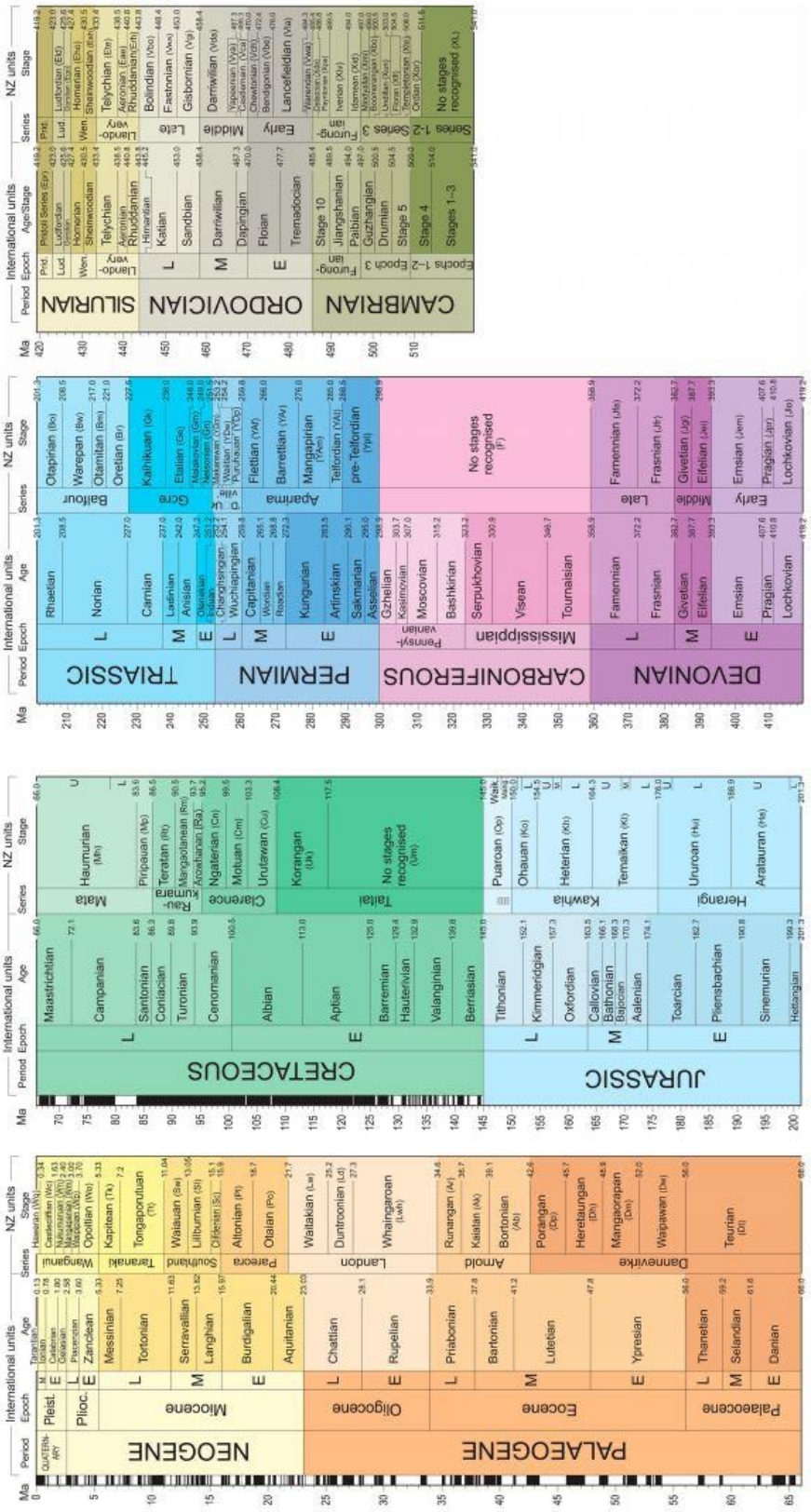

Appendix B – Seismic Lines interpreted in the study

81a-03-1018_matched	ar90-436-107-1627_matched
81a-05-1018_matched	ar90-436-108-1627_matched
81a-06-1018_matched	ar90-445-116-1628_matched
81a-08-1018_matched	cnl95b-003-3054_matched
81a-10-1018_matched	cnl95b-011-3054_matched
81a-11-1018_matched	cnl95b-040-3054_matched
81sy-01-2303_matched	cnl95b-044-3054_matched
81sy-04-1018_matched	cnl95b-048-3054_matched
81sy-05-2303_matched	cnl95b-050b-3054_matched
81sy-06a-2303_matched	ds1-04-917-geosphere_matched
81sy-08a-2303_matched	ds1-10-917-geosphere_matched
81sy-09-2303_matched	ds1-14a-917-geosphere_matched
81sy-10a-2303_matched	ds1-16-917-geosphere_matched
81sy-12-2174_matched	ds1-17-917-geosphere_matched
81sy-16-2095_matched	ds1-18-917-geosphere_matched
81sy-17_2-2303_matched	ds1-22-917-geosphere_matched
81sy-19_1-2303_matched	ds1-82-03-917_matched
81sy-19_2-2303_matched	ds1-82-08-917_matched
81sy-21-2303_matched	ds1-82-09-917_matched
81z-19-1018_matched	ds1-82-12-917_matched
81z-32-2271_matched	dsr89-01-dsir_matched
ar88-103-1398_matched	dtb01-01-2847_matched
ar88-106-1398_matched	dtb01-05-2847_matched
ar88-136-1647_matched	dtb01-32-2847_matched
ar88-140-1647_matched	dtb01-34-2847_matched
ar89-436-101-1474_matched	es89-003-1978_matched
ar89-446-108-1475_matched	es89-005-1978_matched
ar89-447-102-1476_matched	es89-007a-1978_matched
ar89-447-105-1476_matched	es89-007b-1978_matched
ar89-447-107-1476_matched	es89-012-1978_matched
ar89-447-108-1476_matched	es89-015-1978_matched
ar89-447-109-1476_matched	es89-017-1978_matched
ar89-447-112-1476_matched	es89-023-1978_matched
ar89-447-113-1476_matched	es89-029-1978_matched
ar89-447-114-1476_matched	es89-031-1978_matched

ar89-447-117-1476_matched	es89-032-1978_matched
ar90-436-102-1627_matched	es89-102-1978_matched
ar90-436-103-1627_matched	es89-106-1978_matched
ar90-436-104-1627_matched	es89-107-1978_matched
ar90-436-106-1627_matched	es89-108-1978_matched
es89-109-1978_matched	nm-20_1-2708_matched
es89-110-1978_matched	nm-21_2-638_matched
es89-111a-1978_matched	nm-22-638_matched
es89-113-1978_matched	nm-31-2512_matched
es89-114-1978_matched	nm-34-2512_matched
es89-116-1978_matched	nm-35-2708_matched
es89-118-1978_matched	nm-37-geosphere_matched
es89-119-1978_matched	p10781-23-2303_matched
es89-120-1978_matched	p10781-27-2303_matched
es89-122-1978_matched	p10781-28-2303_matched
es89-123-1978_matched	p10781-29-2303_matched
es90-01-1773_matched	p10781-31-2303_matched
es90-03-1773_matched	p10781-32-2303_matched
es90-04-1773_matched	p10781-34-2303_matched
es90-11-1773_matched	p10781-35-2303_matched
es90-12-1773_matched	p10781-35a-2303_matched
es91-01-03-1900_matched	p10781-40-2303_matched
hf1090-2174_matched	p95-001a-2708_matched
hf1100n-2174_matched	p95-103-geosphere_matched
hf1110s-2174_matched	p95-107-geosphere_matched
hf-11x-1963_matched	p95-113-2261_matched
hf-23x-1963_matched	p95-123-geosphere_matched
hf600-2174_matched	p95-127-2261_matched
hz-111-1980_matched	p95-131-2261_matched
hzt82b-204-900_matched	p95-133-2261_matched
hzt82b-206-900_matched	p95-134-2261_matched
hzt82b-210-900_matched	p95-142-2261_matched
hzt82b-212-900_matched	p95-145-2261_matched
hzt82b-214-900_matched	p95-146-2261_matched
hzt82b-216-900_matched	p95-150-2261_matched
hzt82b-218-900_matched	p95-152-2261_matched
nm-02_0-2708_matched	p95-157-2261_matched

nm-03_1-2512_matched	p95-158-2261_matched
nm-14_01-geosphere_matched	p95-162-2261_matched
nm-15-2512_matched	p95-164-2261_matched
nm-16-2512_matched	p95-168-2261_matched
nm-17-2512_matched	p95-172a-2261_matched
nm-18-2512_matched	p95-174-2261_matched
nm-18ext-638_matched	p95-176-2261_matched
nm-19-2512_matched	p95-184-2261_matched
p95-188-2261_matched	s1382-105-2708_matched
p95-194-2261_matched	s1382-108-2708_matched
p95-198-2261_matched	s1382-109-2708_matched
p95-206-geosphere_matched	sunz91-122-1948_matched
p95-208-2261_matched	sunz91-123-1948_matched
s1382-001-2708_matched	sunz91-124-1948_matched
s1382-003-2708_matched	ta88-2003-1615_matched
s1382-015-2708_matched	

Appendix C – Two way travel time and velocity maps used in the creation of structure contour and isopach maps

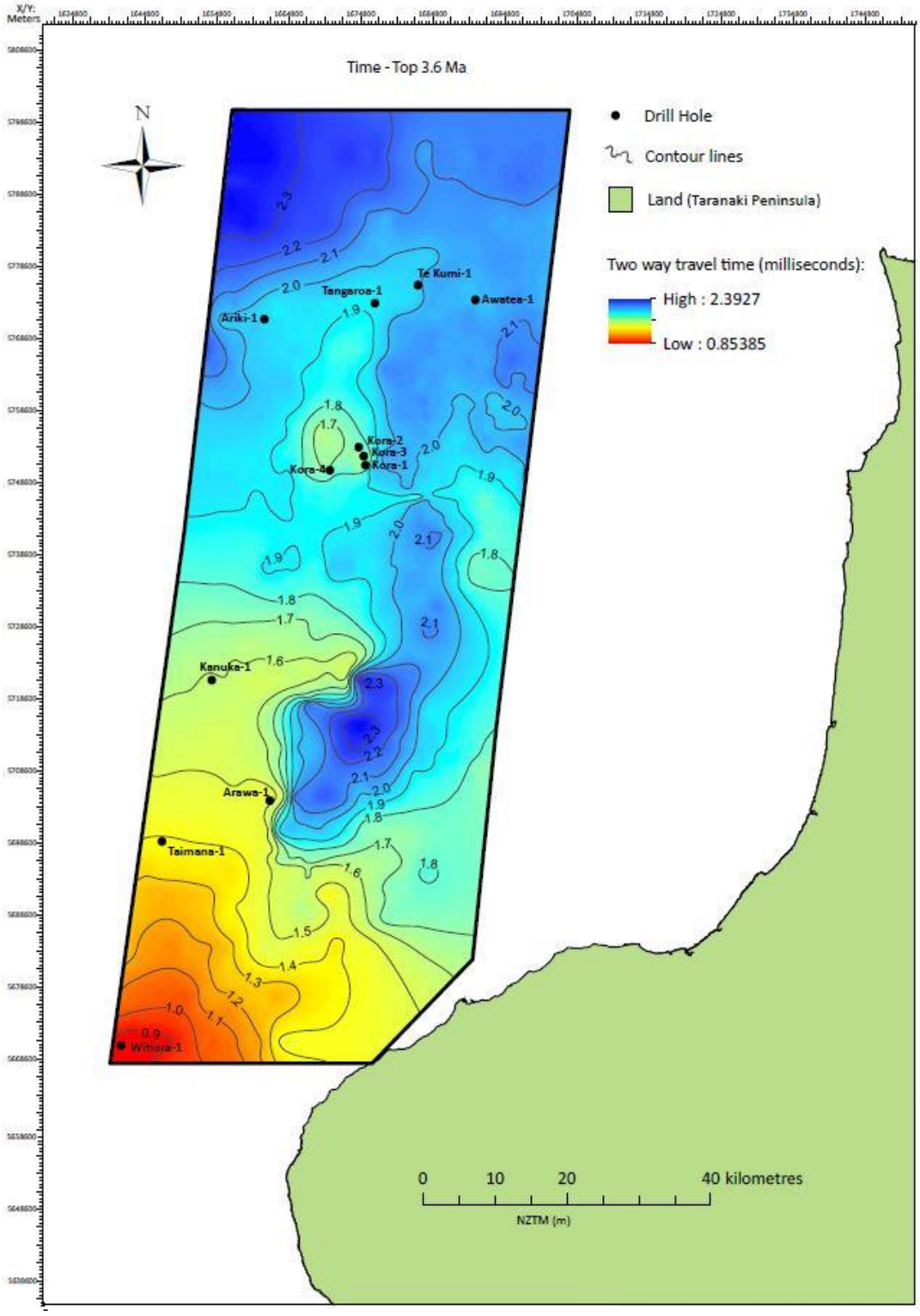

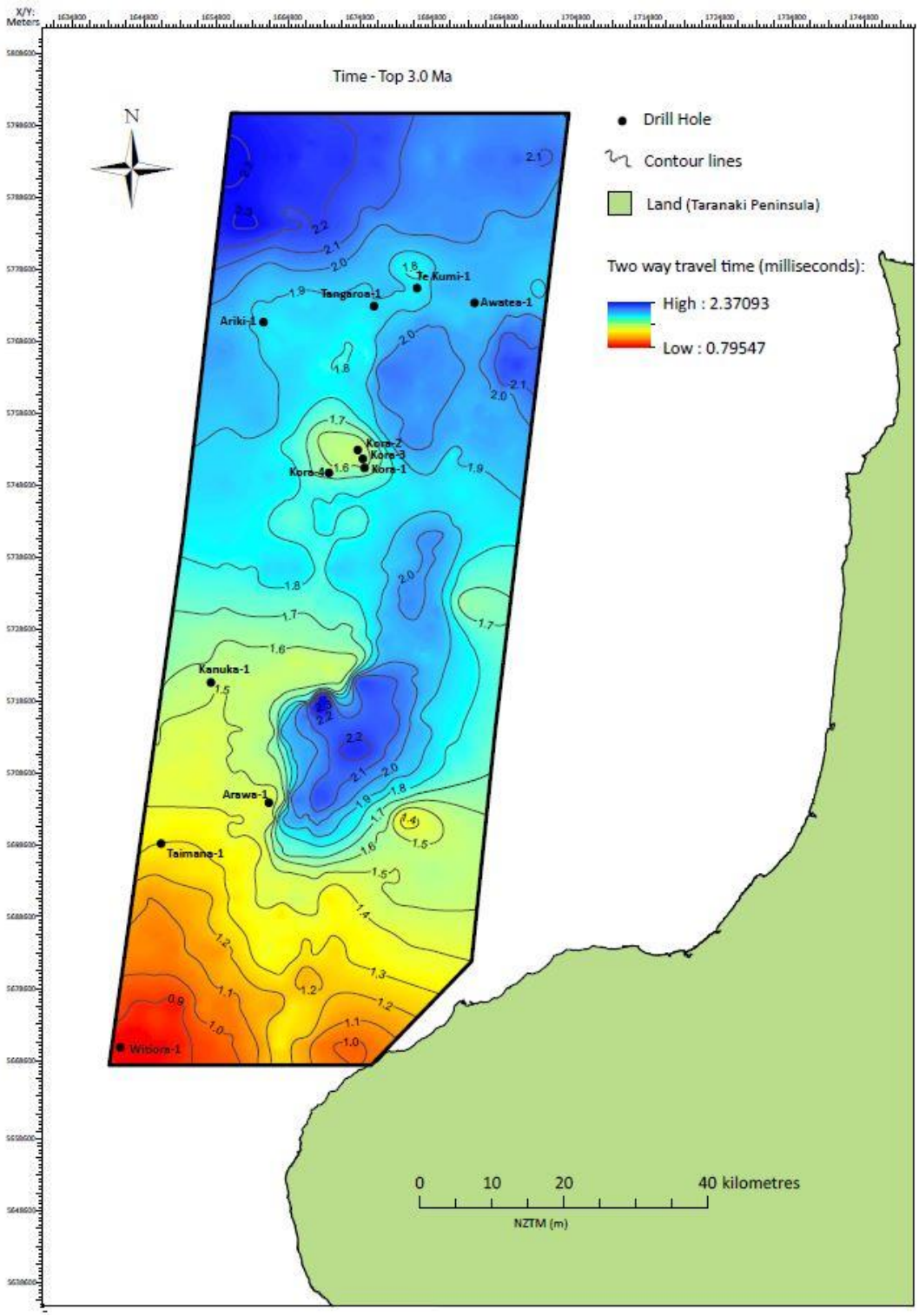
Time - Top 3.0 Ma
N
Drill Hole
Contour lines
Land (Taranaki Peninsula)
Two way travel time (milliseconds):
High : 2.37093
Low : 0.79547
Te Kumi-1
Tangaroa-1
Awatea-1
Ariki-1
Kora-2
Kora-3
Kora-4
Kora-1
Kanuka-1
Arawa-1
Taimana-1
Wilson-1
0
10
20
40 kilometres
NZTM (m)

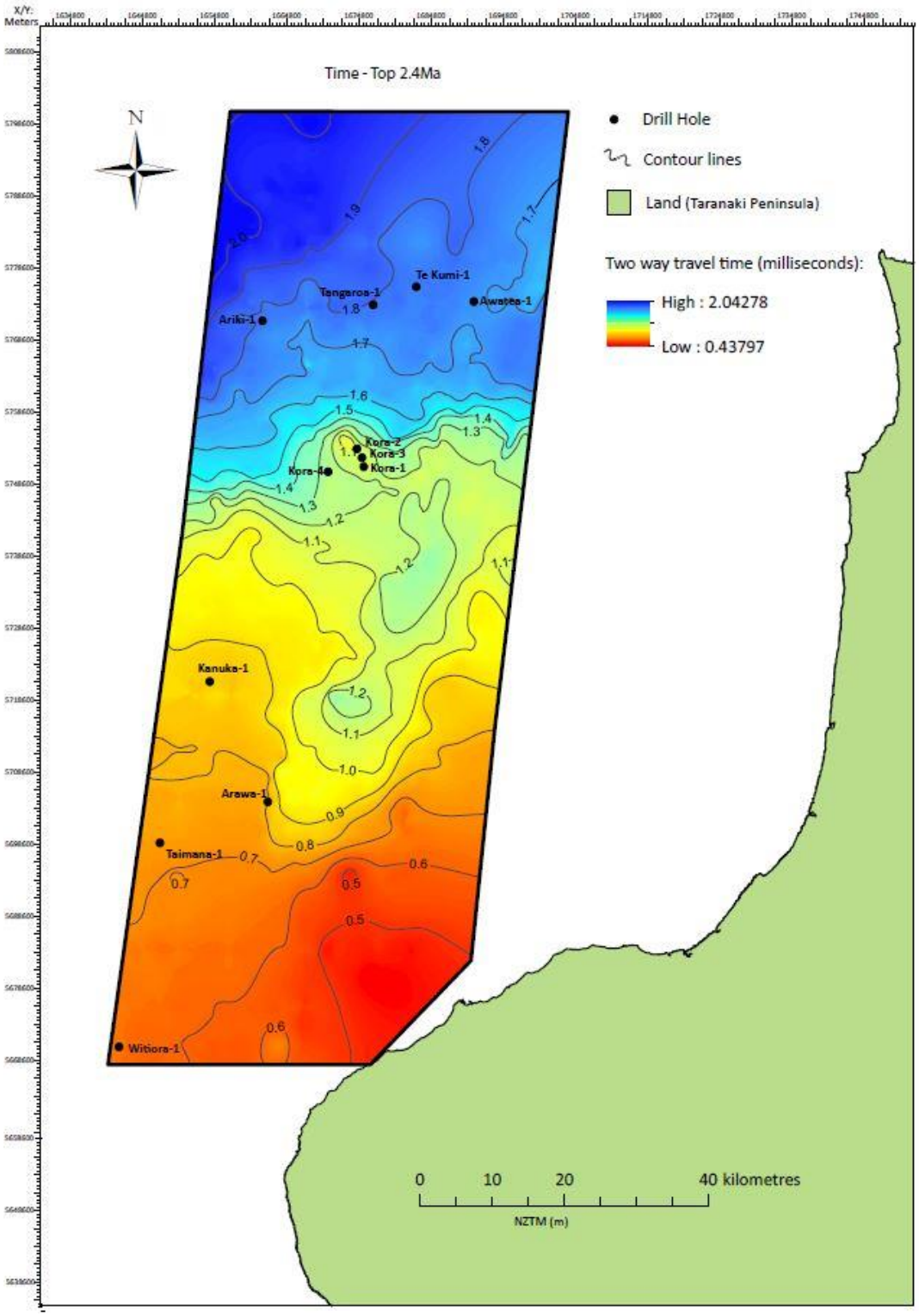
X/Y: Meters
Time - Top 2.4Ma
N
Drill Hole
Contour lines
Land (Taranaki Peninsula)
Two way travel time (milliseconds):
High : 2.04278
Low : 0.43797
Te Kumi-1
Tangaroa-1
Awatea-1
Ariki-1
Kora-2
Kora-3
Kora-1
Kora-4
Kanuka-1
Arowa-1
Taimana-1
Witiora-1
0
10
20
40 kilometres
NZTM (m)

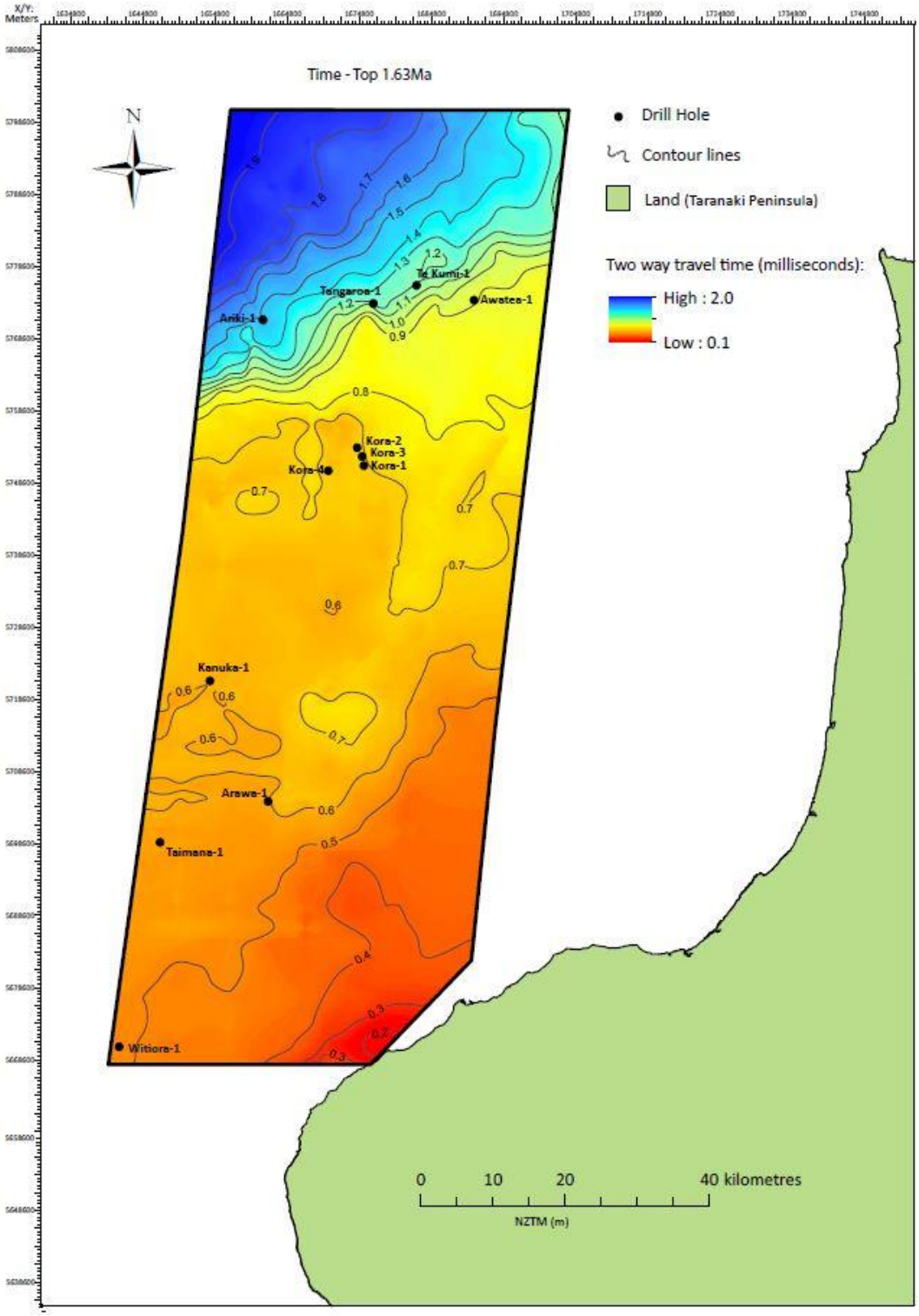
X/Y: Meters
Time - Top 1.63Ma
N
Drill Hole
Contour lines
Land (Taranaki Peninsula)
Two way travel time (milliseconds):
High : 2.0
Low : 0.1
Tengaroa-1
Te Kumi-1
Awatea-1
Aniki-1
Kora-2
Kora-3
Kora-1
Kora-4
Kanuka-1
Arawa-1
Taimana-1
Witiora-1
1.9
1.8
1.7
1.6
1.5
1.4
1.3
1.2
1.1
1.0
0.9
0.8
0.7
0.6
0.5
0.4
0.3
0.2
0
10
20
40 kilometres
NZTM (m)

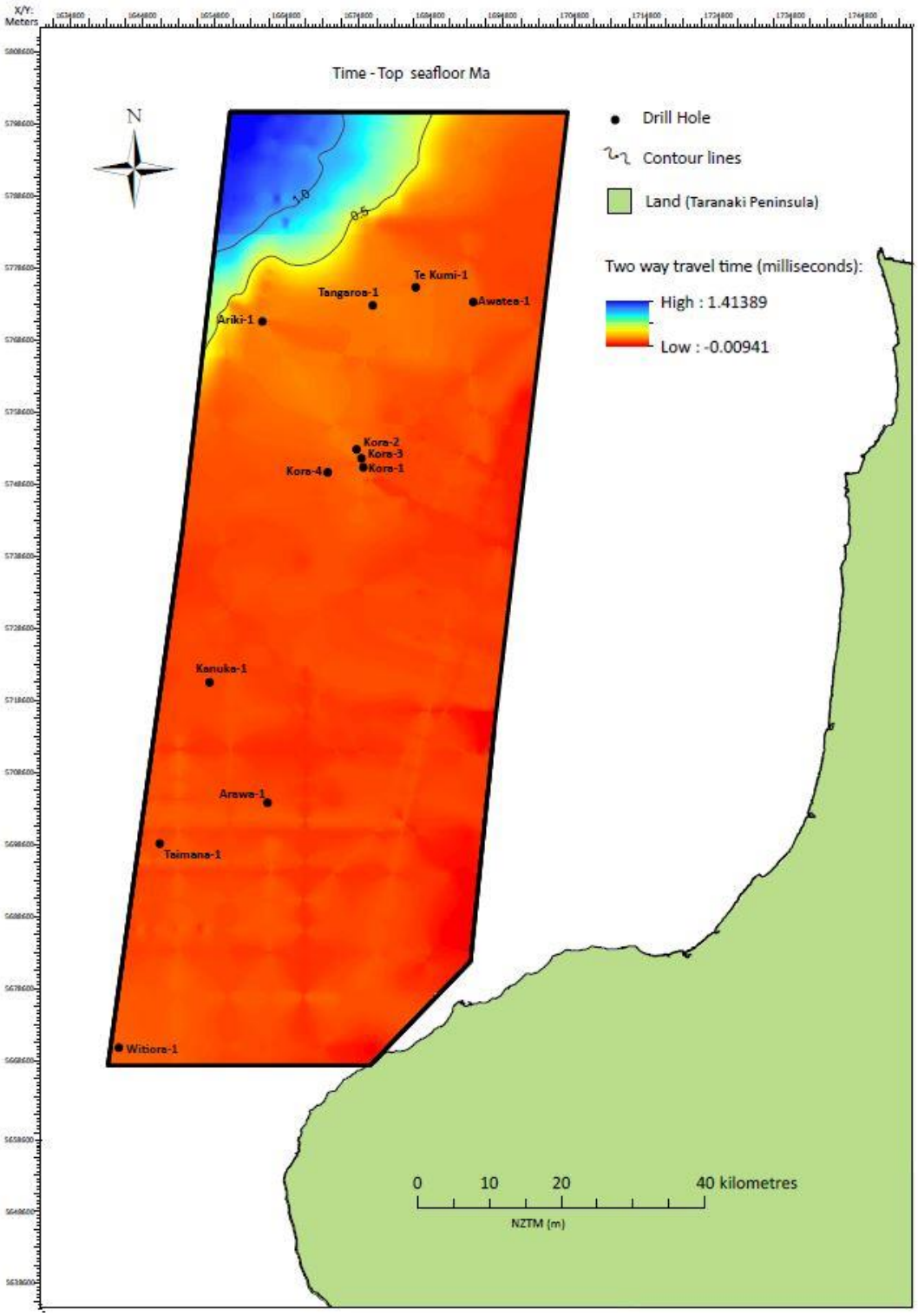
X/Y: Meters
Time - Top seafloor Ma
N
1.0
0.5
Drill Hole
Contour lines
Land (Taranaki Peninsula)
Two way travel time (milliseconds):
High : 1.41389
Low : -0.00941
Te Kumi-1
Tangaroa-1
Awatea-1
Ariki-1
Kora-2
Kora-3
Kora-1
Kora-4
Kanuka-1
Arawa-1
Taimana-1
Witiora-1
0
10
20
40 kilometres
NZTM (m)

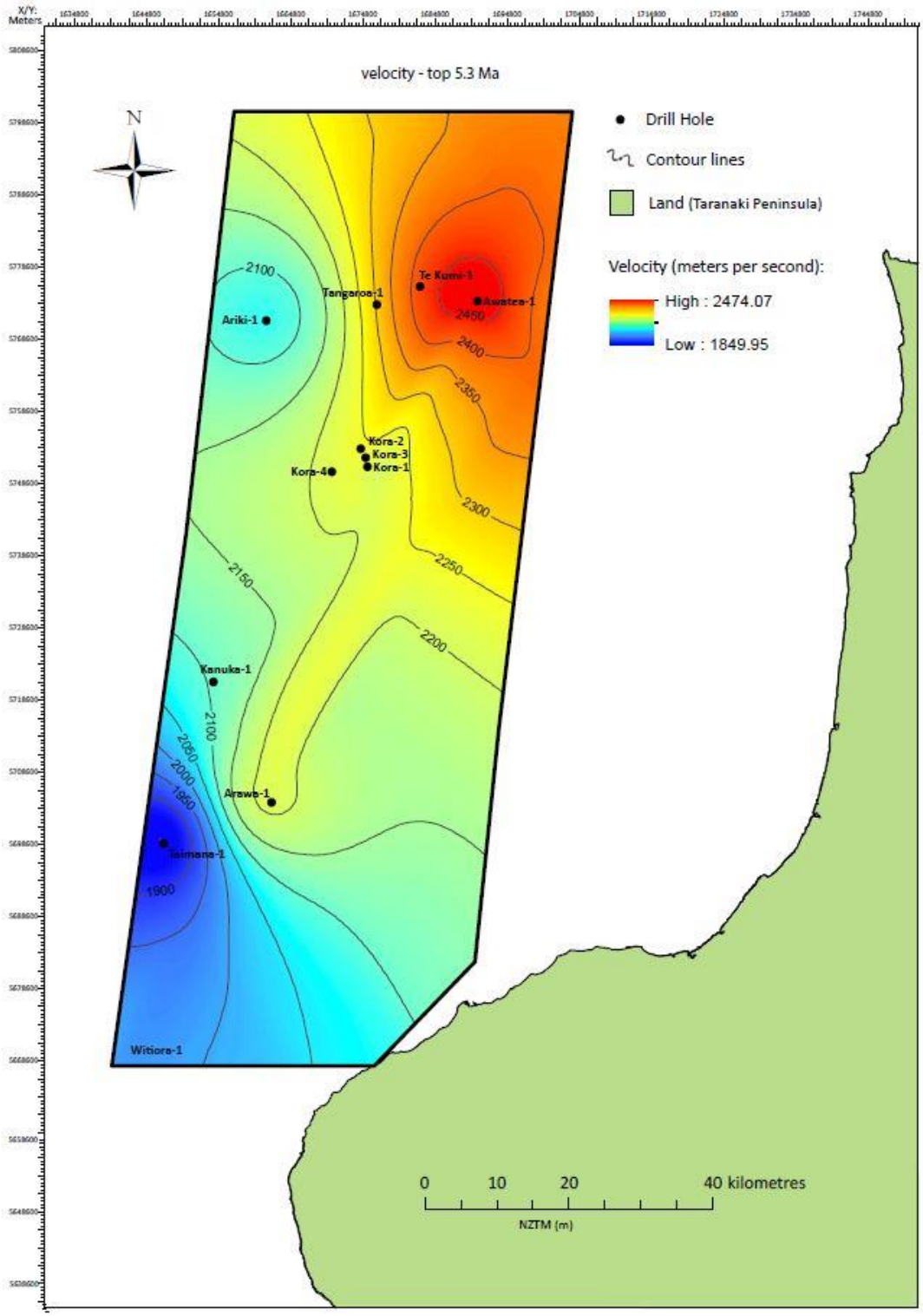
velocity - top 5.3 Ma
N
Drill Hole
Contour lines
Land (Taranaki Peninsula)
Velocity (meters per second):
High : 2474.07
Low : 1849.95
Ariki-1
Tangaroa-1
Te Kumi-1
Awatea-1
Kora-2
Kora-3
Kora-1
Kora-4
Kanuka-1
Arawa-1
Taimana-1
Witiora-1
2100
2450
2400
2350
2300
2250
2200
2150
2100
2050
2000
1950
1900
0
10
20
40 kilometres
NZTM (m)

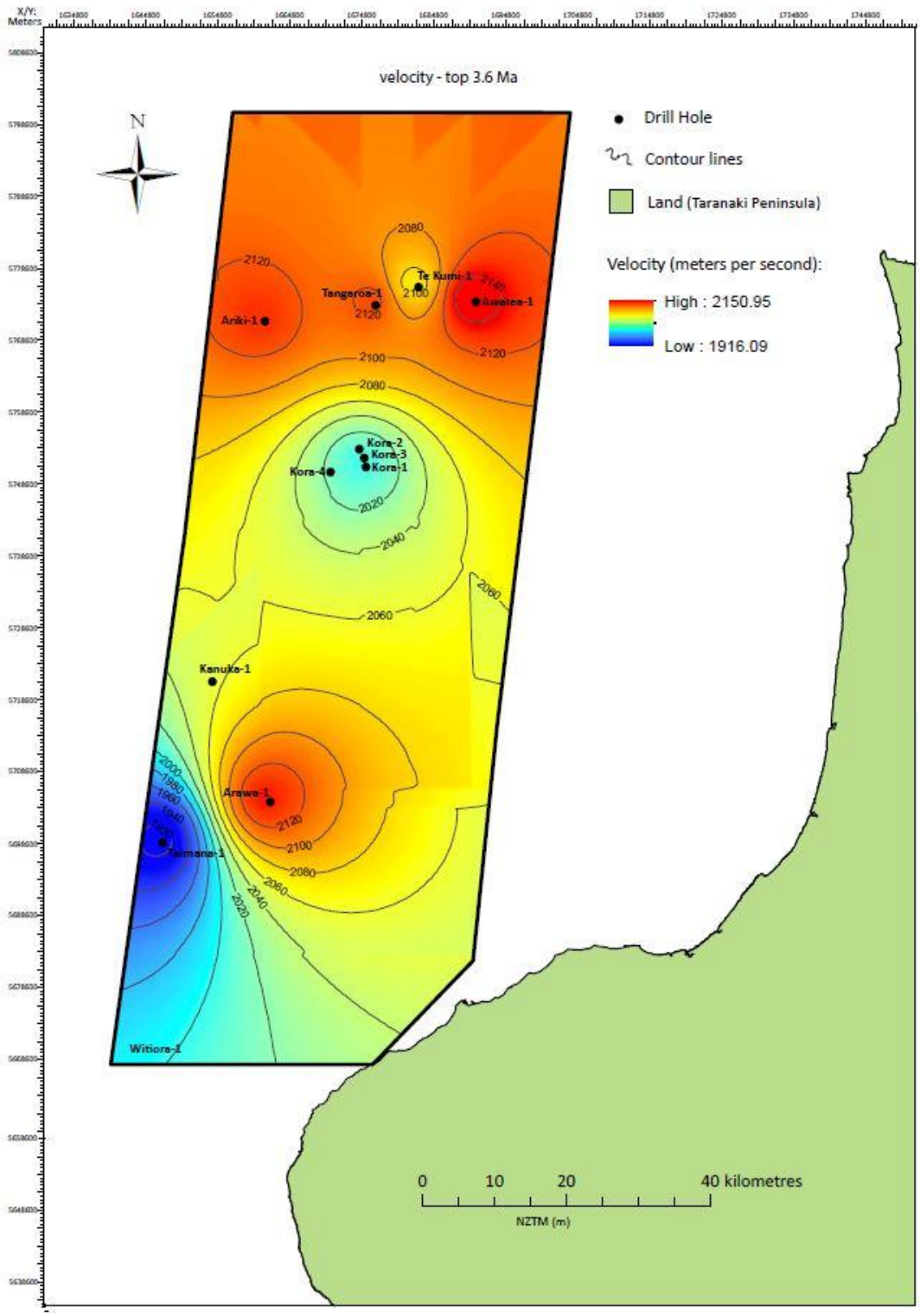
velocity - top 3.6 Ma
N
Drill Hole
Contour lines
Land (Taranaki Peninsula)
Velocity (meters per second):
High : 2150.95
Low : 1916.09
Ariki-1
Tangaroa-1
Te Kumi-1
Awatea-1
Kora-2
Kora-3
Kora-1
Kora-4
Kanuka-1
Arawa-1
Witiora-1
2120
2100
2080
2060
2040
2020
2000
1980
1960
1940
0
10
20
40 kilometres
NZTM (m)

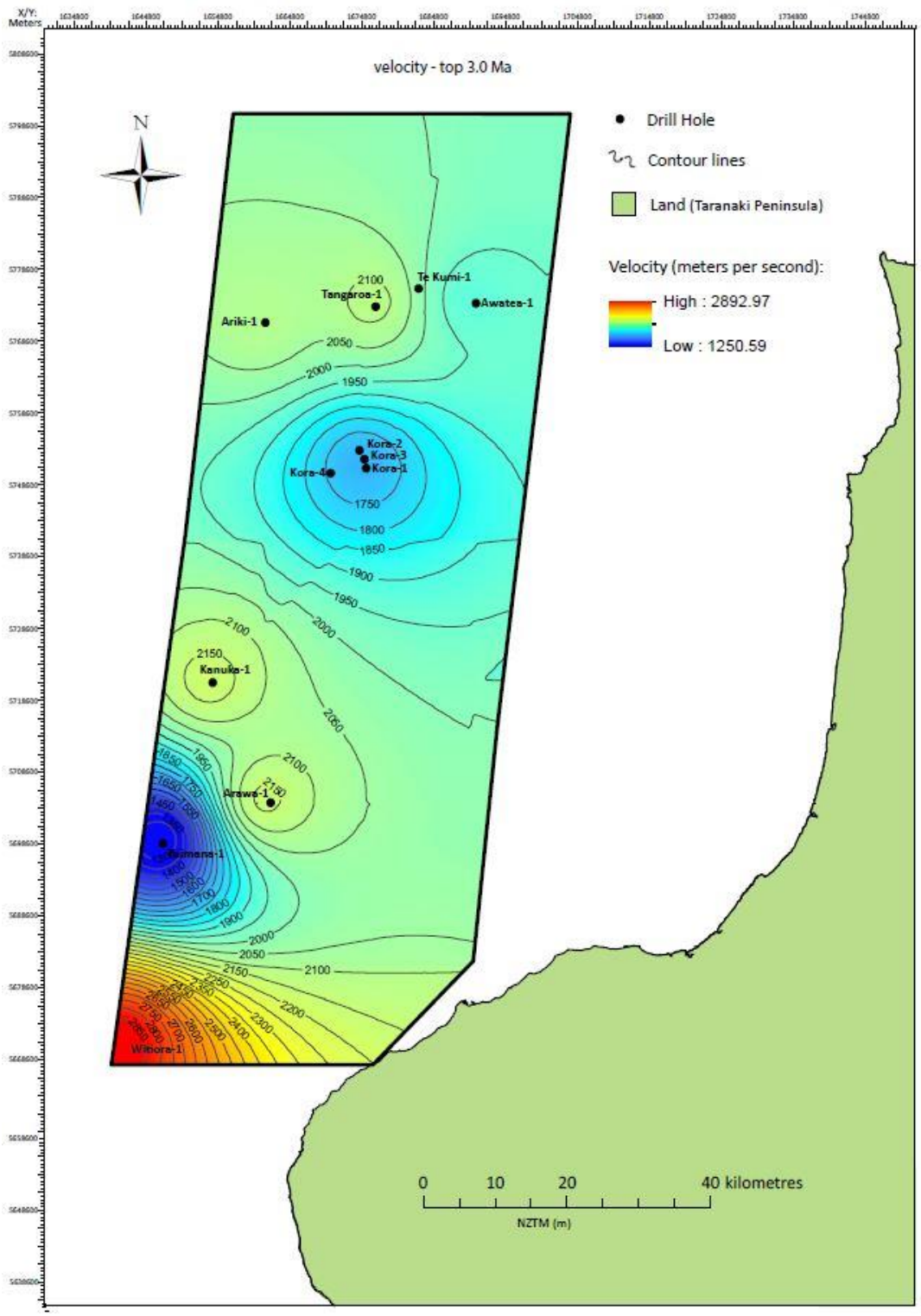
velocity - top 3.0 Ma
N
Drill Hole
Contour lines
Land (Taranaki Peninsula)
Velocity (meters per second):
High : 2892.97
Low : 1250.59
Te Kumi-1
Tangaroa-1
Awatea-1
Ariki-1
Kora-2
Kora-3
Kora-1
Kora-4
Kanuka-1
Arawa-1
Wihoa-1
0
10
20
40 kilometres
NZTM (m)

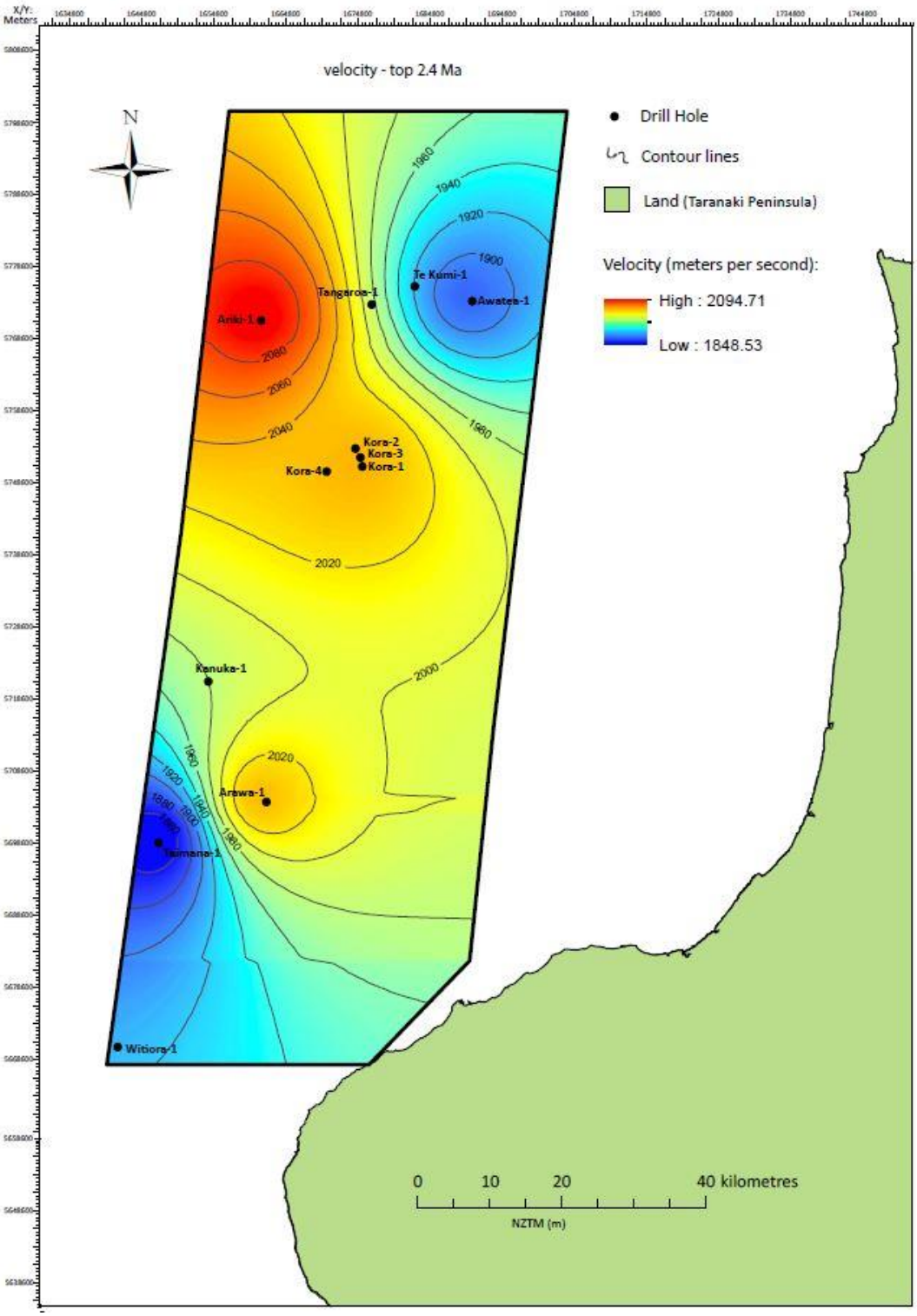
velocity - top 2.4 Ma
N
Drill Hole
Contour lines
Land (Taranaki Peninsula)
Velocity (meters per second):
High : 2094.71
Low : 1848.53
Tangaroa-1
Te Kumi-1
Awatea-1
Aniki-1
Kora-2
Kora-3
Kora-1
Kora-4
Kanuka-1
Arawa-1
Witiora-1
2020
2000
1980
1960
1940
1920
1900
2080
2060
2040
0
10
20
40 kilometres
NZTM (m)

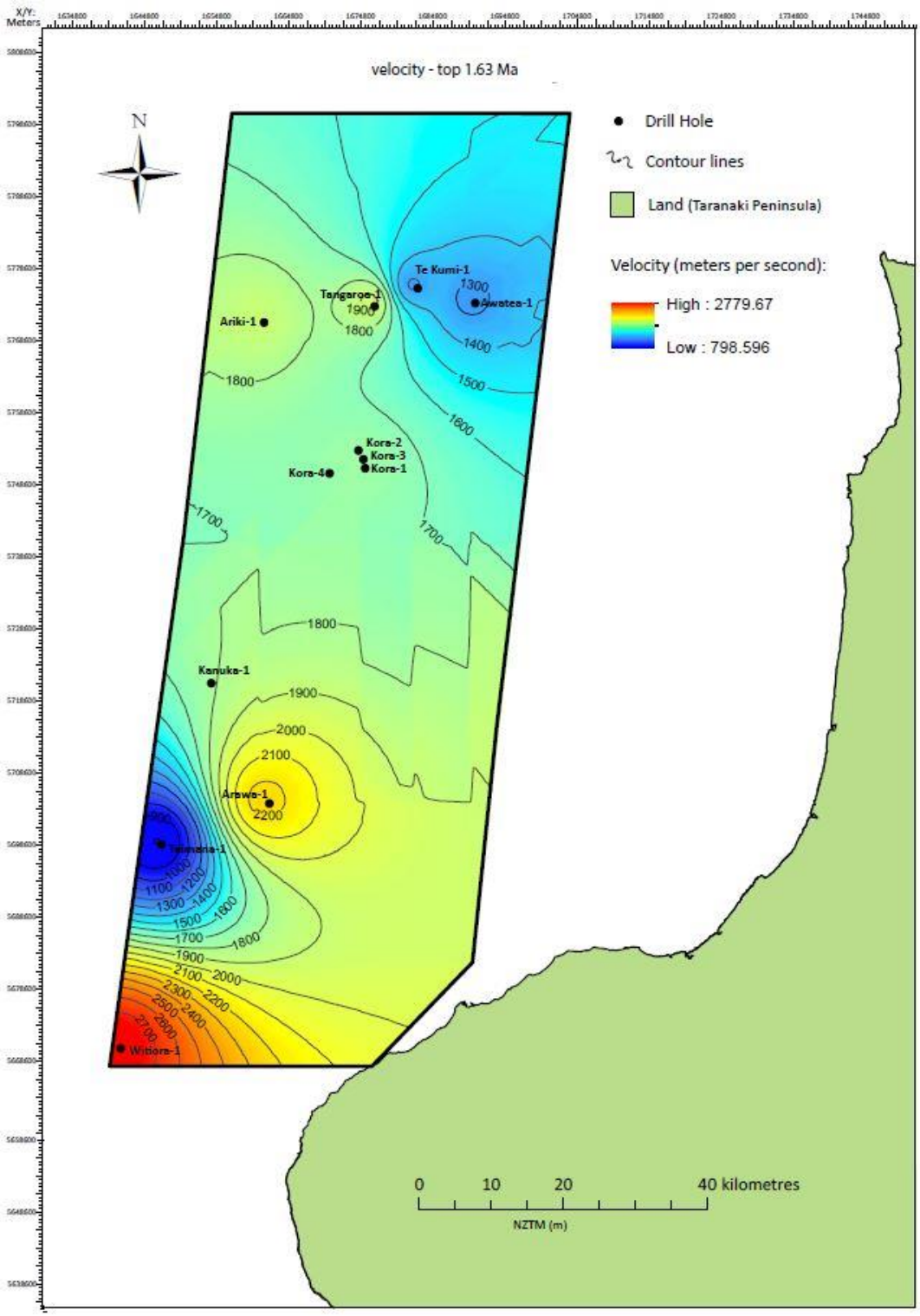
X/Y: Meters
velocity - top 1.63 Ma
N
Drill Hole
Contour lines
Land (Taranaki Peninsula)
Velocity (meters per second):
High : 2779.67
Low : 798.596
Te Kumi-1
Tangaroa-1
Ariki-1
Awatea-1
Kora-2
Kora-3
Kora-1
Kora-4
Kanuka-1
Arawa-1
Tainaria-1
Witiora-1
1300
1900
1800
1400
1500
1800
1700
1700
1800
1900
2000
2100
2200
1000
1100
1200
1300
1400
1500
1600
1700
1800
1900
2000
2100
2200
2300
2400
2500
2600
2700
0
10
20
40 kilometres
NZTM (m)

Appendix D: Detailed methodology outlining Kingdom SMT and map creation

1. Kingdom TM Software

1.1 Creating Time Grids

- Before the time grids are created, the tools that need to be used need to be employed. In the tabs up the top, select **'View'** and then **'Toolbars'**.
- Ensure that both **'Horizon picking'** and **'Fault picking'** are ticked. Two new separate windows will open up, which will be used to map the horizons.
- In the **'Project tree'**, on the left hand side of the Kingdom page, select the chosen horizon. A new base map window will open up.
- Click on any seismic line connected to a well that has biostratigraphic control loaded onto it.
- Select the corresponding horizon in the **'Horizons Picking'** toolbar.
- Find the closest physical seismic reflector to that entered biostratigraphic depth, and follow that horizon along the entire seismic line.
- If any faults are observed, draw them onto the seismic by using **'Fault Picking'** Toolbox to select the associated fault.
- As another seismic line is crossed, click on the new line and map that same reflector. The goal is to create several large loops between wells which have biostratigraphic control, and then expand these loops until the majority of the study area has been covered.
- At this stage, in the tabs across the top of the Kingdom main page, push **'Grids'** and then **'Create Grid'.** A new window will pop up.
- In the 'Data and Algorithm tab'; complete the following (Figure 1 below)
    - For 'Category' – **'Horizon'** is selected
    - For 'Gridding Algorithm' –**'Flex Gridding'** is chosen
    - For constrain by polygon – Select your created study area polygon, for example **'Jessica's Study Area'** and make sure **'Inside polygon'** is ticked.
    - Name the new grid and match the colour to the associated horizon colour.
    - Ensure that for the 'Units', **'Time'** is selected

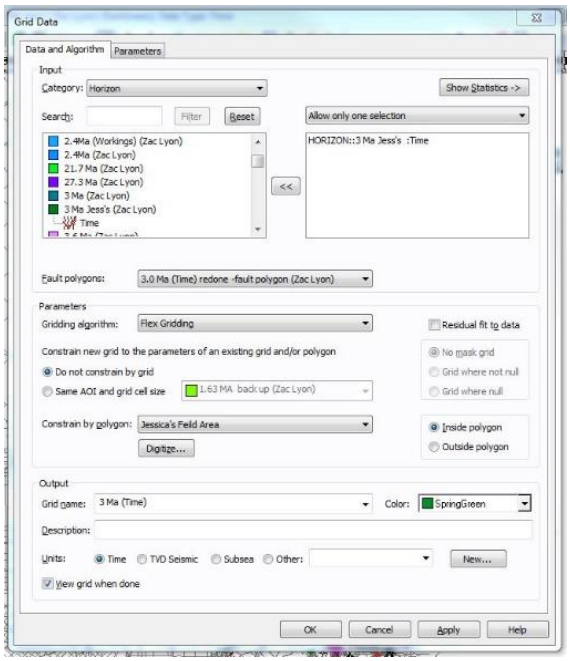

Figure 4

1.2 Creating Structure Contour Maps

- Select '**Tools**', then **'Depth Conversion'**, and **'Compute Velocity Map'**
- Complete the following (Figure 2 below):
    - Fill in **'New Velocity Name'**
    - Change the colour to match the horizon you have chosen
    - Average velocity type – **'Apparent'**
    - Input map type - **'Grid'**
    - Select a **'Time Grid'** and corresponding **'Formation Top'**
    - Location – **'Mid-point'**
    - Select **'OK'** – The program will go through all the wells in the study area, finding a marker at the 1.63Ma boundary previously loaded into Kingdom Software, and then extending this across the entire grid.
    - Ensure the **'View Map When Done'** box is ticked.
- At this point a new window will pop up – **'Grid: Specify Grid Parameters (for Velocity/Depth Map)**'
- To create the right boundaries, the parameters need to be set.
- Complete the following (Figure 2):
    - Select **'Digitize'** and then draw a box around the study area on the base map.

- Ensure that the **‘Extrapolate XY Bounds’** box is ticked.
- Select **‘OK’**
- A list of wells will pop up informing the user of the wells that are not intersecting the created grid. It is fine to ignore this box.

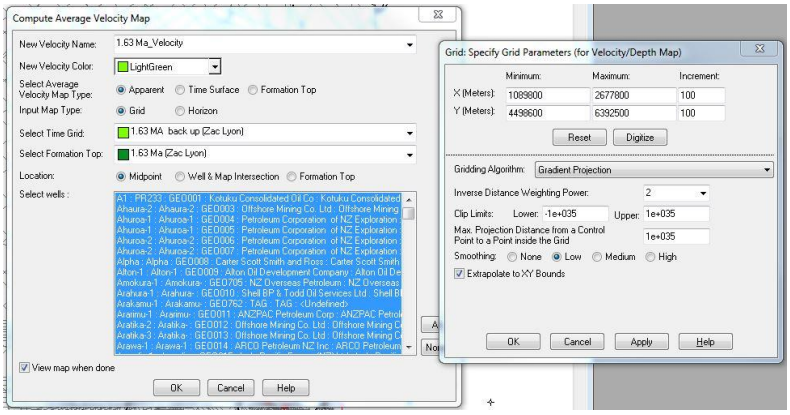

Figure 5

- Push **‘Tools’**, then go to **‘Depth Conversion’** again, and finally **‘Depth Map by Average Velocity Map’**
- Complete the following (Figure 3 Below)
  - Input map type – select **‘Grid’**
  - Select the appropriate time grid
  - Select the Velocity Map that was just created
  - New Depth Map – Use the Horizon name underscore Depth (1.63Ma_Depth)
  - Change the New Depth Map Colour to the colour matching the chosen horizon
  - Select **‘OK’**
- Define the parameters as described above in section 1.2, and shown in Figure 2.

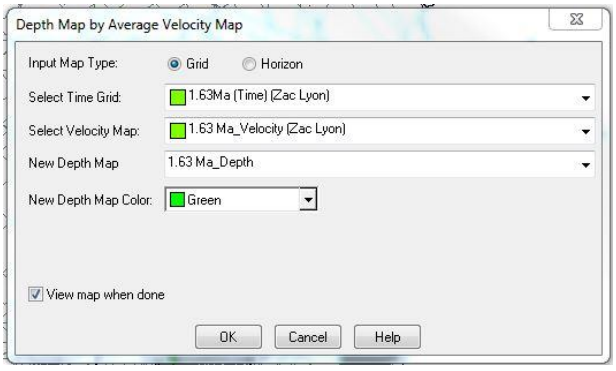

Figure 6

- On the created depth map:
    - Select **'Compute Contour'** button.
    - Select **'Grids'** within the tabs at the top of the new box.
    - Select the chosen depth grid
    - On the right hand side of the box where it says 'Contour Overlay', select **'Parameters'**
    - Change the contour interval in metres.
    - Apply the contouring based on what is happening in each individual map created (50m is generally a good number)

1.3 Compute Internal Velocity Map

- Select **'Tools'**, then **'Depth Conversion'** and finally **'Compute Internal Velocity Map'**
- Select the following things (Figure 4 below):
    - New Velocity Name – Horizon underscore intvelocity (2.4Ma_int velocity)
    - Ensure the colour is changed to the appropriate colour of chosen horizon.
    - Select Internal Velocity Map Type – **'Apparent'**
    - Input Map Type – **'Grid'**
    - Select two **'Time Grids'** adjacent to each other, as well as the corresponding **'Formation Tops'**, for example 2.4Ma (Mangapanian) and 3.0Ma (Waipipian)
    - Location – **'Midpoint'**
    - Ensure the **'View Map when Done'** box is ticked
    - Select **'OK'**
- Specify Grid Parameters as described above in section 1.2 and shown in Figure 2

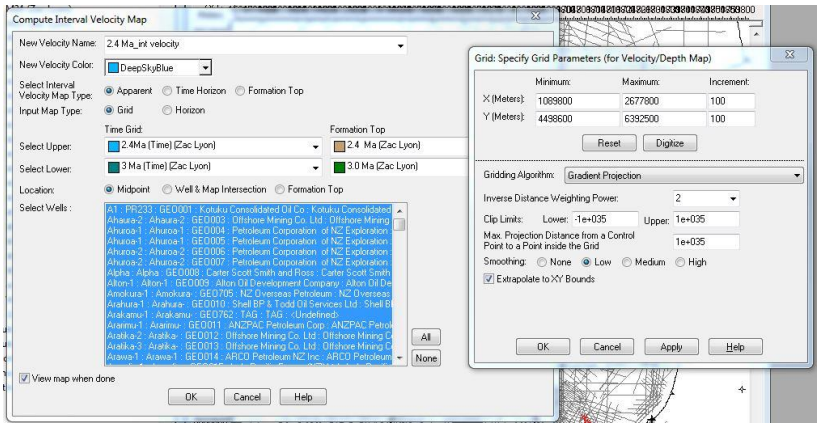

Figure 7

1.4 Compute Isopach Map

- Select **'Tools'**, then **'Depth Conversion'** and finally **'Compute Isopach'**
- Complete the following things (Figure 5 below):
    - New Isopach Map Name – Horizon underscore isopach (2.4Ma_Isopach)
    - Ensure the colour is changed to the appropriate colour of chosen horizon.
    - Input Map Type – **'Grid'**
    - Grid Type – **'Time'**
    - Select both an upper time grid and a lower time grid
    - Velocity Type – **'Velocity Map'**
    - Choose the internal velocity map as created before.
    - Ensure **'View Isopach Map when done'**
    - Select **'OK'**
- Specify Grid Parameters as described above in section 1.2 and shown in Figure 2

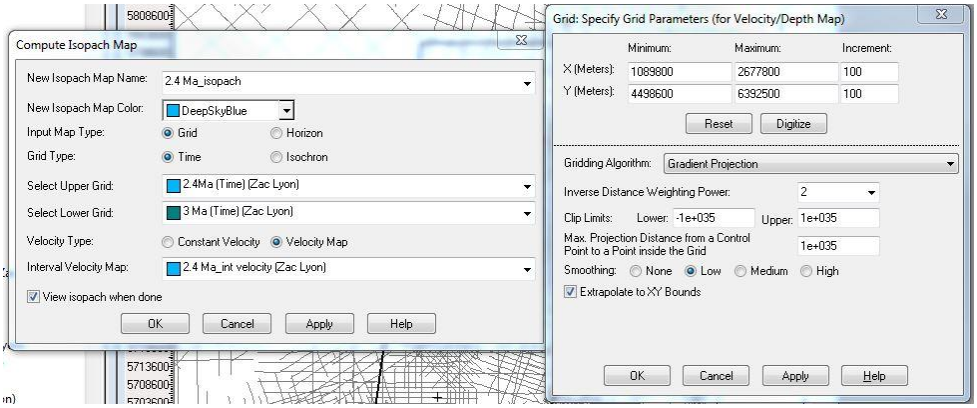

Figure 8

2. Initial manipulation of Images using ArcGIS software

2.1 Creating a CSV file through Microsoft Excel

- In Kingdom, select **'Grids'** and then **'Export X, Y, Z, Points…'**
- Save the file name as the stage boundary/what type of map it is (i.e. 1.63 Depth)
- Drag this newly created file into excel so it opens up on its own
- Ensure that all the data in the **'A'** column is highlighted and selected
- In excel, select the **'Data'** tab along the top, and then select **'Text to Columns'**
- The **'Convert Text to Columns Wizard'** box will pop up (Figure 6 below).
- When choosing the file type that best describes the data, ensure that **'Delimited'** is selected
- Select **'Next'**

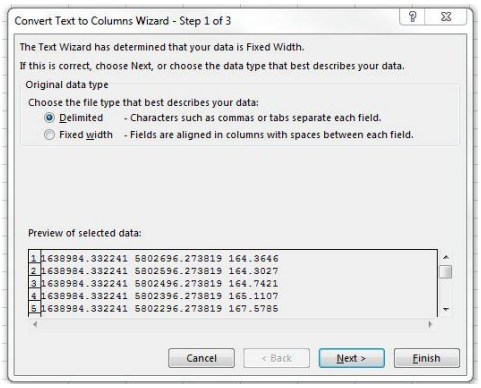

Figure 9

- Ensure that the **'Space'** tick box is selected. The **'Tab'** tick box will be still selected (Figure 7 below)
- Select **'Finish'**

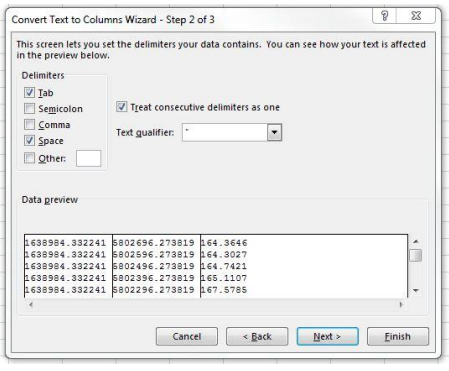

Figure 10

- Label the three produced columns as X, Y, Z, respectively.
- Save the excel file as a CSV file, (comma delimited)

2.2 Using ArcMAP program

- To add the newly created CSV file into ArcMAP, select **'File'** then **'Add Data'** and finally **'XY Data'**
- Select the following things (Figure 8 below):
    - Select the yellow folder to the right of the pop up window and add the created CSV file
    - Set the Z Field to **'Z'**
    - Ensure that the projected coordinate system is **'NZGD_2000_NZ_Transverse_Mercator'**

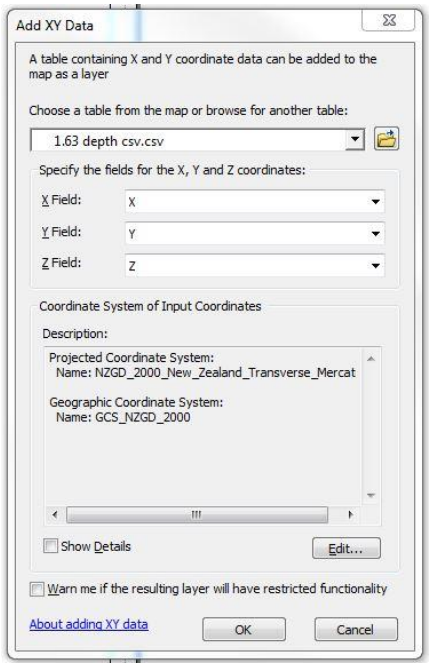

Figure 11

- Click on the new point data created in order to highlight it
- Search in the search bar on the right hand side of the screen '**Point to Raster'** - a new pop up box will appear.
- Select the following things (See Figure 9 below):
    - Input Features – Insert the created CSV file
    - Value Field – **'Z'**
    - Cell Assignment type – **'MEAN'**
    - Push **'OK'**

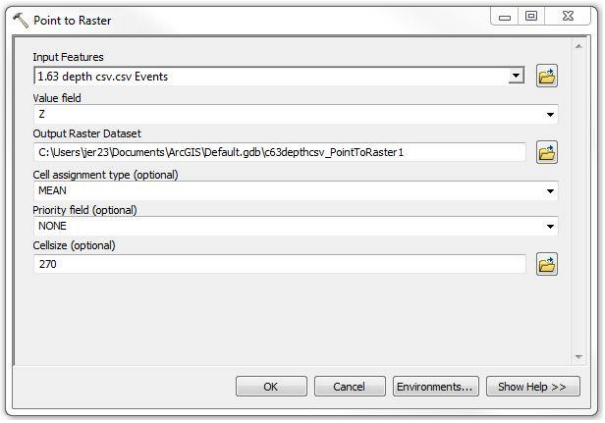

Figure 12

- Change the ramp colours from a black and white ramp to one more suited to the project, and then turn off the point data by unticking the box next to the name.
- To put contour lines onto the created raster image, search **'Contour'** in the search bar on the right. The function you want is **'Contour 3D Analyst'**
- Select the following things (Figure 10 below):
    - Input Raster – Insert the newly created raster file
    - Contour Interval – Choose an appropriate contour interval (50 or 100 works well depending on how detailed the contours need to be)
    - Select **'OK'**

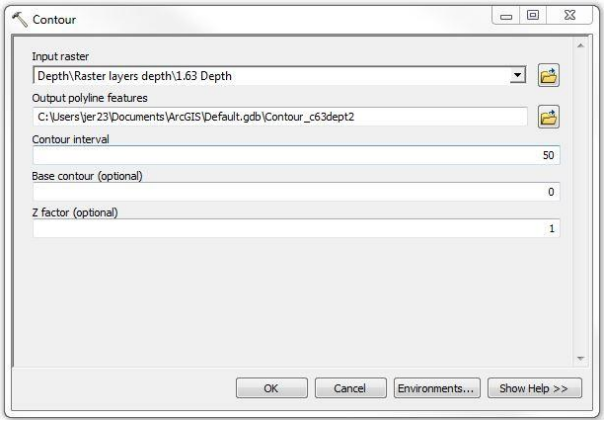

Figure 13

- Export the created maps for future editing in Adobe Illustrator by clicking **'File'**, then **'Save As'** an Adobe Illustrator (AI) file

2.3 Exporting Faults and wells from Kingdom TM software

- Both the locations of faults and drill holes, as well as the (georeferenced locator tick marks) for the final maps were exported separately as an EMF map file directly from Kingdom Software
- With the base map active, select the following things (Figure 11 below):
    - Select **'Map'** and then **'Presentation Plot'**.
    - In the pop up window, ensure that the **'Print to meta file'** tick box is selected and export the grid with the faults as an EMF file by selecting **'OK'**

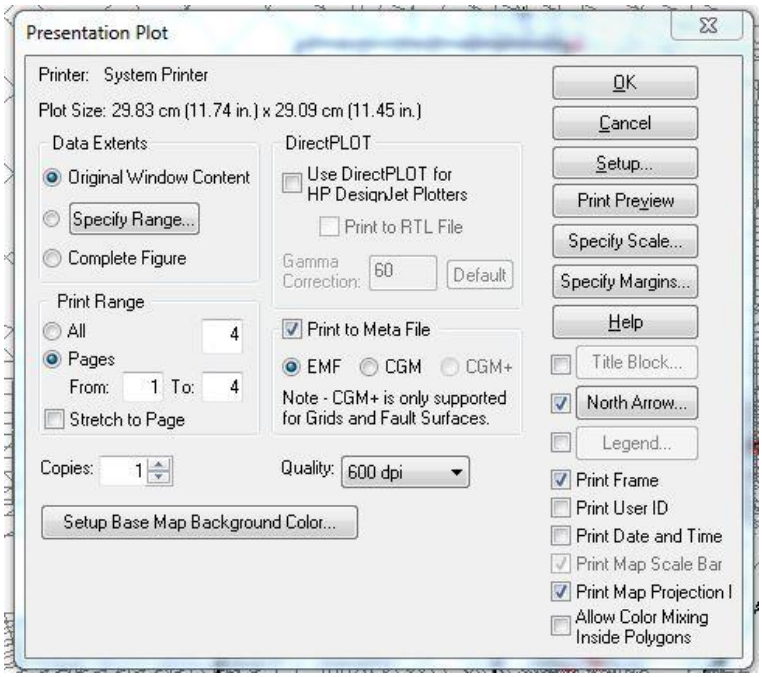

Figure 14

3. Final Manipulation of images in Adobe Illustrator

- The ArcGIS exported maps, Kingdom exported faults and drill hole EMF files were edited, starting with the georeferencing EMF files to the Arc GIS exported map file using the New Zealand Coastline as a reference.
- Final manipulation/tidying of all the maps was completed in Adobe Illustrator, including but not limited to the cutting of contours to faults, smoothing of contours, adding North points and scales, as well as labelling and annotation of key features on the images.